Analytical models for fatigue life prediction of metals in the stress life approach

Politecnico di Bari

Department of Mechanics, Mathematics and Management
MECHANICAL AND MANAGEMENT ENGINEERING
Ph.D. Program
SSD: ING-IND/14-MECHANICAL DESIGN AND MACHINE CONSTRUCTION

Final Dissertation

ANALYTICAL MODELS FOR FATIGUE LIFE PREDICTION OF METALS IN THE STRESS-LIFE APPROACH

---

by
Pietro D'Antuono

Supervisors:
Prof. M. Ciavarella
Prof. G. P. Demelio

Coordinator of Ph.D Program:
Prof. G. P. Demelio

Course n°32, 01/11/2016-31/10/2019

Politecnico di Bari

Department of Mechanics, Mathematics and Management

MECHANICAL AND MANAGEMENT ENGINEERING

Ph.D. Program

SSD: ING-IND/14-MECHANICAL DESIGN AND MACHINE CONSTRUCTION

Final Dissertation

ANALYTICAL MODELS FOR FATIGUE LIFE PREDICTION OF METALS IN THE STRESS-LIFE APPROACH

---

by

Pietro D'Antuono

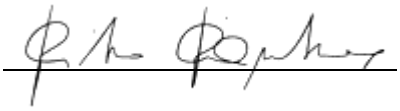

Referees.

Prof. F. Berto

Prof. F. Cianetti

Prof. D. Taylor

Supervisors:

Prof. M. Ciavarella

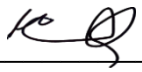

Prof. G. P. Demelio

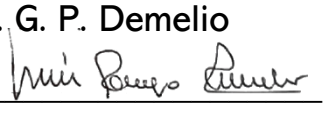

Coordinator of Ph.D Program:
Prof. G. P. Demelio

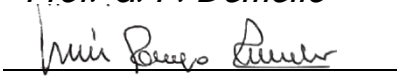

Course n°32, 01/11/2016-31/10/2019

La fatica non è mai sprecata.
Soffri, ma sogni.
Pietro Mennea

Io vidi gente sotto infino al ciglio;
e 'l gran centauro disse: «E' son tiranni
che dier nel sangue e ne l'aver di
piglio…».
Dante, Inferno – Canto XII

Declaration

I hereby declare that the work presented in this thesis has not been submitted for any other degree or professional qualification, and that it is the result of my own independent work.

Full Name

Pietro D'Antuono

Date

23 October 2019

Acknowledgements

Publications associated with this research

[1] D'Antuono P, Ciavarella M. Mean stress effect on Gaßner curves interpreted as shifted Wöhler curves. *arXiv preprint arXiv:1909.13324*. 2019 Sep 29.

[2] D'Antuono P. An analytical relation between Weibull's and Basquin's laws for smooth and notched specimens and application to constant amplitude fatigue. *arXiv preprint arXiv:1909.10741*. 2019 Sep 24.

[3] Ciavarella M, D'Antuono P, Papangelo A. On the connection between Palmgren-Miner rule and crack propagation laws. *Fatigue & Fracture of Engineering Materials & Structures*. 2018 Jul;41(7):1469-75.

[4] Ciavarella M, D'Antuono P, Demelio GP. Generalized definition of "crack-like" notches to finite life and SN curve transition from "crack-like" to "blunt notch" behavior. *Engineering Fracture Mechanics*. 2017 Jun 15;179:154-64.

[5] Ciavarella M, D'Antuono P, Demelio GP. A simple finding on variable amplitude (Gassner) fatigue SN curves obtained using Miner's rule for unnotched or notched specimen. *Engineering Fracture Mechanics*. 2017 May 1;176:178-85.

List of symbols

$\bar{a}$:	Basquin fatigue strength coefficient at 1 cycle.	A_C, B_C:	Ciavarella constants for $a_0(N)$.
$\bar{b}$:	Basquin exponent.	r:	material constant to determine A_C, B_C.
k,C_B:	Basquin's law constants (alternate form).	A_{ST}, B_{ST}:	Susmel and Taylor constants for $a_0(N)$.
a, b, B:	Weibull's law parameters.	2a:	crack/notch characteristic size.
$\check{b}, \check{a}, \check{B}, \check{\alpha}$:	corrected Weibull's law parameters.	c_L:	Leve's exponent
A_N:	Neuber's constant.	D:	damage.
A_P:	Peterson's material constant.	f:	geometric factor.
C_a:	coefficient of variation.	G:	shift factor.
f_a:	slope factor.	k_{CL}:	slope of the power law in the crack
K:	multiplier of the standard error.	like	region for notched specimen.
K_f:	effective stress concentration factor.	L/2:	critical distance in the TCD-P.
K_n:	technical stress concentraiton factor.	N, S:	number of cycles and stress.
K_t:	theoretical elastic stress concentration factor.	N_B:	number of load blocks in a load history.
κ(N):	life dependent stress concentration factor.	j:	load block on N_B
q:	notch sensitivity factor.	N_e:	cycles to the fatigue limit.
$\hat{C}_1$, $\hat{C}_2$:	least squares method fitting constants.	N_H:	number of cycles in the load history.
$\bar{X}$,$\bar{Y}$:	average values of X and Y.	n_j:	number of cycles in a load block j.
X, Y:	variables of the least squares regression line.	N_j:	fatigue life at load block j.
Y_L:	lower limit of Y.	n_f:	number of experimental tests.
α:	exponent of Weibull's law in S/log(N) coordinates.	N_i:	inflection point in Weibull's law.
Δ^2:	sum of the squared deviations.	N_u:	number of cycles at S_u for Basquin's law.
ϵ:	random error.	ν_j:	life proportion spent at block j.
ρ:	notch root radius.	w_j:	work adsorbed during the block j
σ:	sample standard error of Y_j on X_j.	W:	total work
σ^2:	standard deviation of experimental data.	R:	load ratio.
$a_0(N)$:	life dependent crack size.	S'_f:	fatigue strength at one cycle.
a_0:	El Haddad intrinsic crack size.	S_{ae}:	effective stress amplitude.
a_0^u:	a_0 at the ultimate strength.	S_{max}:	maximum stress.
C,m: S_e:	Paris' law constants.	S_{min}:	mininum stress.
Γ,η,ς,:	constants for a generic power law crack growth equation	S_{mj}, S_{aj}:	mean and alternate stress at load block j.
γ:	Walker's law exponent.	$S_{nom,max}$:	maximum nominal alternate stress of the load history.
ΔK:	stress intensity factor range.	$S_{nom,max}$:	maximum nominal alternate stress of the load history.
ΔK_{th}:	threshold stress intensity factor range.	S_e:	fatigue limit stress.
K_{Ic}:	mode I fracture toughness.	S_u:	ultimate tensile strength.
		β:	multiplicative factor of the spectrum.
		ΔS:	stress range.
		ΔS_e:	fatigue limit stress range.
		a_i, a_f:	initial and final crack sizes.
		ψ:	generic function of N

Table of Contents

List of Figures

List of tables

Outline

This Thesis provides a collection of stress-life (S/N) models for fatigue life evaluation of both pristine and notched metallic components. The document is subdivided into five Chapters, the first being a Literature Overview of fatigue in general, and, in the specific, of the tools needed in the subsequent Chapters. In Chapter 2 the "crack like to blunt" notch transition is adapted to the stress-life approach using the theory of the critical distances, therefore a new S/N curve to model this transition is defined. Chapter 3 relies on the new S/N curve model for variable amplitude fatigue loading by demonstrating that fatigue life assessment under these conditions can be performed through a constant shift of the Wöhler curve if adopting a linear damage accumulation rule. The method is quite general since there is no need of hypothesizing specific constraints on loading history as the shift accounts for mean stress effects, albeit suffering from the weaknesses of the underlying linear damage accumulation rule. The models proposed have been experimentally validated through the SAE Keyhole test program data, publicly available online at https://www.efatigue.com/benchmarks/SAE_keyhole/SAE_keyhole.html.

Chapter 4 discusses the limits of validity of a linear damage accumulation rule, giving special attention to its relationship with crack propagation laws of the generalized Paris type. Specifically, the Chapter proves that supposing a linear damage accumulation exactly corresponds to integrating a power law of the stress and the crack size in the form of Paris' or Walker's law. Ergo, this result is valid even for non-zero mean stress, yet neither accounting for load sequence nor for crack closure is considered. Thenceforth, despite some clear limitations, no difference in terms of accuracy is expected between the application of a linear damage accumulation rule vs. integration of a crack growth equation. Finally, Chapter 5 presents an investigation of the advantages in the application of a (maybe more realistic) four parameters S/N curve directly obtained postulating that the two parameters curve corresponds to the first derivative of the former one in its inflection point. The accuracy of the new curve is compared with the former employing an experimental campaign fatigue data on steel and aluminum alloy conducted by the National Advisory Committee for Aeronautics (NACA).

1 Overview

Introduction

This Chapter provides an overview of the notions used in this Thesis, starting with the derivation of stress vs. number of cycles (S/N) curve models for short cracks, since the work of these years is relying on the stress-life approach. Then, an overview of crack propagation models is given, in fact power law type crack propagation equations are integrated to recharacterize the concept of S/N curve for long cracks. Subsequently, the effect of notches in the stress-life formulation is treated mostly by means of the theory of the critical distances. Besides providing a variety of fatigue S/N curve models, a brief overview of damage accumulation rules for fatigue prediction deriving from variable amplitude loading is given. The Chapter concludes with a brief overview of the regulatory aspects of fatigue tolerance evaluation for rotorcrafts.

1.1 The S/N curve

The advent of the First Industrial Revolution in the 18th century caused a dramatic increase of the frequency of work of the machines; this event could be identified as the trigger for the widespread study of fatigue in the last two centuries. Indeed, even if it has been known for centuries that repeatedly applying a load causes early ruptures, as it used to happen to long distance travelling boats, it was only around 1830s that engineers and scientists started investigating how a load much lower than the material strength can cause failure if applied many times. The first reference to the fatigue of metals dates to 1837 when Albert [1], a German mining administrator, published the first document in history relating to a fatigue test was published. The test was aimed to understand the causes of the failure of the conveyor chains in the Clausthal mines in 1829. The test involved the entire component, not only a representative specimen of material. Therefore, since the replacement hemp rope was an expensive good, Albert invented the wire rope which certainly is the innovation he is remembered for. Independently, in 1839 Poncelet [2], a French military engineer, used the adjective "tired" (in French, fatigué) to describe steels under cyclic stress and assumed that steel components experience a decrease of durability when they undergo repeated variable loads. In 1843 Rankine [3] and York [4], [5] focused their attention on railway axles thanks to the establishment of the Her Majesty's Railway Inspectorate instituted due to the increasing number of accidents, amongst which the so-called Versailles disaster where at least 55 people lost their lives due to the failure of the axle tree of the first engine on the 5th October 1842. Anyway, the term fatigue was coined only in 1854 by the Englishman Braithwaite [6], who discussed the fatigue failures of multiple components as water pumps, brewery equipment and, of course, railway axles. Many other English and German studies on the deterioration of railway axles were conducted in those years [7]–[10], but the work of Wöhler, Royal "Obermaschinenmeister" of the "Niederschlesisch-Mährische Railways in Frankfurt an der Oder", was the milestone paving the way for the modern

Wilhelm A. J. Albert (1787/01/24 – 1846/07/04)

Disaster on the Railway between Versailles and Bellevue, 8th May 1842. (55 - 200 casualties)

A. Provost (1834-1855)

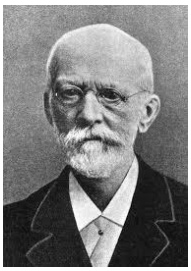

August Wöhler (1819/06/22 – 1914/03/21)

conception of fatigue testing and interpretation of results. In 1858 [11] and 1860 [12] August Wöhler measured for 22,000 km the service loads of railway axles with deflection gages personally developed and from his studies concluded that *"If we estimate the durability of the axles to be 200,000 miles with respect to wear of the journal bearings, it is therefore only necessary that it withstands 200,000 bending cycles of the magnitude measured without failure"*. Such statement represents the first suggestion for a safe life design philosophy with retirement time (or distance travelled). Wöhler then calculated the stresses deriving from service loads and concluded that the higher the stress amplitude is, the more detrimental influence on the axle will be, plus a tensile mean stress anticipates the rupture. Furthermore, he even stated that a replacement of the axle would have been necessary if radial flaws propagated up to 20 mm into the material, and this procedure could be interpreted as an ancestor of the flaw tolerant safe life methodology [13]. Notwithstanding, Wöhler's test results were tabulated and not plotted until 1875, when Spangenberg [14] adopted unusual linear axes to present these data. Furthermore, stress vs. number of cycles (S/N) curves were addressed as Wöhler curves only in 1936 by Kloth and Stroppel [15]. The idea to plot many fatigue test data, including the 60 years old Wöhler's experiments, in logarithmic axes and interpolate them with a power law is from 1910 by Basquin [16]. The equation relating maximum or alternate stress with the number of cycles is

$$S = \bar{b} \cdot N^{\bar{a}} \qquad \text{(BASQUIN) (1.1)}$$

Where S denotes the stress, alternate or maximum, N the number of cycles and $\bar{a}$ and $\bar{b}$ are constants depending on the material. Later such law took his name. The proof of existence of a fatigue limit was given four years later by Stromeyer [17]. In 1914 he conducted tests on small scale specimens in order to reduce to a minimum the difference in terms of chemical composition and mechanical properties in the component under test. The specimens were loaded in bending and twisting moment and the stress plotted against the empirical formula $(10^6/N)^{1/4}$ resulted in a straight line corresponding to the fatigue limit. Stromeyer also theorized that if the maximum stress would have exceeded the yielding, the constant slope ¼ would have certainly changed. The final form of Stromeyer's law simply adds a constant term to (1.1).

$$S = \bar{b} \cdot N^{\bar{a}} + S_e \qquad \text{(STROMEYER) (1.2)}$$

Where S_e is the fatigue limit and for the same material $\bar{a}$ and $\bar{b}$ defined in (1.2) have different values from the corresponding quantities defined in (1.1). In 1924

Palmgren [18] in his studies for the ball bearings life estimation introduced a term B to (1.2), i.e.

$$S = b \cdot (N + B)^a + S_e \qquad \text{(WEIBULL) (1.3)}$$

The B introduces an inflection point in the equation both when plotted in S/log(N) and when plotted in log(S)/log(N) axes, consequently low cycle fatigue data are better fitted by this model. Indeed, as suggested by Shanley [18] in the 1956 "Colloquium on Fatigue" [20], Basquin's law fails to model low cycle fatigue since it does not predict correctly the strain at high stresses, while by using (1.3) one supposes that a stress close to the ultimate tensile strength causes much lower strain, hence it can be applied a certain number of times without failure. This is also confirmed by Epremian and Mehl [21] that in 1952 showed that an S/N diagram, when the alternate strength is close to the ultimate tensile strength, can be fit with very good agreement by a probability scale instead of a logarithmic scale and this suggests that at high stresses alternating plastic strain dependence on stress amplitude is primarily of statistic nature. The model found by Palmgren has been widely used by Weibull since 1949 [22]. For this reason, (1.3) will be addressed here as Weibull's law. Engineer and mathematician, Ernst Hjalmar Waloddi Weibull (1887-1979) gave a huge contribution to material science and statistics in his prolific scientific career. Concerning fatigue, there are tens of documents, many of which are ICAF (International Committee on Aeronautical Fatigue and Structural Integrity) proceedings [23]–[26] and reports to the Aeronautical Research Institute of Sweden (FFA) [27]–[31]. His contribution to the field is principally, but not only, related with the statistical aspects of fatigue. Weibull, in Sweden, approached material science by developing a theory of static strength [32], then his interest extended to fatigue [22]–[26], [28]–[31]. (1.3) has been used by the author in Chapter 5. It is worth of mention that Yokobori [33] and Shanley [19] developed independently theories for interpreting the parameters b and a from physical quantities as absolute temperature, loading frequency, number of preferred nucleation sites per unit volume, etc. As stated by Weibull, (1.3) is the most realistic way of describing S/N data pretty much all over the domain, nevertheless the model has not been extensively used in history and usually Basquin's law is preferred because of its simplicity. Indeed, most usually the simplified power law is preferred to the four parameters law, and for this reason most of the databases in Literature are available as Basquin's constants $\bar{b}, \bar{a}$. This is also due to some generalizations and links that can be derived quite naturally starting from a pure power law fatigue behavior.

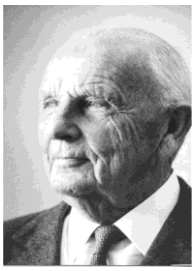

E. H. Waloddi Weibull (1887/06/18 – 1979/10/18)

1.2 The crack growth curves

Crack growth curve equations have been extensively studied since the '50s of the last century, almost in conjunction with the first catastrophic accident of the first jet transportation aircraft, the De Havilland Comet 1 [34]–[36] (1954), where the propagation of fatigue cracks in the upper fuselage panels, starting from the sharp corner of the top rectangular windows brought 35 deaths. As Frost and Dugdale [37] already pointed out in 1958, the cylindrical specimens were the protagonists of the first half of the 20th century in the panorama of fatigue, and this typology of specimens makes really complex the study of crack growth, meaning that no special attention up to that moment was given to crack growth testing of sheet specimens. Secondly, Frost and Dugdale observed that *"In aircraft structures the 'fail-safe' design philosophy requires the structure to be constructed in such a way that fatigue cracks do not cause catastrophic failure before corrective measures can be taken"*. The first scientist that emphasized the necessity to have polished surfaces to minimize the hotspots from where a crack can propagate is Griffith [38] who extended the theorem of minimum potential energy to the phenomena of rupture of elastic solids. Griffith's work was motivated by Inglis' [39] linear elastic solution for the stress around an elliptical hole asymptotically loaded in tension, from which he predicted that the stress would go to infinite as the ratio between the minor and major axis goes to zero. Griffith's theory provides correct predictions as long as brittle materials, such as glass or ceramics, are considered. Starting from the pioneering work of Griffith, Berto and Lazzarin [40] provided an exhaustive overview of local approaches for the description of brittle and quasi-brittle fracture of engineering materials. Anyway, since in structural materials there is almost always some inelastic deformations around the crack faces, Griffith's hypothesis of linear elastic medium in structural metals application becomes highly unrealistic. For this reason, the first crack growth equation relating the stress with the crack growth rate (i.e. the crack length increment per cycle) did not make use of the elastic energy approach. The formulation dates 1953 and has been proposed by Head [41]; it is based on Inglis' [39] solution and the final simplified form of the crack growth equation is

Fatigue test on the Comet G-ALYU fuselage (Farnborough, GB)

The fuselage was hydraulically pressurized, and the first detectable crack was found after 1836 cycles. In service failure occurred after 1221 cycles.

$$\frac{da}{dN} = \varphi\left(S_a, S_y, S_f'\right) \cdot a^{\frac{3}{2}} \cdot t_p^{-\frac{1}{2}} \qquad \text{(HEAD) (1.4)}$$

Where N is the number of cycles, φ(S) is (asymptotically) a linear function of the stress, yielding, and strength, a is the half crack size, and t_p is the thickness of the plastic zone ahead of the crack tip. Frost and Dugdale [37] argued that t_p is not a constant independent of crack length and derived the exponential model for crack propagation, seldom used up to nowadays

$$\frac{da}{dN} = k_{FD}(S_a^3) \cdot a \quad (a)$$
$$\ln\left(\frac{a}{a_i}\right) = k_{FD}(S_a^3) \cdot N \quad (b) \qquad \text{(FROST-DUGDALE) (1.5)}$$

In which a_i is the initial size of the crack and k_{FD} is an experimental quantity depending on the cubic power of the remote alternating stress S_a. During WWII, a group of researchers of the U.S. Naval Research Labs headed by George Rankine Irwin realized that plasticity plays an important role in [42] in fracture mechanics. On this purpose, Griffith's energy formulation was modified in order to make it account for plasticity, too, i.e. the energy release was redefined by adding a plastic dissipation term. Another major achievement of Irwin's work is certainly the relation between the energy release rate $\overline{G}$ and the stress intensity factor in opening mode K_I:

George R. Irwin (1907/02/26 – 1998/10/09)

$$\overline{G} = K_I^2/E^* \qquad (1.6)$$

Where E^*=E for plane stress or $E/(1-\nu)^2$ for plane strain. The critical stress intensity factor is the value of K beyond which a crack starts to propagate and is addressed as fracture toughness K_C. Namely, the toughness is the resistance to fracture of a material, it is a material property and is defined as the stress intensity factor required for a crack to advance from length a to a_C. The fracture toughness values have been grouped by material family by Ashby [43], [44] and are shown in Figure 1.1.

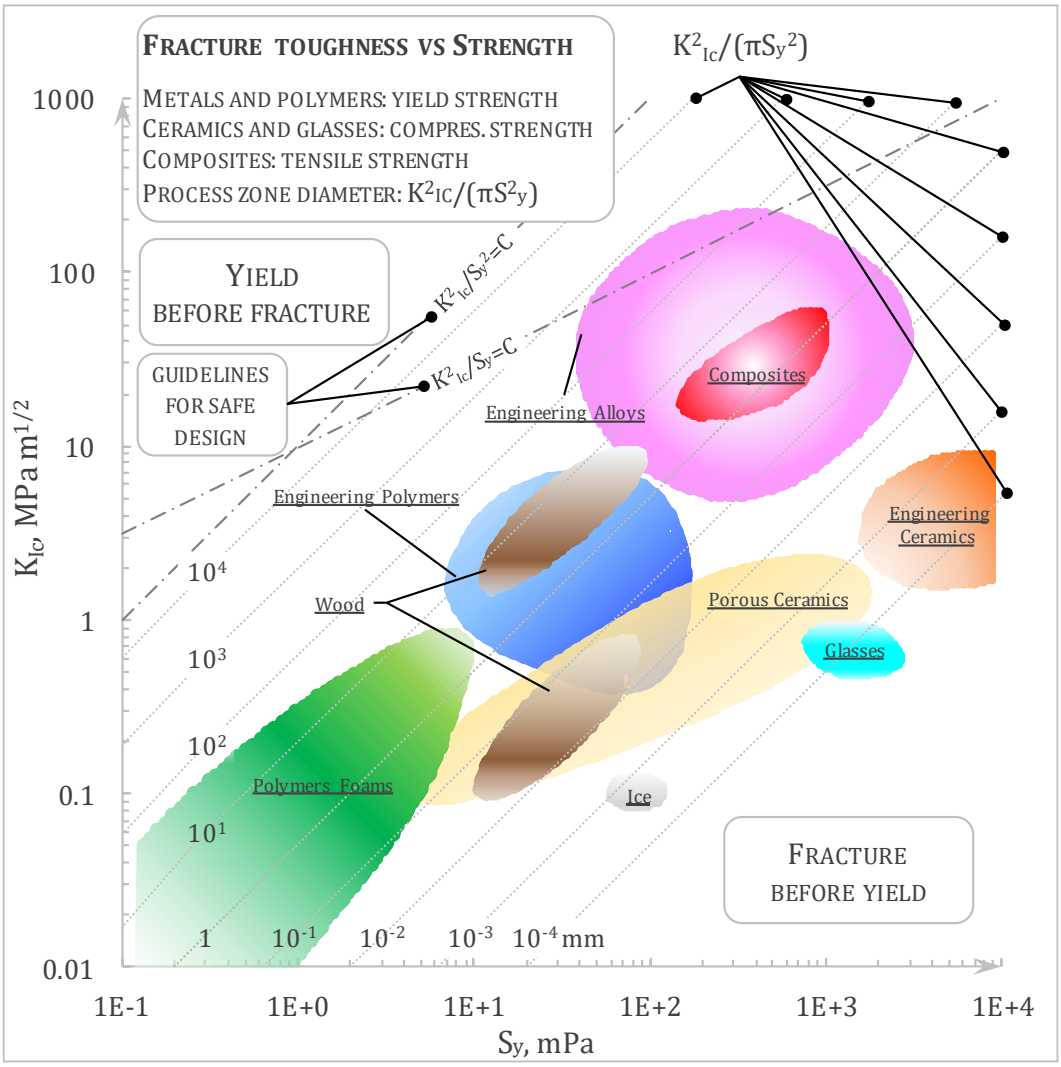

Figure 1.1: Fracture toughness against yield strength (from Ashby [43], [44]). The dottted lines are the value of $K^2_{Ic}/(\pi S_y^2)$, i.e. approximately the diameter of the process zone

Few years later, in 1963, Paris and Erdogan [45] published a work substantiated by many experimental tests where they postulated, differently from Head or Frost and Dugdale, that the crack growth is described by a power law of the stress intensity factor, viz.

$$\frac{da}{dN} = C\,\Delta K^m \qquad \text{(PARIS-ERDOGAN) (1.7)}$$

At the time of publication, the authors were uncertain on the value of the exponent m, in fact there is a famous statement in their paper saying: *"The authors are hesitant but cannot resist the temptation to draw the straight line slope 1/4 through the data..."*. Therefore, the so-called Paris' law, or Paris-Erdogan law, has been formulated in principle with fixed m=4. Indeed, as evident from Figure 1.2 (taken from Ashby [43], [44]), the majority of engineering alloys is concentrated in the neighborhood of m=4, and this may have tricked the authors.

Paul Croce Paris (1930/08/07 – 2017/01/15)

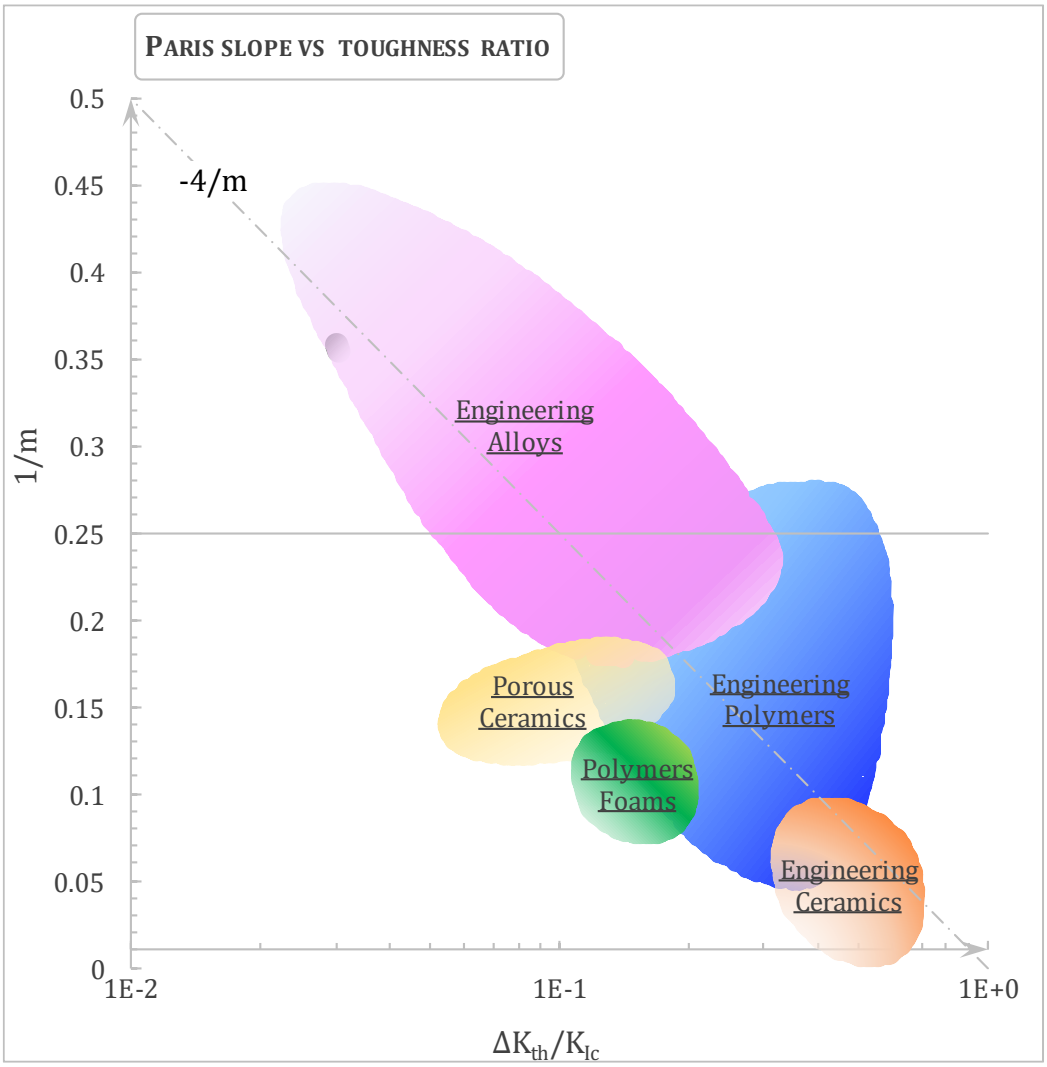

Figure 1.2: Ashby map for Paris' slope against toughness ratio (from [43], [44]). Many engineering alloys are concentrated in the range ($\Delta K_{th}/K_{Ic}$=0.1, m=4)

Paris' law is considered valid within the range $\Delta K_{th}<\Delta K<\Delta K_{cr}$, where ΔK_{cr} is the critical stress intensity factor range which depends on the toughness as $\Delta K_{cr}=(1-R)K_{Ic}$, with R load ratio, and ΔK_{th} is the threshold value below which the crack should not propagate[1]. In the following years there have been many attempts to generalize Paris' law, mainly to account for mean stress effect, crack closure and near threshold/near failure modelling. The simplest model of Paris' law for mean stress effect has been proposed in 1970 by Walker [47]:

$$\frac{da}{dN} = C_0 \left(\frac{\Delta K}{(1-R)^{1-\gamma}}\right)^m \qquad \text{(WALKER) (1.8)}$$

With γ being Walker exponent and R the load ratio. A more general form of Walker equation had already been given in 1967 by Forman et al. [48]:

[1]The crack behavior below threshold is still a quite challenging quantity to predict and measure. The reader is advised to read the work of Zerbst et al. [46] to have a better insight of the topic.

$$\frac{da}{dN} = C\frac{\Delta K^m}{K_c - \frac{\Delta K}{1-R}}$$ (FORMAN ET AL.) (1.9)

Forman equation is, to some extent, the ancestor of the most sophisticated crack propagation equation available in Literature: the NASGRO™ equation

$$\frac{da}{dN} = C \cdot \left(\frac{1-\varphi}{1-R} \cdot \Delta K\right)^m \cdot \frac{\left(1 - \frac{\Delta K_{th}}{\Delta K}\right)^p}{\left(1 - \frac{K_{max}}{K_c}\right)^q}$$ (NASGRO) (1.10)

Where the mean stress effect is accounted for through (1–R), and the crack closure effect through (1–φ). The equation is shown in Figure 1.3 for a sample ASTM A579 Grade 75 steel, forged. Three stages of the crack propagation are easily identified: (i) in the near threshold regime (so-called stage I) slight changes in the microstructure imply high changes in the crack growth rate; (ii) in the stable propagation the crack grows as a power law (Paris' law); (iii) when the crack reaches a length close to the critical a_c, the propagation becomes unstable. Generally, Stage I and II take almost the 90% of the entire life.

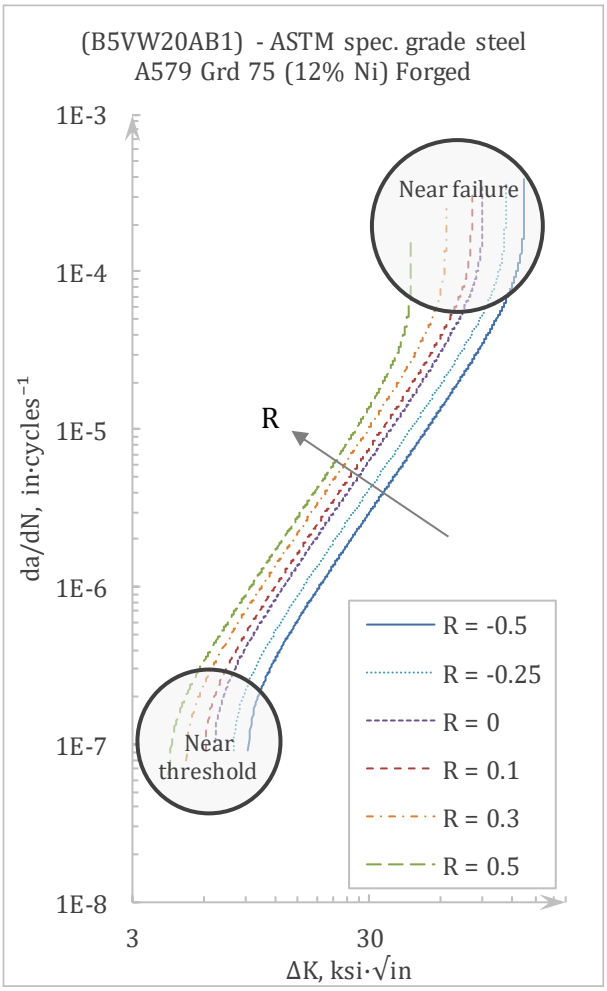

Figure 1.3: Example crack growth curves according to NASGRO 3.0 equation for an ASTM A579 steel. The mean stress effect is clearly visible from the figure.

The quantity f in Equation is called Newman [49] opening function and is the ratio between the opening and maximum stress (intensity factor). i.e.:

$$\varphi = \frac{K_{op}}{K_{max}} = \begin{cases} \max\left(R, \sum_{j=0}^{3} A_j \cdot R^j\right) & R \geq 0 \\ \sum_{j=0}^{1} A_j \cdot R^j & -2 \leq R < 0 \end{cases} \tag{1.11}$$

Where A_j are some empirical constants depending on a value α ranging from 1 (plane stress) to 3 (plane strain), the maximum stress S_{max} and the flow stress $S_0=½\cdot(S_u+S_y)$ (average between the yielding and ultimate tensile strength).

$$\begin{cases} A_0 = & (0.825 - 0.34 \cdot \alpha + 0.05 \cdot \alpha^2) \cdot \sqrt[\alpha]{\cos\left(\frac{\pi}{2} \cdot \frac{S_{max}}{S_0}\right)} \\ A_1 = & (0.415 - 0.071 \cdot \alpha) \cdot \frac{S_{max}}{S_0} \\ A_2 = & 1 - A_0 - A_1 - A_3 \\ A_3 = & 2 \cdot A_0 + A_1 - 1 \end{cases} \tag{1.12}$$

The near threshold and near failure areas are dealt through the exponents p and q. As regards the calculation of the ΔK_{th}, the NASGRO 3.0 [50][2] equation defines

$$\Delta K_{th} = \Delta K_0 \frac{\sqrt{\frac{a}{a + a_0}}}{\left(\frac{1 - \varphi}{(1 - A_0)(1 - R)}\right)^{1 + C_{th} R}} \tag{1.13}$$

Being C_{th} a constant to be calibrated and ΔK_0 the threshold stress intensity factor for long cracks calculated at R=0. Equation (1.13) has been derived to take into consideration the small crack effect demonstrated by Tanaka et al. [51]. The value a_0 is a quantity of paramount importance: the intrinsic crack size. It was defined for the first time in 1980 by El Haddad [52]. El Haddad's constant is, by definition, proportional to the square of the ration between the fatigue threshold and the fatigue limit (at fixed load ratio), i.e.

$$a_0 = \frac{1}{\pi} \left(\frac{\Delta K_{th}}{\Delta S_e}\right)^2 \tag{1.14}$$

Cracks smaller than El Haddad intrinsic size do not follow Paris' law even for $\Delta K > \Delta K_{th}$, whereas the fatigue behavior in this range of crack size is ruled by the fatigue limit. The quantity a_0 is also used in the famous interpolating equation proposed by El Haddad-Dowling-Topper-Smith [52] and modified by Atzori and Lazzarin [53]–[56] in the following form:

$$\Delta S_e = \frac{\Delta K_{th}}{\sqrt{\pi(f \cdot a + a_0)}} \tag{1.15}$$

This equation fits the data of the Kitagawa-Takahashi [57] diagram[3] first proposed in 1976:

[2] NASGRO 3.0 is the last free version of the equation. Indeed, since the version 4.0 the equation has been amended considerably especially in the calculation of the threshold stress intensity factor.

[3] Data have been collected in the form of Kitagawa-Takahashi diagram already in 1973 by Sprowls et al. [58], as also pointed out by Sadananda and Sarkar [59], but Kitagawa and Takahashi were the first observing that below a_0 the threshold stress remains constant and propagation is ruled by the fatigue limit.

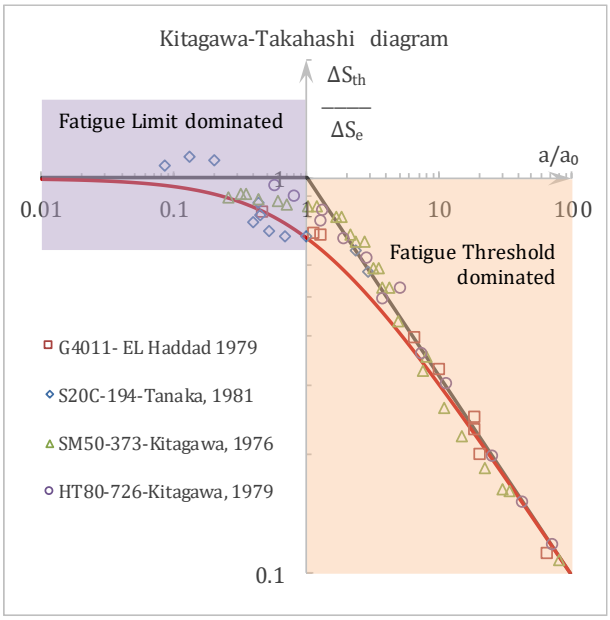

Figure 1.4: Kitagawa-Takahashi diagram for some material data taken from [51], [52], [57]. The red line is El Haddad equation, while the grey line is the Kitagawa-Takahashi criterion.

1.3 Notch fatigue

The idea behind Equation (1.14) is one aspect of the "Theory of the Critical Distances" (TCD) whose ancestor, as summarized by Taylor [60], and Yao et al. [61], can be identified in the effective stress concentration factor K_f first proposed by Neuber [62] in 1946, then picked up by Kuhn and Hardrath [63] who in the early '50s assumed that the notched specimen fails if the averaged stress over the distance A_{KH} ahead of the notch root is equal to the fatigue limit S_e of the plain specimen. From this hypothesis, K_f was calculated as

$$K_f = 1 + \frac{K_t - 1}{1 + \frac{\pi}{\pi - \omega}\sqrt{A_{KH}/\rho}} \tag{1.16}$$

Where K_t is the theoretical stress concentration factor (e.g. 3 for a circular hole in an infinite plate, from Kirsch [64] solution), ω is the notch flank angle, ϱ is the notch root radius and the distance A_{KH} is a material constant. The stress concentration factor equation was later modified by Neuber as

$$K_f = 1 + \frac{K_t - 1}{1 + \sqrt{a_N/\rho}} \tag{1.17}$$

a_N is known as Neuber's material constant

In 1949 Peterson [65] derived his version of the stress concentration equation based on the hypotheses that (i) the notched material fails if the point stress at a distance d_0

away from the notch root is at least equal to the fatigue strength of the plain specimen and (ii) the stress ahead of the notch root drops linearly up to d_0 obtaining

$$K_f = 1 + \frac{K_t - 1}{1 + a_P/\rho} \tag{1.18}$$

Where a_P is Peterson's material constant. Nevertheless, as also confirmed by Topper et al. [66], as ϱ increases the fatigue limit is actually fully controlled by the theoretical stress concentration factor, thus $K_f \rightarrow K_t$ since $a_P/\varrho \rightarrow 0$ and the notch is addressed as blunt notch. From a mathematical point of view, a notch can be effectively be addressed as blunt when its characteristic size a^* excedes [54]–[56], [67]

$$a^* \geq K_t^2 \cdot a_0 \tag{1.19}$$

Hence, for instance for a hole in an infinite plate this occurs when the circle radius is almost one order of magnitude larger than a_0. For aluminum alloys and steels, typically 10 μm$<a_0<$100 μm respectively implying 0.1 mm$< a^*<$1 mm respectively. Therefore, Atzori and Lazzarin suggested the following infinite life design criterion for notched components

$$K_f = \min\left(\sqrt{1 + a/a_0},\ K_t\right) \tag{1.20}$$

The combination of Equations (1.19) and (1.20) implies that below a^* notches behave similarly to cracks, and above a^* they behave as blunt notches. In the last decades, tens of notch sensitivity estimation models for infinite life design have been proposed. Most of them have been collected in 2004 by Ciavarella and Meneghetti [68] who reviewed a series of classical and modern approaches to the stress concentration factor estimate concluding that Neuber's method [62] is the most conservative and accurate among the "classical" approaches whilst the Atzori-Lazzarin criterion is the most conservative yet easy-to-use between the "modern" ones. Therefore, they proposed their personal modification to the Atzori-Lazzarin criterion to make it consistent with Lukáš and Klesnil [69] discussion which can be interpreted as a modification of Neuber's rule including the effect of cyclic plasticity. The Ciavarella-Meneghetti criterion for infinite life design is:

$$K_f = \min\left((1 + (a/a_0)^r)^{1/2r},\ K_t\right) \quad 0 < r \leq 1 \tag{1.21}$$

Equation (1.21) for r=1 obviously returns the Atzori-Lazzarin criterion, while for r=0.5 gives Lukáš-Klesnil criterion. Bazant [70] has shown in detail that the expression $(1+(a/a_0)^r)^{1/2r}$ is an asymptotic matching with truncation at the first order between the large-size ($a \gg a_0$) and the short-size ($a \ll a_0$) expansions of the crack propagation criterion in terms of stress intensity factor, concluding that El Haddad equation can

be interpreted as a "matching asymptotics" solution for the transition between fatigue endurance towards fatigue threshold dominated threshold.

The first modern reformulation of Neubers' idea is attributed to Tanaka [71]. The formulation is based on the assumption, confirmed by experimental evidence, that the stress that can be withstood at the notch root/crack tip without causing defect can be higher than $K_t \cdot S_{nom}$. Thus, Tanaka averaged the local stress ahead of the notch root/crack tip up to a distance $l_0=2a_0$

$$S_{l_0} = \frac{1}{l_0}\int_a^{a+l_0} S(x)\,dx \tag{1.22}$$

From this assumption, the effective stress intensity factor according to the TCD is

$$K_f = \frac{S_{l_0}}{S_{nom}} \tag{1.23}$$

Tanaka's model has been picked up and extended to other variants by Taylor who formulated *"a unifying theoretical model"* in 1999. Indeed, Taylor's extension of the TCD defines three variants: (i) point, (ii) line, and (iii) area. Considering the system as described in Figure 1.5, the stress according to the TCD is:

$$S_{l_0} = S(l_0) = S(½a_0) \quad \text{(POINT)} \tag{1.24}$$

$$S_{l_0} = \frac{1}{l_0}\int_a^{a+l_0} S(x)\,dx = \frac{1}{2a_0}\int_0^{2a_0} S(x+a)\,dx \quad \text{(LINE)} \tag{1.25}$$

$$S_{l_0} = \frac{2}{\pi\, a_0^2}\int_{-\frac{\pi}{2}}^{\frac{\pi}{2}}\int_0^{a_0} S(r)\,\varphi(\theta)\,r\,dr\,d\theta \quad \text{(AREA)} \tag{1.26}$$

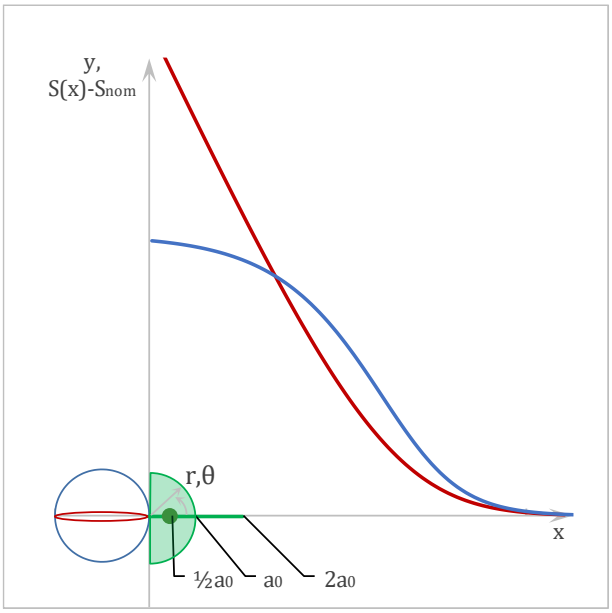

Figure 1.5: Stress field ahead of a crack (red) and of a circular notch(blue) for r, θ=0°. The green point, line and circle express the TCD process zones in its variants.

The design criterion just mentioned can be easily extended to finite life. This has been done by Susmel and Taylor [72]–[75] and by Ciavarella et al. [76] through similar, yet different approaches. The key assumption is postulating that the intrinsic crack size follows a power law of the number of cycles up to a critical value a_0^u defined as a function of the toughness and the fatigue strength at one cycle (or the ultimate tensile strength), i.e.

$$a_0^u = \frac{1}{\pi}\left(\frac{K_{Ic}}{S_f'}\right)^2 \tag{1.27}$$

Through this assumption the Atzori-Lazzarin diagram can be extended to finite life and a general S/N curve model valid for both crack and notches can be obtained. The model is described in Chapter 2. The validation has been done with experimental data available in Literature (from the SAE Keyhole test program [77]) both considering constant and variable amplitude loading.

1.4 Damage accumulation rules

The majority of the mechanical components undergo complex load histories in their operating life, called variable-amplitude (VA) loading. For this reason, VA life prediction still attracts the attention of engineers and researchers, indeed multiple damage models keep being proposed until very recently. Especially the most recent models tend to be more and more sophisticated; for example, in 2019 Susmel et al. [78] proposed a strain energy density based model to predict VA life of notched components. Another energy based method was recently (2018) proposed by Braccesi

et al. [79] to predict VA fatigue life in multiaxial stress state. The model is formulated in the frequency domain and converts the multiaxial stress state into an equivalent uniaxial Von Mises stress that is then used to perform the life prediction calculation. Going back to the basics, the simplest VA fatigue prediction rule has been proposed about a century ago (1924) by Palmgren [18] for the fatigue calculation of ball-bearings. Supposing that the load history consists of N_H cycles that have been counted through one of the multiple cycle-counting algorithms available in Literature. The counted cycles are then grouped into N_B load blocks, each one containing n_j cycles at the stress amplitude S_{aj} and the corresponding fatigue strength $N(S_{aj})=N_j$. Therefore, the damage rule is expressed as

$$D = \sum_{j=1}^{N_B} n_j/N_j = 1 \tag{1.28}$$

In other words, Palmgren postulated the linear accumulation of the fatigue damage, postulating that the failure occurs as the damage goes to unity without providing a derivation for the rule, and the same holds for Langer [80] that in 1937 postulated the same rule applied separately to the crack initiation and to the crack propagation phases. The first derivation of the linear damage accumulation rule has been formulated by Miner [81]. His hypothesis was that the work that can be adsorbed until failure is a constant value and that the amount of work adsorbed during n_j is directly proportional to n_j. Thus, said W the total work and w_j the work adsorbed during the block n_j, the criterion is $\Sigma_j w_j=W$. The use of Miner hypothesis ($n_j/N_j=w_j/W$) leads immediately to Equation (1.28). Miner conducted a series of tests on smooth and riveted 2024-T3 aluminum alloy sheet specimens by applying load histories having $2\leq N_B\leq 4$ and found $0.61\leq\Sigma_j n_j/N_j\leq 1.45$, very close to 1 on average. Since then the linear damage accumulation rule has been addressed very often as Miner's rule, but probably Palmgren-Miner's (PM) rule, is the more corrected form and it is how the rule will be called in this work. Since that time many works have been published to verify the PM rule and to find its limits of validity. For example, also the author, together with Ciavarella and Papangelo [82] has co-authored a work which will be dealt with in Chapter 4 where they show that the limit values of PM rule range from 0.001 to 10. Several theories that tried to overcome this limit and generalize the rule have been proposed. The most comprehensive overview of cumulative fatigue damage theories was published by Fatemi and Yang [83] in 1997. The authors identified eight categories of damage rules that they grouped in as many tables, some of which are listed hereafter:

- Phenomenologically based damage theories (work before 1970)

  To this period belong theories categorizable into five groups: the damage curve approach, endurance limit-based approach, S/N curve modification approach, two stage damage approach, and crack growth-based approach. The damage curve approach defines the damage curve by plotting damage D vs. cycle ratio n_j/N_j. Therefore, the damage curve of the PM rule simply corresponds to the bisector of the first quadrant. The major limitations of PM rule are: (i) no load level dependence, (ii) no load sequence dependence, (iii) no load interaction accountable. Marco and Starkey [84] proposed a load level dependent damage theory that modifies the damage curves at each level j, i.e.

$$D = \sum_{j=1}^{N_B} \left(\frac{n_j}{N_j}\right)^{\zeta_j} = 1 \tag{1.29}$$

  Where ζ_j varies at each level j.

  Concerning endurance limit reduction theories, they have been introduced to model the effect of residual stresses on the fatigue behavior, as stated by Kommers [85], [86]. The S/N curve modification has been used by Corten and Dolon [87] and by Freudenthal [88] to include load interaction effects. Basically, these methods correspond to a rotation of the power law around a point at low cycles. The first damage theory based on crack growth concept was presented by Valluri [89], [90]. The damage model is based on dislocation theory and elastoplastic fracture mechanics.

$$\frac{da}{dN} = C_V \, \varphi(S) \, a \tag{1.30}$$

- Refined double linear damage rule and refined damage curve approach

  The double linear damage rule (DLDR) basically defines a knee in the damage curve. In the refined version (R-DLDR) the knee point is derived from a first order series expansion of the damage curve approach (DCA) which was empirically formulated by Manson and Halford [91], [92]. Said a_i and a_f the initial and final crack length, the damage curve approach defines an effective crack growth depending on some material parameters β_1 and β_2, i.e.:

$$D_j = \frac{a_j}{a_f} = \frac{a_0}{a_f} + \left(1 - \frac{a_0}{a_f}\right) \cdot \left(\frac{n_j}{N_j}\right)^{\beta_1 N_j^{\beta_2}} \tag{1.31}$$

A comparison between some damage curves is provided Figure 1.6. It can be seen how the slope of the R-DLDR equals the first derivative of the DCA at the extremes.

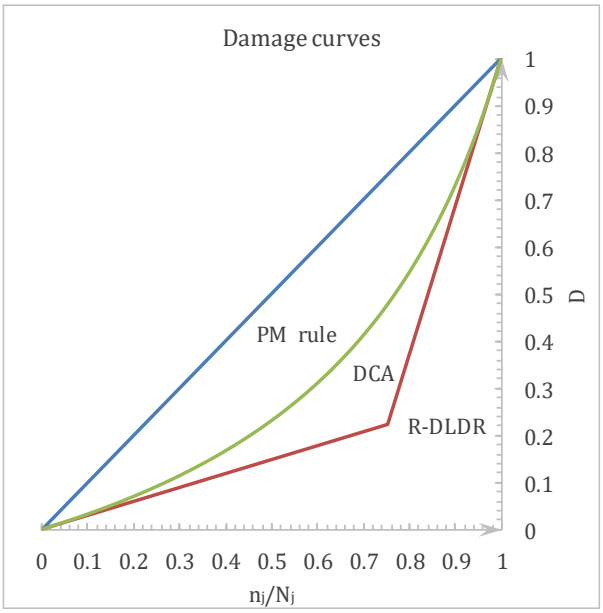

Figure 1.6: Comparison between the damage curves for linear damage rule (PM rule), damage curve approach (DCA) and refined double linear damage rule (R-DLDR)

- Theories using the crack growth concept

  Crack growth approaches have met a wide approval among the damage calculation theories because crack length is the simplest measure of damage. One of the most famous approaches in this direction was proposed by Barsom [93] and translates the VA load history in an equivalent CA load by calculating the root-mean-square of the stress intensity factor range, i.e. ΔK_{rms}

$$\Delta K_{rms} = 1/N_B \sqrt{\sum_{j=1}^{N_H} \Delta K_j^2} \tag{1.32}$$

  Where N_H is the total number of cycles in the load history. It is noteworthy that this empirical method does not require the cycles to be counted, and that it does not account for load sequence effects.

Tens of other cumulative fatigue damage theories have been described by Fatemi and Yang, based on the S/N curve modification approach [94]–[96], or energy-based [97], [98] or even continuum damage mechanics-based [99], [100].

Despite hundreds of damage accumulation theories have been proposed in the last decades, the PM rule remains by far the most used damage accumulation method. Maybe because of its simplicity, or maybe because no other simple rule has demonstrated to be more accurate without proper calibration or even because it has

been demonstrated that applying the PM rule corresponds to the integration of the Paris' law, which for its part still is widely used in crack propagation calculations. As regards this Thesis, the PM rule has been chosen because its application led to some interesting generalizations shown in Chapters 3 and 4.

1.5 Brief outline of regulatory aspects in rotorcrafts

The oldest method to perform fatigue tolerance evaluation of metallic rotorcraft structures is addressed as *safe life*. The expression is derived from the concept of safety by retirement, which means that the component is not allowed to show any defect that may weaken it below the design value during its entire lifespan. Safe life breaks down when loads are too high (usually high altitudes/speeds), when fatigue lives shall be extended (for economic reasons), or when stronger materials with poorer fatigue properties shall be used. A graphical representation of the safe life philosophy is given in Figure 1.7.

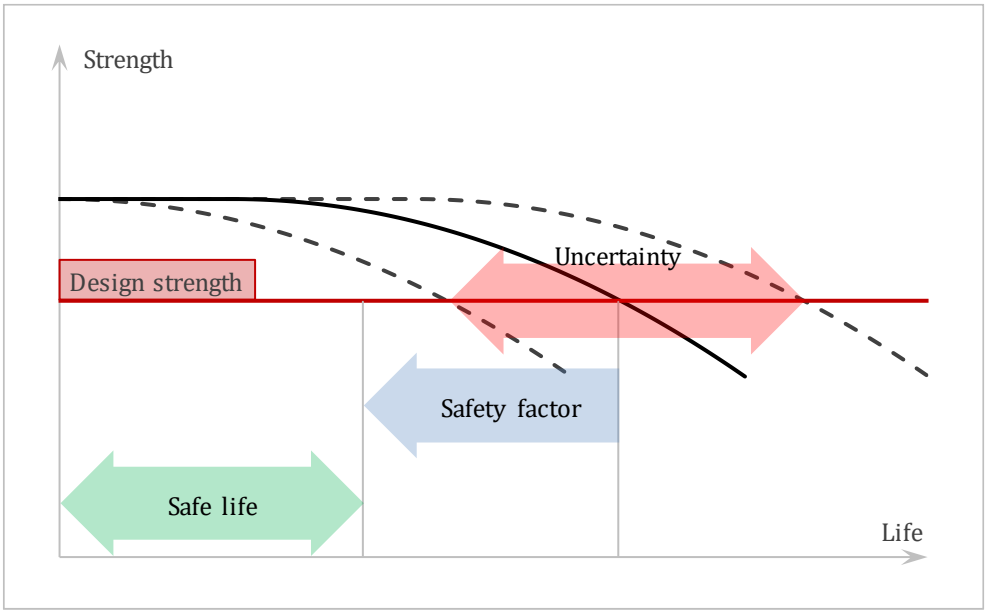

Figure 1.7: Strength vs. life plot showing the strength trend along the component lifespan and the safe life which must be lower than the "minimum expected life".

After the abovementioned Comet accidents, safe life design philosophy was integrated with a safe by design approach called *fail-safe*. According to this design philosophy, the structure must safely withstand the maximum load without catastrophic failure for all the time between two inspections, even after partial or total failure of one of its principal structural elements. Fail-safe structures must have some redundancies to do so. Obviously, redundancies imply higher weight, which makes the fail-safe design not optimal where not strictly necessary. For this reason, fail-safe has been integrated with the most modern design philosophy called *damage tolerance*, defined as the ability of the

structure to withstand fatigue loads, corrosion or accidental damage until such damage is detected through inspections or malfunctions and it is repaired. A damage tolerant structure is assumed to be flawed and the initial dimension of this defect corresponds conventionally to the maximum non-detectable flaw size. Such sizes are defined in the certification process and are listed, for each component, in a document called threat assessment. A hybrid philosophy between damage tolerance and safe life is addressed as flaw-tolerance safe life design [101], [102]. A flaw-tolerant structure is a safe life structure which can withstand fatigue loads for its entire lifetime even if a flaw (introduced by manufacturing, or inspection) is present. The Authorities (FAA, EASA) clearly state that the safe life design can be applied only after demonstrating that damage tolerance cannot be applied. Typically, in rotorcrafts this happens for the landing gears, main and tail rotor shafts, etc. Therefore, damage tolerance design philosophy is becoming progressively of widespread application, also under the pressure of the Airworthiness Authorities that, after the successful application to the military and commercial fixed wing world as well as to engines, are convinced that this is the gold standard to ensure safety against fatigue cracking and accidental damages. All the concepts just given, together with the duties regarding fatigue substantiation of a rotorcraft principal structural element (PSE), are detailly described in the Federal Aviation Administration (FAA), DOT rules 29.571 (for metals) and 29.573 (for damage tolerance and composites).

"***§ 29.571 Fatigue Tolerance Evaluation of Metallic Structure.***

(a) A fatigue tolerance evaluation of each principal structural element (PSE) must be performed, and appropriate inspections and retirement time or approved equivalent means must be established to avoid catastrophic failure during the operational life of the rotorcraft. The fatigue tolerance evaluation must consider the effects of both fatigue and the damage determined under paragraph (e)(4) of this section. Parts to be evaluated include PSEs of the rotors, rotor drive systems between the engines and rotor hubs, controls, fuselage, fixed and movable control surfaces, engine and transmission mountings, landing gear, and their related primary attachments.

(b) For the purposes of this section, the term:

(1) Catastrophic failure means an event that could prevent continued safe flight and landing

(2) Principal structural element (PSE) means a structural element that contributes significantly to the carriage of flight or ground loads, and the fatigue failure of that structural element could result in catastrophic failure of the aircraft.

(c) The methodology used to establish compliance with this section must be submitted to and approved by the Administrator.

(d) Considering all rotorcraft structure, structural elements, and assemblies, each PSE must be identified.

(e) Each fatigue tolerance evaluation required by this section must include:

(1) In-flight measurements to determine the fatigue loads or stresses for the PSEs identified in paragraph (d) of this section in all critical conditions throughout the range of design limitations required by § 29.309 (including altitude effects), except that maneuvering load factors need not exceed the maximum values expected in operations.

(2) The loading spectra as severe as those expected in operations based on loads or stresses determined under paragraph (e)(1) of this section, including external load operations, if applicable, and other high frequency power-cycle operations.

(3) Takeoff, landing, and taxi loads when evaluating the landing gear and other affected PSEs.

(4) For each PSE identified in paragraph (d) of this section, a threat assessment which includes a determination of the probable locations, types, and sizes of damage, taking into account fatigue, environmental effects, intrinsic and discrete flaws, or accidental damage that may occur during manufacture or operation.

(5) A determination of the fatigue tolerance characteristics for the PSE with the damage identified in paragraph (e)(4) of this section that supports the inspection and retirement times, or other approved equivalent means.

(6) Analyses supported by test evidence and, if available, service experience.

(f) A residual strength determination is required that substantiates the maximum damage size assumed in the fatigue tolerance evaluation. In determining inspection intervals based on damage growth, the residual strength evaluation must show that the remaining structure, after damage growth, is able to withstand design limit loads without failure.

(g) The effect of damage on stiffness, dynamic behavior, loads, and functional performance must be considered.

(h) Based on the requirements of this section, inspections and retirement times or approved equivalent means must be established to avoid catastrophic failure. The inspections and retirement times or approved equivalent means must be included in the Airworthiness Limitations Section of the Instructions for Continued Airworthiness required by Section 29.1529 and Section A29.4 of Appendix A of this part.

(i) If inspections for any of the damage types identified in paragraph (e)(4) of this section cannot be established within the limitations of geometry, inspectability, or good design practice, then supplemental procedures, in conjunction with the PSE retirement time, must

be established to minimize the risk of occurrence of these types of damage that could result in a catastrophic failure during the operational life of the rotorcraft.

[Doc. No. FAA-2009-0413, Amdt. 29-55, 76 FR 75442, Dec. 2, 2011]"

"***§ 29.573 Damage Tolerance and Fatigue Evaluation of Composite Rotorcraft Structures.***

(a) Each applicant must evaluate the composite rotorcraft structure under the damage tolerance standards of paragraph (d) of this section unless the applicant establishes that a damage tolerance evaluation is impractical within the limits of geometry, inspectability, and good design practice. If an applicant establishes that it is impractical within the limits of geometry, inspectability, and good design practice, the applicant must do a fatigue evaluation in accordance with paragraph (e) of this section.

(b) The methodology used to establish compliance with this section must be submitted to and approved by the Administrator.

(c) Definitions:

(1) Catastrophic failure is an event that could prevent continued safe flight and landing.

(2) Principal Structural Elements (PSEs) are structural elements that contribute significantly to the carrying of flight or ground loads, the failure of which could result in catastrophic failure of the rotorcraft.

(3) Threat Assessment is an assessment that specifies the locations, types, and sizes of damage, considering fatigue, environmental effects, intrinsic and discrete flaws, and impact or other accidental damage (including the discrete source of the accidental damage) that may occur during manufacture or operation.

(d) Damage Tolerance Evaluation:

(1) Each applicant must show that catastrophic failure due to static and fatigue loads, considering the intrinsic or discrete manufacturing defects or accidental damage, is avoided throughout the operational life or prescribed inspection intervals of the rotorcraft by performing damage tolerance evaluations of the strength of composite PSEs and other parts, detail design points, and fabrication techniques. Each applicant must account for the effects of material and process variability along with environmental conditions in the strength and fatigue evaluations. Each applicant must evaluate parts that include PSEs of the airframe, main and tail rotor drive systems, main and tail rotor blades and hubs, rotor controls, fixed and movable control surfaces, engine and transmission mountings, landing gear, other parts, detail design points, and fabrication techniques deemed critical by the FAA. Each damage tolerance evaluation must include:

(i) The identification of all PSEs;

(ii) In-flight and ground measurements for determining the loads or stresses for all PSEs for all critical conditions throughout the range of limits in § 29.309 (including altitude effects), except that maneuvering load factors need not exceed the maximum values expected in service;

(iii) The loading spectra as severe as those expected in service based on loads or stresses determined under paragraph (d)(1)(ii) of this section, including external load operations, if applicable, and other operations including high-torque events;

(iv) A threat assessment for all PSEs that specifies the locations, types, and sizes of damage, considering fatigue, environmental effects, intrinsic and discrete flaws, and impact or other accidental damage (including the discrete source of the accidental damage) that may occur during manufacture or operation; and

(v) An assessment of the residual strength and fatigue characteristics of all PSEs that supports the replacement times and inspection intervals established under paragraph (d)(2) of this section.

(2) Each applicant must establish replacement times, inspections, or other procedures for all PSEs to require the repair or replacement of damaged parts before a catastrophic failure. These replacement times, inspections, or other procedures must be included in the Airworthiness Limitations Section of the Instructions for Continued Airworthiness required by § 29.1529.

(i) Replacement times for PSEs must be determined by tests, or by analysis supported by tests, and must show that the structure is able to withstand the repeated loads of variable magnitude expected in-service. In establishing these replacement times, the following items must be considered:

(A) Damage identified in the threat assessment required by paragraph (d)(1)(iv) of this section;

(B) Maximum acceptable manufacturing defects and in-service damage (i.e., those that do not lower the residual strength below ultimate design loads and those that can be repaired to restore ultimate strength); and

(C) Ultimate load strength capability after applying repeated loads.

(ii) Inspection intervals for PSEs must be established to reveal any damage identified in the threat assessment required by paragraph (d)(1)(iv) of this section that may occur from fatigue or other in-service causes before such damage has grown to the extent that the component cannot sustain the required residual strength capability. In establishing these inspection intervals, the following items must be considered:

(A) The growth rate, including no-growth, of the damage under the repeated loads expected in-service determined by tests or analysis supported by tests;

(B) The required residual strength for the assumed damage established after considering the damage type, inspection interval, detectability of damage, and the techniques adopted for damage detection. The minimum required residual strength is limit load; and

(C) Whether the inspection will detect the damage growth before the minimum residual strength is reached and restored to ultimate load capability, or whether the component will require replacement.

(3) Each applicant must consider the effects of damage on stiffness, dynamic behavior, loads, and functional performance on all PSEs when substantiating the maximum assumed damage size and inspection interval.

(e) Fatigue Evaluation: If an applicant establishes that the damage tolerance evaluation described in paragraph (d) of this section is impractical within the limits of geometry,

inspectability, or good design practice, the applicant must do a fatigue evaluation of the particular composite rotorcraft structure and:

(1) Identify all PSEs considered in the fatigue evaluation;

(2) Identify the types of damage for all PSEs considered in the fatigue evaluation;

(3) Establish supplemental procedures to minimize the risk of catastrophic failure associated with the damages identified in paragraph (d) of this section; and

(4) Include these supplemental procedures in the Airworthiness Limitations section of the Instructions for Continued Airworthiness required by § 29.1529.

[Doc. No. FAA-2009-0660, Amdt. 29-59, 76 FR 74664, Dec. 1, 2011]"

Conclusion

All the basic concepts regarding the topics covered in this work have been given, alongside with a brief overview of regulatory aspects in rotorcrafts fatigue tolerance evaluation. Specifically, the reader now has a deeper insight of (i) two and four parameters S/N curve, (ii) constant and variable amplitude fatigue, (iii) damage accumulation rules, (iv) theory of the critical distances for crack/notch stress-life evaluation, (v) crack propagation, (vi) design philosophies.

References

[1] W. A. J. Albert, 'Uber Treibseile am Harz. Archiv fur Mineralogie, Georgnosie', *Bergbau Huttenkunde*, vol. 10, p. 215, 1837.

[2] J. V. Poncelet, *Introduction à la mécanique industrielle, physique ou expérimentale*. Thiel, 1839.

[3] W. J. M. Rankine, 'On the causes of the unexpected breakage of the journals of railway axles; and on the means of preventing such accidents by observing the law of continuity in their construction.', *Minutes Proc. Inst. Civ. Eng.*, vol. 2, no. 1843, pp. 105–107, Jan. 1843.

[4] J. O. York, 'Account of a series of experiments on the comparative strength of solid and hollow axles.', *Minutes Proc. Inst. Civ. Eng.*, vol. 2, no. 1843, pp. 89–91, Jan. 1843.

[5] C. Geach *et al.*, 'Discussion. a series of experiments on the comparative strength of solid and hollow axles.', *Minutes Proc. Inst. Civ. Eng.*, vol. 2, no. 1843, pp. 91–94, Jan. 1843.

[6] F. Braithwaite, C. W. Williams, D. K. Clark, J. Hawkshaw, H. Grissell, and J. Simpson, 'Discussion on the fatigue and consequent fracture of metals.', *Minutes Proc. Inst. Civ. Eng.*, vol. 13, no. 1854, pp. 467–475, Jan. 1854.

[7] P. Stopfl, 'Achsenbrüche an Lokomotiven, Tender und Wagen, ihre Erklärung und Beseitigung', *Org Eisenbahnw*, vol. 3, pp. 55–67, 1848.

[8] V. D. Eisenbahnverwaltung, *Organ für die Fortschritte des Eisenbahnwesens*. Springer, 1848.

[9] J. E. McConnell, 'On Railway Axles', *Proc Inst Mech Engrs*, vol. 1, pp. 13–27, 1849.

[10] J. E. McConnell, 'On the deterioration of railway axles', *Proc Inst Mech Engrs*, pp. 5–19, 1850.

[11] A. Wöhler, 'Bericht über die Versuche, welche auf der Königl. Niederschlesisch-Märkischen Eisenbahn mit Apparaten zum Messen der Biegung und Verdrehung von Eisenbahnwagen-Achsen während der Fahrt angestellt wurden', *Z. Für Bauwes.*, vol. 8, no. 1858, pp. 641–652, 1858.

[12] A. Wöhler, 'Versuche zur Ermittlung der auf die Eisenbahnwagenachsen einwirkenden Kräfte und die Widerstandsfähigkeit der Wagen-Achsen', *Z. Für Bauwes.*, vol. 10, no. 1860, pp. 583–614, 1860.

[13] 'Flaw Tolerant Safe-Life Methodology', SIKORSKY AIRCRAFT CORP STRATFORD CT, Feb. 2000.

[14] L. Spangenberg, *Über das verhalten der metalle bei wiederholten anstrengungen, etc.* Ernst & Korn, 1875.

[15] W. Kloth and T. Stroppel, 'Krafte, Beanspruchungen und Sicherheiten in den Landmaschinen', *Z-VDI*, vol. 80, p. 85, 1936.

[16] O. H. Basquin, 'The exponential law of endurance tests', in *Proc Am Soc Test Mater*, 1910, vol. 10, pp. 625–630.

[17] C. E. Stromeyer, 'The determination of fatigue limits under alternating stress conditions', *Proc. R. Soc. Lond. Ser. Contain. Pap. Math. Phys. Character*, vol. 90, no. 620, pp. 411–425, 1914.

[18] A. G. Palmgren, 'Die Lebensdauer von Kugellagern (Life Length of Roller Bearings. In German)', *Z. Vereines Dtsch. Ingenieure VDI Z. ISSN*, pp. 0341–7258, 1924.

[19] F. R. Shanley, 'A proposed mechanism of fatigue failure', in *Colloquium on Fatigue / Colloque de Fatigue / Kolloquium über Ermüdungsfestigkeit*, 1956, pp. 251–259.

[20] W. Weibull and F. K. G. Odqvist, *Colloquium on Fatigue / Colloque de Fatigue / Kolloquium über Ermüdungsfestigkeit: Stockholm May 25–27, 1955 Proceedings / Stockholm 25–*

27 Mai 1955 Comptes Rendus / Stockholm 25.–27. Mai 1955 Verhandlungen. Springer Science & Business Media, 2012.

[21] E. Epremian and R. F. Mehl, *Investigation of statistical nature of fatigue properties*. National Advisory Committee for Aeronautics, 1952.

[22] W. Weibull, W. Weibull, S. Physicist, W. Weibull, S. Physicien, and W. Weibull, *A statistical representation of fatigue failures in solids*. Elander, 1949.

[23] W. Weibull, 'Scatter in fatigue tests', in *Proc. Second ICAF Conf*, Stockholm, 1953, p. App. 2.

[24] W. Weibull, 'The propagation of fatigue cracks in light-alloy plates', in *Proc. Third ICAF Conf*, Cranfield, 1955, p. App. 3.

[25] W. Weibull, 'Scatter in fatigue life of 24S-T alclad plates', in *Proc. Third ICAF Conf*, Cranfield, 1955, p. App. 4.

[26] W. Weibull, 'Scatter of fatigue life and fatigue strength of aircraft materials', in *Proc. Fourth ICAF Conf.*, Zurich, 1956, p. Doc. 94.

[27] W. Weibull, 'New methods for computing parameters of complete or truncated distributions', Aeronautical Research Institute of Sweden, AMR 8 FFA Rep. 58, 1955.

[28] W. Weibull, 'Static strength and fatigue properties of threaded bolts', Aeronautical Research Institute of Sweden, FFA Rep. 59, 1955.

[29] W. Weibull, 'Effect of crack length and stress amplitude on growth of fatigue cracks', Aeronautical Research Institute of Sweden, FFA Rep. 65, 1956.

[30] W. Weibull, 'Static strength and fatigue properties of unnotched circular 75S-T specimens subjected to repeated tensile loading', Aeronautical Research Institute of Sweden, FFA Rep. 68, 1956.

[31] W. Weibull, 'Scatter of fatigue life and fatigue strength in aircraft structural materials and parts', Aeronautical Research Institute of Sweden, FFA Rep. 73, 1957.

[32] W. Weibull, *A statistical theory of strength of materials*. Stockholm: Generalstabens Litografisky Anstalts F6rlag, 1939.

[33] T. Yokobori, 'The statistical aspect of fatigue fracture of metals', *Title 東京大學理工學研究所報告*, vol. 8, no. 1, p. 5, 1954.

[34] P. A. Withey, 'Fatigue failure of the de Havilland comet I', *Eng. Fail. Anal.*, vol. 4, no. 2, pp. 147–154, 1997.

[35] P. A. Withey, 'Fatigue Failure of the De Havilland Comet I', in *Failure Analysis Case Studies II*, Elsevier, 2001, pp. 185–192.

[36] D. Lawson, *Engineering disasters*. 2005.

[37] N. E. Frost and D. S. Dugdale, 'The propagation of fatigue cracks in sheet specimens', *J. Mech. Phys. Solids*, vol. 6, no. 2, pp. 92–110, Jan. 1958.

[38] A. A. Griffith, 'VI. The phenomena of rupture and flow in solids', *Philos. Trans. R. Soc. Lond. Ser. Contain. Pap. Math. Phys. Character*, vol. 221, no. 582–593, pp. 163–198, 1921.

[39] C. E. Inglis, 'Stresses in a plate due to the presence of cracks and sharp corners', *Trans Inst Nav. Arch.*, vol. 55, pp. 219–241, 1913.

[40] F. Berto and P. Lazzarin, 'Recent developments in brittle and quasi-brittle failure assessment of engineering materials by means of local approaches', *Mater. Sci. Eng. R Rep.*, vol. 75, pp. 1–48, Jan. 2014.

[41] A. K. Head, 'XCVIII. The growth of fatigue cracks', *Lond. Edinb. Dublin Philos. Mag. J. Sci.*, vol. 44, no. 356, pp. 925–938, Sep. 1953.

[42] G. R. Irwin, 'Analysis of stresses and strains near the end of a crack transversing a plate', *Trans ASME Ser E J Appl Mech*, vol. 24, pp. 361–364, 1957.

[43] M. F. Ashby, 'Overview No. 80: On the engineering properties of materials', *Acta Metall.*, vol. 37, no. 5, pp. 1273–1293, May 1989.

[44] M. F. Ashby, *Materials Selection in Mechanical Design. PergamonPress*. Oxford—New York—Seoul—Tokyo, 1992.

[45] P. C. Paris and F. Erdogan, *A Critical Analysis of Crack Propagation Laws*. ASME, 1963.

[46] U. Zerbst, M. Vormwald, R. Pippan, H.-P. Gänser, C. Sarrazin-Baudoux, and M. Madia, 'About the fatigue crack propagation threshold of metals as a design criterion – A review', *Eng. Fract. Mech.*, vol. 153, pp. 190–243, Mar. 2016.

[47] K. Walker, 'The Effect of Stress Ratio During Crack Propagation and Fatigue for 2024-T3 and 7075-T6 Aluminum', *Eff. Environ. Complex Load Hist. Fatigue Life*, Jan. 1970.

[48] R. G. Forman, V. E. Kearney, and R. M. Engle, 'Numerical analysis of crack propagation in cyclic-loaded structures', *J. Basic Eng.*, vol. 89, no. 3, pp. 459–463, 1967.

[49] J. J. Newman, 'A crack opening stress equation for fatigue crack growth', *Int. J. Fract.*, vol. 24, no. 4, pp. R131–R135, 1984.

[50] S. R. S. Mettu, 'NASGRO 3.0: A Software for Analyzing Aging Aircraft', 1999.

[51] K. Tanaka, Y. Nakai, and M. Yamashita, 'Fatigue growth threshold of small cracks', *Int. J. Fract.*, vol. 17, no. 5, pp. 519–533, 1981.

[52] M. H. El Haddad, N. E. Dowling, T. H. Topper, and K. N. Smith, 'J integral applications for short fatigue cracks at notches', *Int. J. Fract.*, vol. 16, no. 1, pp. 15–30, 1980.

[53] B. Atzori and P. Lazzarin, 'Analisi delle problematiche connesse con la valutazione numerica della resistenza a fatica', in *AIAS National Conference, Lucca Italy, also Quaderno AIAS*, 2000, pp. 33–50.

[54] B. Atzori and P. Lazzarin, 'Notch Sensitivity and Defect Sensitivity under Fatigue Loading: Two Sides of the Same Medal', *Int. J. Fract.*, vol. 107, no. 1, pp. 1–8, Jan. 2001.

[55] B. Atzori, P. Lazzarin, and G. Meneghetti, 'Fracture mechanics and notch sensitivity', *Fatigue Fract. Eng. Mater. Struct.*, vol. 26, no. 3, pp. 257–267, 2003.

[56] B. Atzori, P. Lazzarin, and G. Meneghetti, 'A unified treatment of the mode I fatigue limit of components containing notches or defects', *Int. J. Fract.*, vol. 133, no. 1, pp. 61–87, Jan. 2005.

[57] H. Kitagawa and S. Takahashi, 'Applicability of fracture mechanics to very small cracks or the cracks in the early stage', in *Proc. of 2nd ICM, Cleveland, 1976*, 1976, pp. 627–631.

[58] D. O. Sprowls, M. B. Shumaker, J. D. Walsh, and J. W. Coursen, 'Evaluation of Stress Corrosion Cracking Susceptibility Using Fracture Mechanics Techniques, Part 1.[environmental tests of aluminum alloys, stainless steels, and titanium alloys]', 1973.

[59] K. Sadananda and S. Sarkar, 'Modified Kitagawa Diagram and Transition from Crack Nucleation to Crack Propagation', *Metall. Mater. Trans. A*, vol. 44, no. 3, pp. 1175–1189, Mar. 2013.

[60] D. Taylor, 'The theory of critical distances', *Eng. Fract. Mech.*, vol. 75, no. 7, pp. 1696–1705, 2008.

[61] W. Yao, K. Xia, and Y. Gu, 'On the fatigue notch factor, Kf', *Int. J. Fatigue*, vol. 17, no. 4, pp. 245–251, May 1995.

[62] H. Neuber, *Theory of notch stresses: Principles for exact stress calculation*, vol. 74. JW Edwards, 1946.

[63] P. Kuhn and H. F. Hardrath, 'An engineering method for estimating notch-size effect in fatigue tests on steel', National Advisory Committee for Aeronautics, Langley Field, Va, NACA Technical Note NACA-TR-2805, 1952.

[64] C. Kirsch, 'Die theorie der elastizitat und die bedurfnisse der festigkeitslehre', *Z. Vereines Dtsch. Ingenieure*, vol. 42, pp. 797–807, 1898.

[65] R. Peterson, Ed., *Manual on Fatigue Testing*. West Conshohocken, PA: ASTM International, 1949.

[66] T. Topper, R. M. Wetzel, and J. Morrow, 'Neuber's rule applied to fatigue of notched specimens', ILLINOIS UNIV AT URBANA DEPT OF THEORETICAL AND APPLIED MECHANICS, 1967.

[67] B. Atzori and P. Lazzarin, 'A three-dimensional graphical aid to analyze fatigue crack nucleation and propagation phases under fatigue limit conditions', *Int. J. Fract.*, vol. 118, no. 3, pp. 271–284, Dec. 2002.

[68] M. Ciavarella and G. Meneghetti, 'On fatigue limit in the presence of notches: classical vs. recent unified formulations', *Int. J. Fatigue*, vol. 26, no. 3, pp. 289–298, Mar. 2004.

[69] P. Lukáš and M. Klesnil, 'Fatigue limit of notched bodies', *Mater. Sci. Eng.*, vol. 34, no. 1, pp. 61–66, Jun. 1978.

[70] Z. P. Bazant, 'Scaling of quasibrittle fracture : asymptotic analysis', *Scaling Quasibrittle Fract. Asymptot. Anal.*, vol. 83, no. 1, pp. 19–40, 1997.

[71] K. Tanaka, 'Engineering formulae for fatigue strength reduction due to crack-like notches', *Int. J. Fract.*, vol. 22, no. 2, pp. R39–R46, 1983.

[72] L. Susmel and D. Taylor, 'A novel formulation of the theory of critical distances to estimate lifetime of notched components in the medium-cycle fatigue regime', *Fatigue Fract. Eng. Mater. Struct.*, vol. 30, no. 7, pp. 567–581, 2007.

[73] L. Susmel and D. Taylor, 'On the use of the Theory of Critical Distances to predict static failures in ductile metallic materials containing different geometrical features', *Eng. Fract. Mech.*, vol. 75, no. 15, pp. 4410–4421, Oct. 2008.

[74] L. Susmel and D. Taylor, 'The Theory of Critical Distances to estimate lifetime of notched components subjected to variable amplitude uniaxial fatigue loading', *Int. J. Fatigue*, vol. 33, no. 7, pp. 900–911, Jul. 2011.

[75] L. Susmel and D. Taylor, 'A critical distance/plane method to estimate finite life of notched components under variable amplitude uniaxial/multiaxial fatigue loading', *Int. J. Fatigue*, vol. 38, pp. 7–24, May 2012.

[76] M. Ciavarella, P. D'Antuono, and G. P. Demelio, 'Generalized definition of "crack-like" notches to finite life and SN curve transition from "crack-like" to "blunt notch" behavior', *Eng. Fract. Mech.*, vol. 179, pp. 154–164, Jun. 2017.

[77] L. Tucker and S. Bussa, 'The SAE Cumulative Fatigue Damage Test Program', *SAE Trans.*, vol. 84, pp. 198–248, 1975.

[78] L. Susmel, F. Berto, and Z. Hu, 'The Strain energy density to estimate lifetime of notched components subjected to variable amplitude fatigue loading', *Frat. Ed Integrità Strutt.*, vol. 13, no. 47, pp. 383–393, 2019.

[79] C. Braccesi, G. Morettini, F. Cianetti, and M. Palmieri, 'Development of a new simple energy method for life prediction in multiaxial fatigue', *Int. J. Fatigue*, vol. 112, pp. 1–8, Jul. 2018.

[80] B. F. Langer, 'Fatigue failure from stress cycles of varying amplitude', *J. Appl. Mech.*, vol. 59, pp. A160–A162, 1937.

[81] M. A. Miner, 'Cumulative Damage in Fatigue', *J. Appl. Mech.*, vol. 3, pp. 159–164, 1945.

[82] M. Ciavarella, P. D'antuono, and A. Papangelo, 'On the connection between Palmgren-Miner rule and crack propagation laws', *Fatigue Fract. Eng. Mater. Struct.*, vol. 41, no. 7, pp. 1469–1475, 2018.

[83] A. B. Fatemi and L. Yang, 'Cumulative fatigue damage and life prediction theories: a survey of the state of the art for homogeneous materials', 1998.

[84] S. M. Marco and W. L. Starkey, 'A concept of fatigue damage', *Trans Asme*, vol. 76, no. 4, pp. 627–632, 1954.

[85] J. B. Kommers, 'The effect of overstress in fatigue on the endurance life of steel', in *PROCEEDINGS-AMERICAN SOCIETY FOR TESTING AND MATERIALS*, 1945, vol. 45, pp. 532–541.

[86] J. A. Bennett, 'A study of the damaging effect of fatigue stressing on SAE X4130 steel, J', *Res. NBS*, vol. 37, p. 133, 1946.

[87] H. T. Corten and T. J. Dolan, 'Cumulative fatigue damage', in *Proceedings of the international conference on fatigue of metals*, 1956, vol. 1, pp. 235–242.

[88] A. M. Freudenthal, 'On stress interaction in fatigue and a cumulative damage rule', *J. Aerosp. Sci.*, vol. 26, no. 7, pp. 431–442, 1959.

[89] S. R. Valluri, 'A unified engineering theory of high stress level fatigue', California Institute of Technology, Graduate Aeronautical Labs, Pasadena, CA, 20, 1961.

[90] S. R. Valluri, 'A theory of cumulative damage in fatigue', United States Air Force, Aeronautical Research Laboratory, Office of Aerospace Research, ARL 182, 1961.

[91] S. S. Manson and G. R. Halford, 'Practical implementation of the double linear damage rule and damage curve approach for treating cumulative fatigue damage', *Int. J. Fract.*, vol. 17, no. 2, pp. 169–192, Apr. 1981.

[92] S. S. Manson and G. R. Halford, 'Correction: Practical implementation of the double linear damage rule and damage curve approach for treating cumulative fatigue damage', *Int. J. Fract.*, vol. 17, no. 4, pp. R35–R42, 1981.

[93] J. M. Barsom, 'Fatigue crack growth under variable-amplitude loading in various bridge steels', in *Fatigue Crack Growth Under Spectrum Loads*, ASTM International, 1976.

[94] H. H. E. Leipholz, T. Topper, and M. El Menoufy, 'Lifetime prediction for metallic components subjected to stochastic loading', *Comput. Struct.*, vol. 16, no. 1–4, pp. 499–507, 1983.

[95] H. H. E. Leipholz, 'Lifetime prediction for metallic specimens subjected to loading with varying intensity', *Comput. Struct.*, vol. 20, no. 1–3, pp. 239–246, 1985.

[96] H. H. E. Leipholz, 'On the modified sn curve for metal fatigue prediction and its experimental verification', *Eng. Fract. Mech.*, vol. 23, no. 3, pp. 495–505, 1986.

[97] D. Kujawski and F. Ellyin, 'A cumulative damage theory for fatigue crack initiation and propagation', *Int. J. Fatigue*, vol. 6, no. 2, pp. 83–88, 1984.

[98] B. N. Leis, 'A nonlinear history-dependent damage model for low cycle fatigue', in *Low Cycle Fatigue*, ASTM International, 1988.

[99] L. Kachanov, 'Rupture time under creep conditions', *Izv Akad Nauk SSSR*, vol. 8, pp. 26–31, 1958.

[100] Y. N. Rabotnov, 'Creep problems in structural members', 1969.

[101] L. Lazzeri and U. Mariani, 'Application of damage tolerance principles to the design of helicopters', *Int. J. Fatigue*, vol. 31, no. 6, pp. 1039–1045, 2009.

[102] D. O. Adams, 'Flaw tolerant safe-life methodology', SIKORSKY AIRCRAFT CORP STRATFORD CT, 2000.

2 “Crack like to blunt” notch S/N curve model

Introduction

In this Chapter the infinite life design philosophy of notched specimens is analyzed, then the same concepts are specialized to finite life design concepts in the context of the “Theory of the Critical Distances” to analyze the transition from “crack-like to blunt” notch. It is shown that a notched specimen behaves very similarly to a crack up to a certain number of fatigue cycles, then its fatigue behavior can be approximated with a plain specimen reduced by the effective stress concentration factor. Accordingly, some fast assessment methods have been suggested: (i) a crack like notch could be replaced by a crack for which there is a wide amount of solutions in Literature and (ii) a blunt notch could be treated through infinite life design concepts only. To verify the analytical method, the SAE Keyhole test program constant amplitude fatigue test data have been used and predictions are in good agreement with experiments, also compared with other methods as strain-life approaches through Neuber’s rule.

2.1 Infinite life design

The effect of notches in infinite life fatigue design can be simply estimated through the concept of crack like notch introduced by Smith and Miller [1] which allows to obtain characteristic diagrams [2]–[5] under the assumption that the governing factor for infinite life modeling is the threshold stress intensity factor range ΔK_{th}, value below which a so-called long crack should not propagate consistently with Paris’ law [6]. Indeed, infinite life fatigue design is governed by the threshold stress intensity factor range for long cracks, and by the fatigue limit stress range ΔS_e for short cracks [7]; hence in order to identify the order of magnitude of the critical length of transition from short to long crack, El-Haddad’s intrinsic defect size a_0 can be introduced

$$a_0 = \frac{1}{\pi}\left(\frac{\Delta K_{th}}{\Delta S_e}\right)^2 \tag{2.1}$$

The equation is given for a prescribed load ratio $R=S_{min}/S_{max}$. Such transition has been studied in principle experimentally in 1976 by Kitagawa and Takahashi [8] which

plotted stress range vs. crack size (ΔS-a) diagrams confirming the validity of the relation connecting the stress intensity factor range ΔK and the stress range ΔS

$$\Delta K = f \cdot \Delta S \sqrt{\pi a} \tag{2.2}$$

Where f is a geometric factor. Then, in 1977 Smith evidenced that Equation (2.2) is valid only beyond a specific value of crack size and later, in 1980, this limit was overcome by El Haddad et al. [9] who proposed the empirical formula

$$\Delta S_e = \Delta K_{th} / \sqrt{\pi (a + a_0)} \tag{2.3}$$

In which the intrinsic defect size has been simply added to Equation (2.2) and the geometric factor f has been set to 1 for simplicity. The idea behind Equation (2.3) is one aspect of the "Theory of the Critical Distances" whose ancestor, as summarized by Taylor [10], and Yao et al. [11], can be identified in the effective stress concentration factor K_f proposed by Neuber [12], Kuhn and Hardrath [13] who in the early '50s assumed that the notched specimen fails if the averaged stress over the distance A_{KH} ahead of the notch root is equal to the fatigue limit S_e of the plain specimen. From this hypothesis, K_f was calculated as

$$K_f = 1 + \frac{K_t - 1}{1 + \frac{\pi}{\pi - \omega} \sqrt{A_{KH}/\rho}} \tag{2.4}$$

Where K_t is the theoretical stress concentration factor (e.g. 3 for a circular hole in an infinite plate), ω is the notch flank angle, ϱ is the notch root radius and the distance A_{KH} depends on the material under exam. Later the equation has been modified as

$$K_f = 1 + \frac{K_t - 1}{1 + \sqrt{a_N/\rho}} \tag{2.5}$$

a_N is known as Neuber's material constant

Few years later Peterson [14] derived an equation based on the hypotheses that (i) the notched material fails if the point stress at a distance d_0 away from the notch root is at least equal to the fatigue strength of the plain specimen and (ii) the stress ahead of the notch root drops linearly up to d_0 obtaining

$$K_f = 1 + \frac{K_t - 1}{1 + a_P/\rho} \tag{2.6}$$

Where a_P is Peterson's material constant. Notwithstanding, as also confirmed by Topper et al. [15], as ϱ increases the fatigue limit is actually fully controlled by the theoretical stress concentration factor, thus $K_f \rightarrow K_t$ since $a_P/\varrho \rightarrow 0$ and the notch is

addressed as blunt notch. From a mathematical point of view, a notch can be effectively be addressed as blunt when its characteristic size a^* is [2]–[5]

$$a^* \geq K_t^2 \cdot a_0 \tag{2.7}$$

Hence, for instance for a hole in an infinite plate (K_t=3) this occurs when the circle radius is almost one order of magnitude larger than El Haddad's intrinsic defect size. For aluminum alloys and steels, typically a_0 is of the order of 10 μm and 100 μm respectively implying a^* of the order of 0.1 mm and 1 mm respectively which are typical orders of magnitude of drilled holes for riveting. Therefore, Atzori and Lazzarin suggested the following infinite life design criterion for notched components

$$K_f = \min\left(\sqrt{1 + a/a_0},\ K_t\right) \tag{2.8}$$

Combining Equation (2.7)with Equation (2.8) implies that below a^* notches behave like cracks, and above a^* they behave as blunt notches. In 2004, with the purpose of collecting and comparing exhaustively the existing notch sensitivity estimation models for infinite life design, Ciavarella and Meneghetti [16] reviewed a series of classical and modern approaches to the stress concentration factor estimate and concluded that Neuber's method [12] is the most conservative and accurate amongst the "classical" approaches whilst the Atzori-Lazzarin criterion is the most conservative yet easy-to-use between the "modern" ones. Moreover, they proposed the following modification to the Atzori-Lazzarin criterion of Equation (2.8) in order to make it consistent with Lukáš and Klesnil [17] discussion which can be interpreted as a modification of Neuber's rule including the effect of cyclic plasticity.

$$K_f = \min\left((1 + (a/a_0)^r)^{1/2r},\ K_t\right) \quad 0 < r \leq 1 \tag{2.9}$$

Equation (2.9) for r=1 obviously returns the Atzori-Lazzarin criterion, while for r=0.5 gives Lukáš-Klesnil criterion. Bazant [18] has shown in detail that the expression $(1+(a/a_0)^r)^{1/2r}$ corresponds to an asymptotic matching with truncation at the first order between the large-size ($a \gg a_0$) and the short-size ($a \ll a_0$) expansions of the crack propagation criterion in terms of stress intensity factor and concluded that the El-Haddad equation can be seen as a "matching asymptotics" solution for the transition between fatigue limit towards fatigue threshold dominated threshold. Nevertheless, Ciavarella and Meneghetti in their review did not discuss the implications of applying the "Theory of the Critical Distances"[10], [19]–[22] (TCD) in its point variant (TCD-P); this shall be done here since the transition from infinite to finite life design here proposed is based on the TCD-P. Anyway, since it has already been demonstrated that

Neuber's (2.5) and Peterson's (2.6) equations are prototypical critical distance approaches, a similar result with respect to Ciavarella and Meneghetti's is expected. Indeed, the basic hypothesis of the TCD-P is that the material fails when the stress at a distance $a_0/2$ from the notch root/crack tip reaches the fatigue strength of the plain material. For instance, considering the Kirsch solution [23] for an infinite plate with a circular hole under uniform remote tension S_{nom} and imposing that the stress S_Y parallel to S_{nom} at distance $r=a+a_0/2$ from the center of the hole is equal to the alternate fatigue limit S_e leads to

$$K_f = \frac{S_Y\left(a+\frac{a_0}{2}\right)}{S_{nom}} = \frac{S_e}{S_{nom}} = \frac{1}{2}\cdot\left(2+\left(\frac{a}{a+\frac{a_0}{2}}\right)^2+3\left(\frac{a}{a+\frac{a_0}{2}}\right)^4\right) \tag{2.10}$$

Returning the well-known $K_t=3$ for $a \gg a_0$. Similarly, considering Westergaard [24] solution for a crack immersed into an infinite plate and loaded perpendicularly to the crack flanks it results, at a distance $a_0/2$ from the crack tip

$$K_f = \frac{S_Y\left(\frac{a_0}{2}\right)}{S_{nom}} = \frac{S_e}{S_{nom}} = \cdot\frac{1+\frac{a_0/2}{a}}{\sqrt{\frac{a_0/2}{a}}\sqrt{2+\frac{a_0/2}{a}}} \tag{2.11}$$

Which goes to infinite for $a \gg a_0$. In Figure 2.1 on the left it is shown the normalized stress component S_Y/S_{nom} ahead of the crack tip/notch root for the Kirsch and Westergaard problems, while on the right there is a comparison between stress concentration factors according to different criteria. Atzori-Lazzarin criterion is extremely close to the TCD-P applied to Westergaard problem for $a<a^*$ and then it becomes constant for $a \geq a^*$ and at the same time it is comparable with the TCD-P applied to the Kirsch solution within the entire domain. However, there is a region where the TCD-P applied to Kirsch solution is more conservative than both Westergaard solution and the Atzori-Lazzarin criterion. This may sound counterintuitive, but comparing the stress gradient ahead of a hole (low) with the stress gradient ahead of a crack (high) provides a simple explanation; indeed, even if the stress immediately ahead of a hole is lower than the stress ahead of a crack, then at a certain distance the situation has to reverse to respect the global equilibrium, as evident from Figure 2.1 (Left).

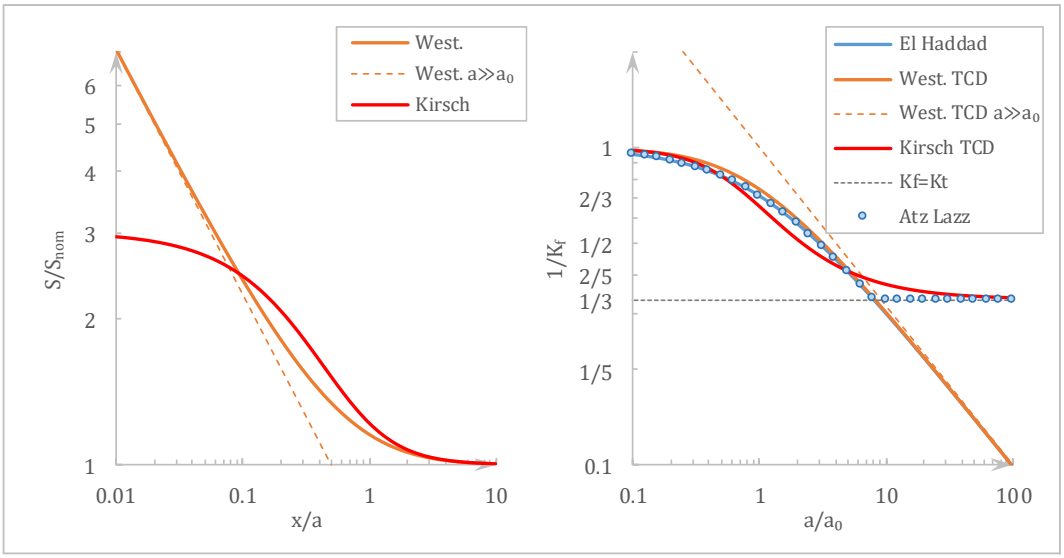

Figure 2.1: (Left) Stress field for Kirsch, Westergard and Westergaard for $a \gg a_0$; (Right) $1/K_f$ as a function of the notch/crack size. El Haddad's equation is nearly indistinguishable from Westergaard TCD. The Atzori-Lazzarin criterion for a hole is equal to El Haddad's equation up to a^*, beyond which it holds $1/K_t$ and it is comparable to Kirsch TCD

The infinite life design approach is useful when there are no other design constraints such as weight limits, but it becomes too limiting in aerospace applications, where the conflicting requirements of lightweight and durable structures must be simultaneously met. For this reason, it is convenient to extend the TCD-P design philosophy to finite life.

2.2 Finite life design

The extension to a finite life design for notched components leading to a generalized Kitagawa-Takahashi diagram has been approached in multiple ways by other authors [25]–[28], but all the approaches are usually less intuitive/straightforward than the corresponding ones for infinite life. As regards the stress-life approach (suitable for short cracks), the classical simplest technique to account for notch effect has been suggested by Fuchs and Stephens [29] in their Textbook, re-edited as Stephens et al. [30]. They suggested to account for the notch effect by using its infinite life effect, then they wrote that *"in the absence of other data, one can estimate the monotonic tensile strength of the notched part for a metal behaving in a ductile manner to be equal to the strength of the smooth part in monotonic testing"*. In other words, notch effect for short cracks can be modeled into an S/N curve by interpolating with a power law between the value $S_{e\text{-plain}}/K_f$ and the fatigue strength of the plain material at a prescribed number of cycles. Such number of cycles generally ranges from 1 to 1,000 cycles to failure, but it is not a general rule. Turning to more general proposals, Ciavarella [27] attempted a generalized finite life

form of the El Haddad equation, postulating a life dependent power law for the intrinsic defect size, i.e. $a_0=a_0(N)$ (life-dependent)

$$a_0(N) = \frac{1}{\pi}\left(\frac{\Delta K_{th}}{\Delta S_e}\right)^2 (N/N_e)^{2\left(\frac{1}{k}-\frac{1}{r}\right)} = A_C \cdot N^{Bc} \tag{2.12}$$

Where $B_C=2(1/k-1/r)$, $A_C=1/\pi\cdot(\Delta K_{th}/\Delta S_e)^2\cdot N_e^{-Bc}$, N_e is the number of cycles to the fatigue limit, $k = -1/\bar{b}$ is Basquin's law exponent and r is a material constant which could coincide with the Paris' law exponent since it has been introduced to the postulate the evolution of $\Delta K_{th}(N)= \Delta K_{th}\cdot(N_e/N)^{1/r}$. A very similar approach to the problem has been proposed by Susmel and Taylor [10], [19]–[22] in their TCD-P in which a life dependent power law evolution of the critical distance L/2 from the crack tip/notch root has been postulated, i.e.

$$L(N)/2 = A_{ST} \cdot N^{B_{ST}} \tag{2.13}$$

Where the constants A_{ST} and B_{ST} have similar meaning to A_C and B_C and can be determined both through experimental fitting of data from notched specimens and from basic material properties. Considering the derivation from the material properties, it is straightforward to define the power law from the El Haddad intrinsic defect size to the equivalent ultimate, or static, one

$$a_0^u = 1/\pi\left(\frac{K_{Ic}}{S'_f}\right)^2 \tag{2.14}$$

Where K_{Ic} is the mode I fracture toughness and S'_f is the fatigue strength at one cycle according to Basquin's law, i.e. $S = \bar{a}\, N^{\bar{b}}$. S'_f has been used instead of the ultimate tensile strength S_u since it is there's still another free parameter to be set: the number of cycles N_u where the a_0^u is assumed to hold. The definition of a_0^u incidentally leads to the definition of an extended Atzori-Lazzarin diagram to finite life (cfr. Figure 2.2) [4], [31], [32]. Atzori and Lazzarin in their conference paper proposal [31] were uncertain if the static failure line could have been always drawn by means of the linear elastic fracture mechanics, i.e. omitting geometric factors:

$$K_{Ic} = S_{nom}\sqrt{\pi\, a} \tag{2.15}$$

Consequently, they proposed the model only for brittle materials.

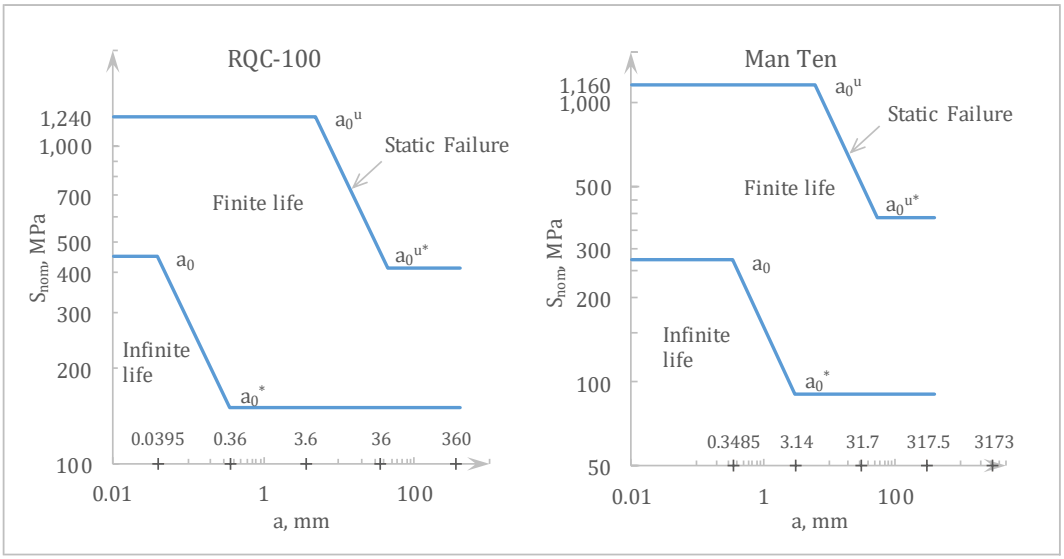

Figure 2.2: Extended Atzori-Lazzarin diagram to finite life considering a circular hole in an "infinite" plate. The materials considered are the RQC-100 steel (higher strength, low carbon, hot rolled, quenched and tempered) and Man Ten (medium carbon, lower strength, higher ductility). Observe that a_0 for RQC-100 is almost 10 times smaller than for Man Ten because of the difference in ductility

However, an experimental measure of the fracture toughness for ductile materials is very challenging, if not even impossible, because most probably in that case a_0^u would be too large and the specimen required to perform the tests would be excessively big. Concerning steels, as said the a_0 lies in the range of 10÷100 μm, whilst a_0^u is in the order of 1÷100 mm. In the current work, two very common steels close to the extremes of the ranges of a_0 have been used as reference: (i) the Bethlehem RQC-100 steel [33] (up to 0.21% carbon content, quenched, tempered and hot rolled) and (ii) the U.S. Man Ten steel [34] (up to 0.35% carbon content, hot rolled), whose properties are listed in Table 2.1. These material properties have been used to draw the finite life Atzori-Lazzarin diagrams in Figure 2.2. The TCD has been used lately also to predict with a certain level of accuracy the static failure of notched cold rolled low carbon steel and in presence of large plastic deformation before failure. Nonetheless, in order to state that the TCD is a fully established approach, a large number of tests is still needed on larger notch radii $a > a_0^u$ and even $a > a_0^{u*}$ and on a wider amount of material classes; for this reason, albeit accurate in the cases analyzed, the current linear elastic approach does not expect to supersede the elastoplastic fracture mechanics. It is however noteworthy that no other simple methods, including strain-life approach applied to notched geometries, give higher accuracy. Thus, in order to draw some conclusions regarding the generalized Atzori-Lazzarin diagram and criterion, some limit cases need to be analyzed and discussed.

Table 2.1: Material properties for RQC-100 and Man-Ten

Property Description	**RQC-100**	**Man Ten**
Elastic Modulus, E, GPa	203	203
Yield Strength, Y, MPa	883	325
Ultimate Strength, S_u, MPA	931	565
Fatigue Limit Strength Range, ΔS_e, MPa	449	272
Fatigue Strength Coefficient, S'_f, MPa	1,240	1,160
Threshold Stress Intensity Range, ΔK_{th}, MPa·√mm	158	285
Fracture Toughness, K_{Ic}, MPa·√mm	4,870	5,091
Fatigue Strength Exponent, b	-0.07	-0.095
Fatigue Ductility Coefficient, ε	1.06	0.26
Fatigue Ductility Exponent, c	-0.75	-0.47
Crack Growth Intercept, C, mm·cycle^{-1}	5.2E-9	3.0E-9
Crack Growth Exponent, m	3.15	3.43

The TCD has been used lately also to predict with a certain level of accuracy the static failure of notched cold rolled low carbon steel and in presence of large plastic deformation before failure. Nonetheless, in order to state that the TCD is a fully established approach, a large number of tests is still needed on larger notch radii $a > a_0^u$ and even $a > a_0^{u*}$ and on a wider amount of material classes; for this reason, albeit accurate in the cases analyzed, the current linear elastic approach does not expect to supersede the elastoplastic fracture mechanics. It is however noteworthy that no other simple methods, including strain-life approach applied to notched geometries, give higher accuracy. Thus, in order to draw some conclusions regarding the generalized Atzori-Lazzarin diagram and criterion, some limit cases need to be analyzed and discussed.

2.3 The crack-like notch

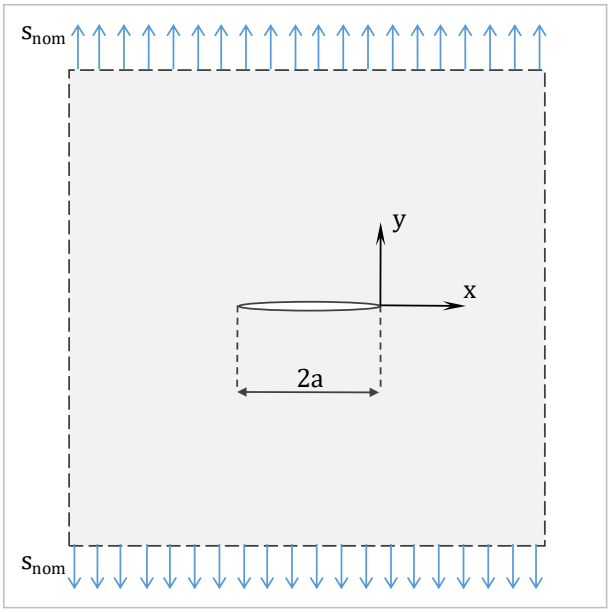

Figure 2.3: Large plate with central crack and remote nominal stress S_{nom}

Consider the very basic case of a large, conceptually infinite, plate having a central crack whose length is 2a, loaded in opening mode (I) by a nominal stress S_{nom} as shown in Figure 2.3. The fully analytical solution to the stress field of the plate has been found in 1934 through the usage of the Airy's stress function by Westergaard [35]. The asymptotic stress field in the region x>0, y=0 is given by

$$S(x) = \frac{K_I}{\sqrt{2\pi\, x}} = \frac{S_{nom}}{\sqrt{2\, x/a}} \tag{2.16}$$

Using the TCD-P implies moving at $a_0/2$ from the crack tip, i.e.

$$S(N) = \frac{S_{nom}}{\sqrt{\frac{A_{ST}}{a} N^{B_{ST}}}} \tag{2.17}$$

Postulating a power law evolution for $a_0(N)$ between a low number of cycles N_u and a high number of cycles N_e gives

$$\begin{aligned} a_0 &= \frac{1}{\pi}\left(\frac{\Delta K_{th}}{\Delta S_e}\right)^2 \quad (a) \\ a_0^u &= \frac{1}{\pi}\left(\frac{K_{Ic}}{S'_f}\right)^2 \quad (b) \end{aligned} \tag{2.18}$$

From which the constants A_{ST} and B_{ST} are easily found as

$$\begin{aligned} B_{ST} &= 2\,\frac{\mathrm{Log}(\Delta K_{th}/K_{Ic}) + \mathrm{Log}(S'_f/\Delta S_e)}{\mathrm{Log}(N_e/N_u)} \quad (a) \\ A_{ST} &= a_0\, N^{-B_{ST}} \quad (b) \end{aligned} \tag{2.19}$$

If the plain material stress-life behavior follows Basquin's law (at fixed load ratio) $S^kN=C_B$, it implies that also the also the stress-life behavior of the "asymptotic crack" is a power law

$$S_{nom}^{k_{ST}}\, N = C_{ST} \tag{2.20}$$

Where $k_{ST} = \frac{k}{1-B_{ST}\,k/2}$ and $C_{ST} = \left(\left(\frac{a}{A_{ST}}\right)^{\frac{k}{2}} 1/C_B\right)^{\frac{k_{ST}}{k}}$ meaning that if $B_{ST}\neq 0$ then $k_{ST}\neq k$. The latter can be valid only if a_0 is constant. Turning to the full Westergaard solution for the opening stress ahead of the crack tip

$$S(x) = \frac{S_{nom}\,(x/a+1)}{\sqrt{x/a}\sqrt{x/a+2}} \tag{2.21}$$

Which obviously tends to Equation (2.16) when $x \ll a$. Substituting (2.13) into (2.21) and then within Basquin's law, leads to the complete S/N curve for a crack

$$\left(\frac{S_{nom}\left(\frac{A_{ST}}{2a}N^{B_{ST}}+1\right)}{\sqrt{\frac{A_{ST}}{2a}N^{B_{ST}}}\sqrt{\frac{A_{ST}}{2a}N^{B_{ST}}+2}}\right)^{k} N = \left(S_{nom}\,\kappa_W(N)\right)^{k} N = C_B \tag{2.22}$$

Where the Greek symbol $\varkappa$ represents a sort of life dependent stress concentration factor Equation (2.22) is an implicit function of the number of cycles and tends to Equation (2.20) for a N higher than a certain number of cycles N^*, as shown in Figure 2.4, where also the Basquin's law for the corresponding plain specimen is plotted. In the cases under exam a=4.75 mm and the transitions to blunt notch behavior occur at ca. $10^4 \div 10^5$ cycles for RQC-100 and $10^5 \div 10^6$ cycles for Man Ten.

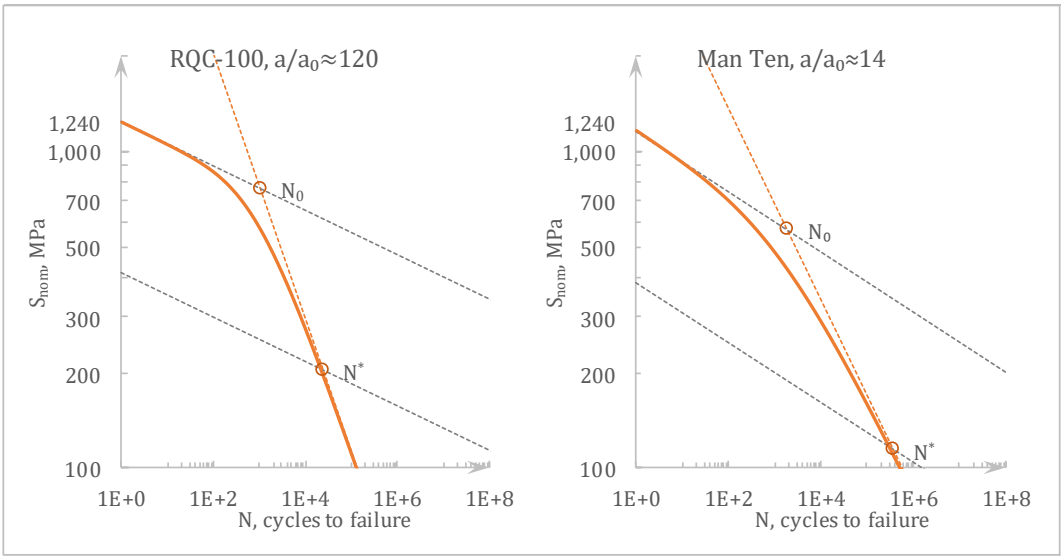

Figure 2.4: The dashed dark gray lines represent the S/N curve for the plain specimen and the same curve reduced by K_t. The orange dashed curve represents the asymptotic S/N curve for a cracked body by means of the TCD-P. Finally, the solid curve is the full S/N curve for a cracked body according to the TCD-P

It is noteworthy that the Basquin's law has not been truncated here neither at the ultimate tensile strength nor at the fatigue limit. Basquin's truncated law will be dealt

with in detail in Chapter 5. By intersecting the Basquin's law for the smooth specimen with the Basquin's law for the "asymptotic crack" the value of N_0 is obtained as

$$N_0 = \left(\frac{a}{A_{ST}}\right)^{\frac{1}{B_{ST}}} \tag{2.23}$$

Since $B_{ST}<0$, N_0 and N^* must decrease as the semi-crack length a increases as intuitively expected from the observation of the change of slope of the orange solid line in Figure 2.4, hence the corresponding stress $S(N_0)$ (and $S(N^*)$) must increase as the crack size is decreased, i.e.:

$$S(N_0) = C_B \left(\frac{a}{A_{ST}}\right)^{-\frac{1}{kB_{ST}}} \tag{2.24}$$

2.4 The transition to blunt notch

The transition from crack like to blunt notch behavior occurs, considering Figure 2.4, at around N^* cycles, i.e.

$$N^* = \left(\frac{a}{K_t^2\, A_{ST}}\right)^{\frac{1}{B_{ST}}} = \frac{N_0}{K_t^{2/B_{ST}}} = N_e \left(\frac{a}{K_t^2\, a_0}\right)^{\frac{1}{B_{ST}}} = N_e \left(\frac{a}{a^*}\right)^{\frac{1}{B_{ST}}} \tag{2.25}$$

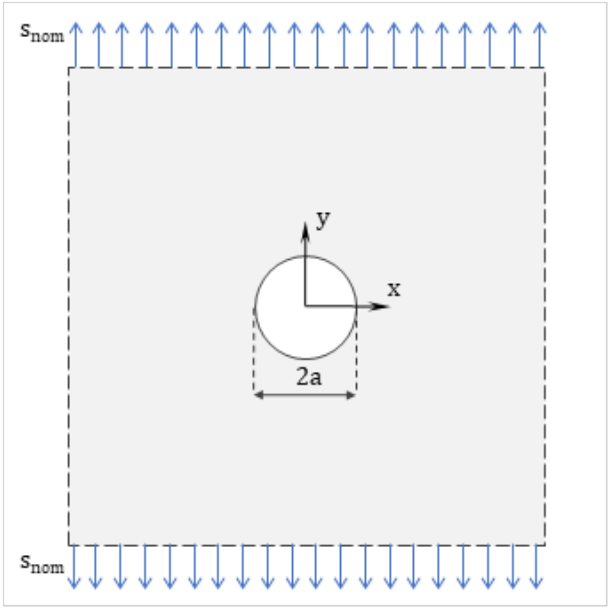

Figure 2.5: Large plate with central hole and remote nominal stress S_{nom}

Equation (2.25) confirms that the transition can occur only if $a>a^*=K_t^2 a_0$; after such point the notch behaves as blunt, extending the Atzori-Lazzarin definition to finite life. Specifically, if the notch is larger than a^*, then for $N>N^*$ the S/N curve for the notched specimen can be approximated with the Basquin's law for the plain specimen reduced by K_t. For instance, considering a circular notch and using the analytical solution to the Kirsch [23] problem (cfr. Figure 2.5rewritten by means of the the TCD-P (cfr. Equation (2.10)) into Basquin's law to reduce the S/N curve by a life- dependent K_t leads to another implicit function of N.

$$\left(S_{nom}\frac{1}{2}\cdot\left(2+\left(\frac{a}{a+\frac{a_0}{2}}\right)^2+3\left(\frac{a}{a+\frac{a_0}{2}}\right)^4\right)\right)^k N=\left(S_{nom}\,\kappa_K(N)\right)^k N=C_B \quad (2.26)$$

It is important to note that Equations (2.22) and (2.26) written in general form as

$$\left(S_{nom}\,\kappa(N)\right)^k N=C_B \quad (2.27)$$

can be used for a much wider range of application than the simple cases from which they have been derived, indeed, deviations from these expressions ahead of a crack or a notch occur at a higher distance with respect to what is required by the TCD. Therefore, this model, despite being simple, has provided satisfactory estimates in an example that nominally should is very different from the ideal cases used to derive Equation (2.27).

2.5 New S/N curve model for notches

The TCD-P allows to draw multiple S/N curves whose shape changes based on the ratio a/a_0. Figure 2.6 and Figure 2.7 show some example for RQC-100 and Man Ten respectively considering the notch sizes evidenced in the extended Atzori-Lazzarin diagrams of Figure 2.2.

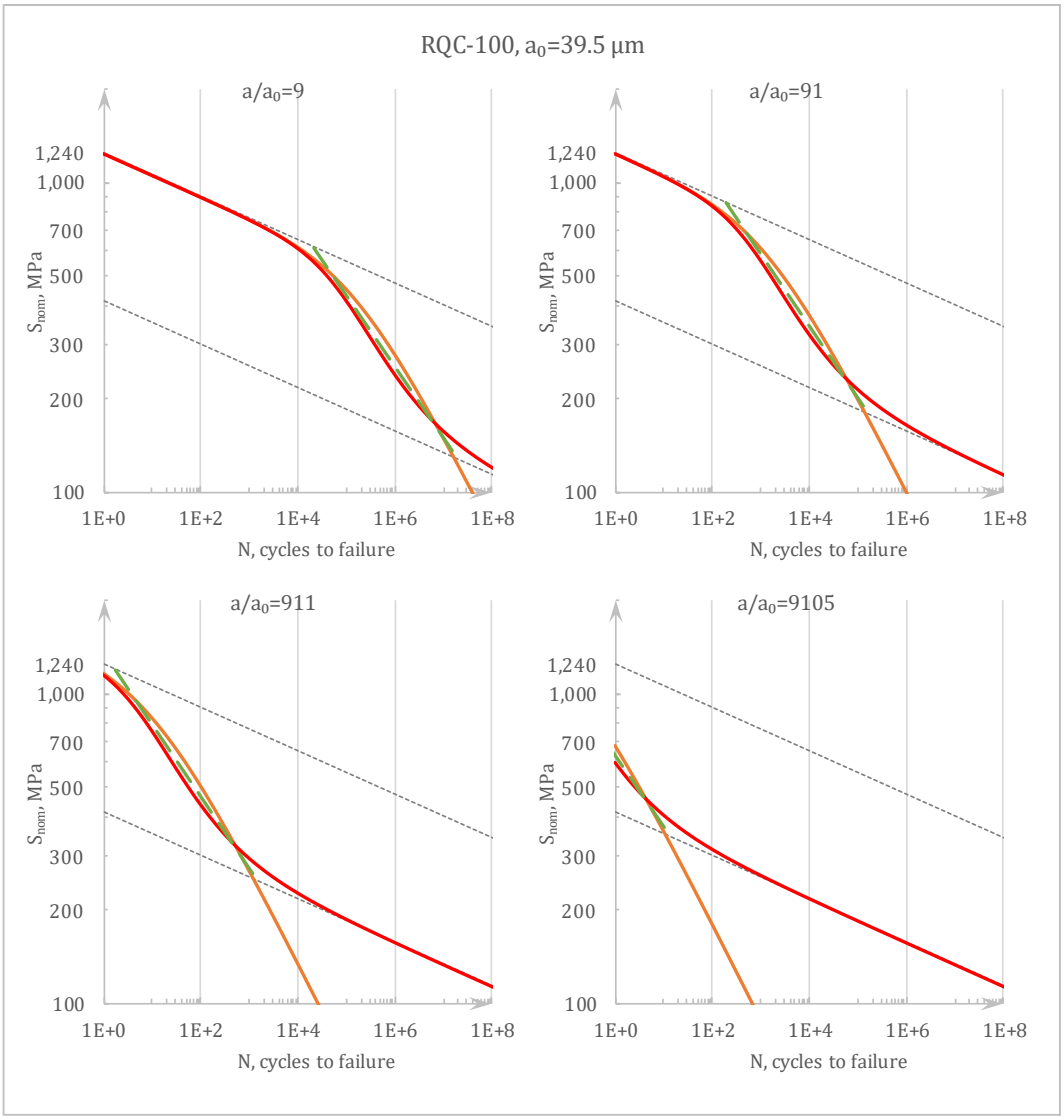

Figure 2.6: RQC-100 S/N curves obtained with increasing notch/crack size. The TCD-P curve with Westergaard solution (orange) is nearly indistinguishable from the TCD-P curve with Kirsch solution (red). The green dashed line is a power law drawn between $N_0/10$ and N^*

Evidently, in first approximation the behavior of the notch and of the crack in the crack like region are almost identical, similarly to what happens in the Atzori-Lazzarin criterion for infinite life under similar conditions. Conversely, at around N^* cycles there is the transition to blunt notch behavior where the "Kirsch" curve behaves similarly to the Basquin's law reduced by K_t. Thus, the new curve follows the S/N curve for the crack up to N^*, then the Basquin's law reduced by K_t should be used.

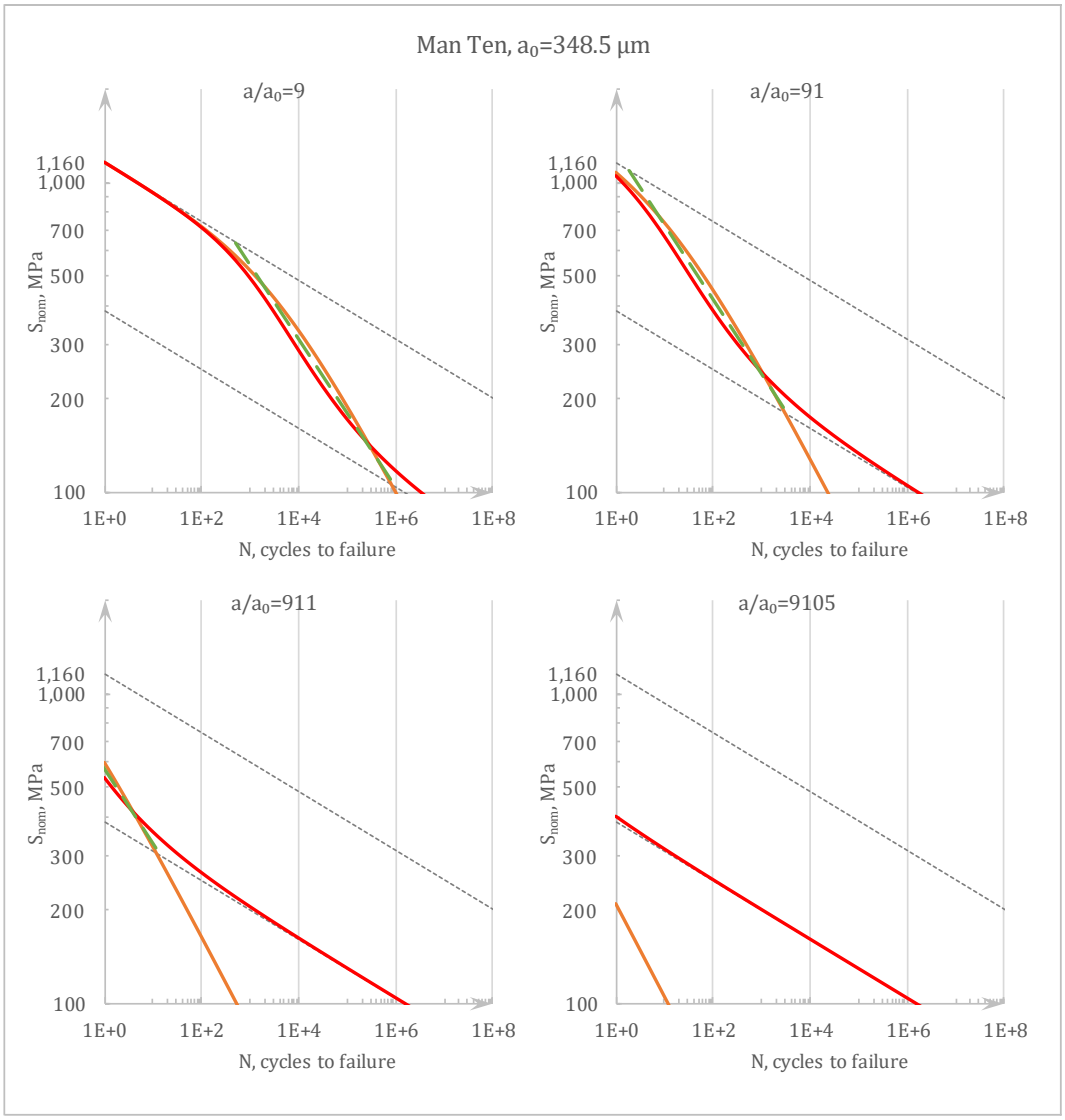

Figure 2.7: Man Ten: S/N curves obtained with increasing notch/crack size. The TCD-P curve with Westergaard solution (orange) is nearly indistinguishable from the TCD-P curve with Kirsch solution (red). The green dashed line is a power law drawn between $N_0/10$

Figure 2.6 and Figure 2.7 confirm Equation (2.25), i.e. the blunt notch region increases as the notch size is increased and for extremely large notches the S/N curve coincides with the reduced Basquin's law. The S/N curves for the circular hole slightly deviate from the S/N curve for the "asymptotic crack". Such difference can accounted for by defining a steeper power law curve between N_0/η (on the Basquin curve) and N^* (on the reduced Basquin curve); using η=10 leads to the green dashed lines in Figure 2.6 and Figure 2.7. A simple proposal, therefore, in the spirit of being conservative in line with the Atzori-Lazzarin criterion for infinite life, would be to take this power law for crack-like and the reduced Basquin's law in the blunt notch region. Clearly at N_e the long crack threshold should be considered, and this may induce a knee in the piecewise power law S/N curve even for materials which do not show a knee in the smooth S/N

curve. In fact, light alloys without a precise fatigue limit are known, but even these still have a fatigue threshold.

2.6 Quantitative validation with experiments

In the 1970s, the Society of Automotive Engineers (SAE) Fatigue Design & Evaluation Committee conducted a test program using a notched member with two steels commonly used in the ground vehicle industry (Bethlehem RQC-100 and U.S. Steel Man-Ten). The test program is explained in details by Tucker and Bussa [36] and in the website https://www.efatigue.com/benchmarks/ under "SAE Keyhole Test Program", finally test program and analysis are described in the book [20]. Most basic material properties were measured for both materials (listed in Table 2.1) and constant amplitude tests were performed on the "component like" specimen, although the main scope of the test program was variable amplitude fatigue testing using three loading histories at several load levels. In fact, many different prediction models for constant and variable amplitude fatigue life have been collected in the SAE Transactions Vol. 84, 1975, § 1. For example, Landgraf et al. [37] and Potter [38] adopted a strain-life approach through Neuber's rule [39] whilst Nelson and Fuchs [40] decided to work with stress-life models called nominal stress range I and II methods. In this work, a strain-life method is used to compare TCD-P the constant amplitude fatigue predictions and make some final considerations.

2.6.1 Calibration of TCD-P constants

As already mentioned, there is a free parameter in the model: N_u, i.e. the number of cycles adopted as upper bound for $a_0(N)$, i.e. $a_0^u=a_0(N_u)$. In the cases under exam N_u has been set to 1,000 cycles both for RQC-100 and for Man-Ten, which implies that $a_0^u=1/\pi\cdot(4{,}870/1{,}240)^2=4.91$ mm and $a_0^u=1/\pi\cdot(5{,}091/1{,}160)^2=6.13$ mm respectively. N_u is the only fitting parameter the required by the model and it should be calibrated through best fitting technique. Other authors also have to recur to similar assumptions when calibrating the constants of the TCD method for finite life [19]. Notice that the plots here presented have not been truncated below N_u and above N_e for cleanliness, albeit some truncations should be considered to have more precise plots. Thereupon, the TCD-P constants are:

$$B_{ST} = 2\,\frac{\mathrm{Log}(158/4{,}870) + \mathrm{Log}(1{,}240/449)}{\mathrm{Log}(10^6/10^3)} \approx -0.70 \quad \text{(a)}$$

$$A_{ST} = \frac{1}{\pi}\left(\frac{158}{449}\right)^2 \cdot 10^{6^{0.70}} \approx 610\ \text{mm} \quad \text{(b)}$$

RQC-100(2.28)

$$B_{ST} = 2\,\frac{\mathrm{Log}(284/5{,}091) + \mathrm{Log}(1{,}160/272)}{\mathrm{Log}(10^6/10^3)} \approx -0.41 \quad \text{(a)}$$

$$A_{ST} = \frac{1}{\pi}\left(\frac{285}{272}\right)^2 \cdot 10^{6^{0.42}} \approx 100\ \text{mm} \quad \text{(b)}$$

Man Ten(2.29)

Notice that, using Ciavarella's proposal [27] and taking r equal to the Paris' law exponent, the constants would be comparable for Man Ten but quite different for RQC-100:

$$B_C = 2\left(\frac{1}{14.28} - \frac{1}{3.15}\right) \approx -0.50 \quad \text{(a)}$$

$$A_C = \frac{1}{\pi}\left(\frac{158}{449}\right)^2 \cdot 10^{6^{0.50}} \approx 40\ \text{mm} \quad \text{(b)}$$

RQC-100(2.30)

$$B_C = 2\left(\frac{1}{10.53} - \frac{1}{3.43}\right) \approx -0.40 \quad \text{(a)}$$

$$A_C = \frac{1}{\pi}\left(\frac{285}{272}\right)^2 \cdot 10^{6^{-0.40}} \approx 74\ \text{mm} \quad \text{(b)}$$

Man Ten(2.31)

In order to have A_C and B_C equal to A_{ST} and B_{ST}, the exponent r should be equal to 2.4 for RQC-100 and 3.3 for Man Ten.

2.6.2 Stress field

The specimen geometry and the test setup the SAE keyhole test program is provided in Figure 2.8, whilst the load set is given in Figure 2.9. Some considerations on the stress field ahead of the notch are necessary since the geometry is very different from the ideal cases considered in the derivation of the equations. From the load set adopted, a nominal stress S_{nom} can be defined for convenience by "cutting" a beam shaped section immediately ahead of the crack tip and by writing the tensile stress from a combined axial-bending load (cfr. Figure 2.9). Concerning the blunt notch region, the presence of the circular notch theoretically raises the stress of a K_t=3 at the notch root. Furthermore, from comparison with finite elements analysis it is observed that a significant part of the stress field is like the Kirsch solution since the critical distance where the stress is computed lies between $4.9 \le a_0^u \le 6.1$ mm (cfr. Figure 2.10) which is comparable with the radius of the hole and much smaller than the width of the beam W.

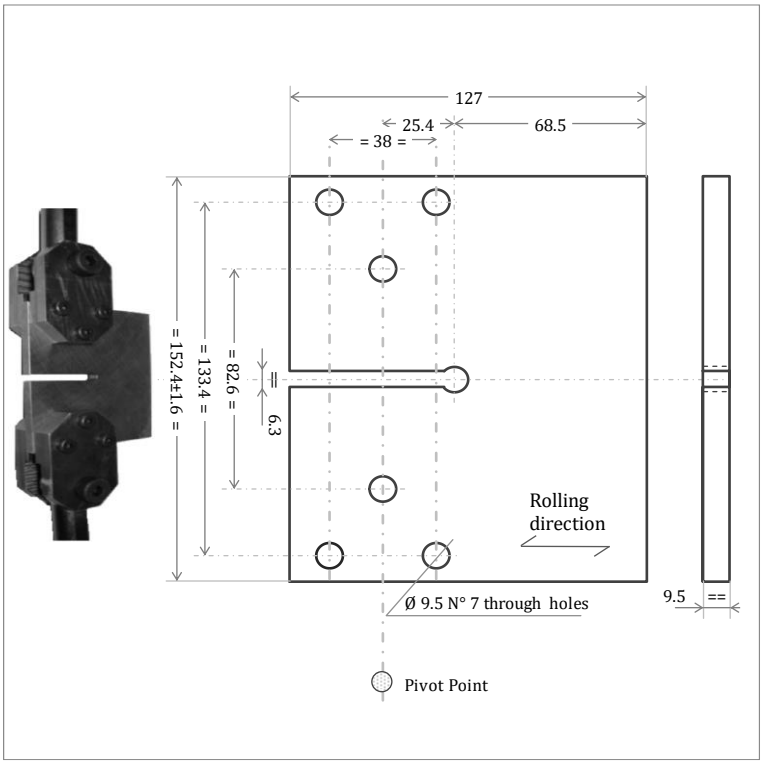

Figure 2.8: SAE keyhole test specimen: (Left) experiment setup and (Right) dimensioned drawing. Units in mm

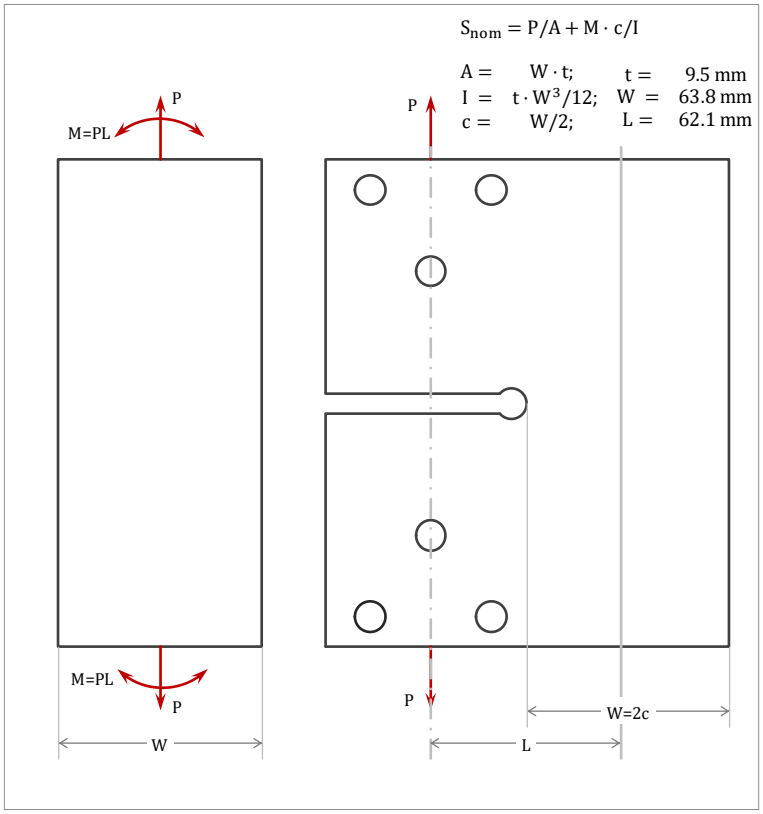

Figure 2.9: SAE Keyhole test specimen: load set. The nominal stress has been calculated through the beam on the left

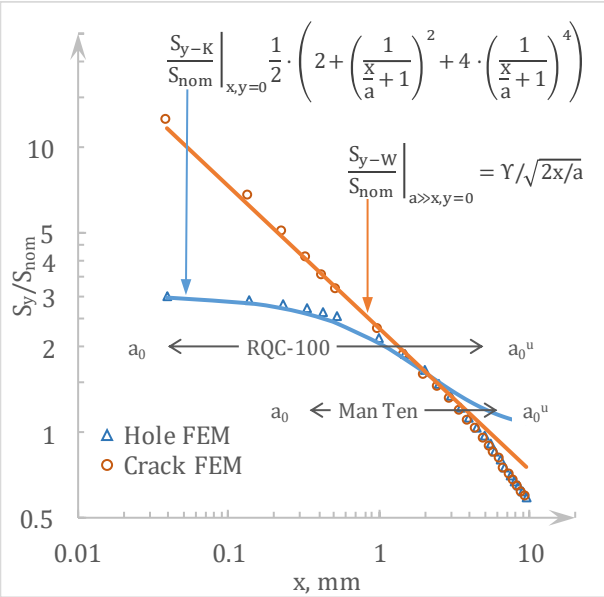

Figure 2.10: Opening stress ahead of the SAE Keyhole specimen (blue ttriangles) compared with Kirsh solution (solid blue), and opening stress ahead of a crack (orange circles) compared with the asymptotic Westergaard solution for the load set shown in Figure 2.9

Obviously at large distances from the notch root the finite elements solution diverges from the ideal notch but, in the range of interest of this model, Kirsch solution is more than appropriate (again cfr. Figure 2.10). As regards the crack-like behavior, the notch is abruptly substituted by a crack in the finite elements model and the stress intensity factor is then estimated via Ansys, obtaining $K_I=\Upsilon\cdot S_{nom}(\pi a)^{1/2}$, with , with $\Upsilon=1.36$. Again, the distance between the numerical and the asymptotic stress increases as the distance from the crack tip increases, but it is acceptable up to a_0^u for both RQC-100 and Man Ten. Then, with the only assumption that $N_u=1000$, the values of beginning for the crack like region N_0 and the transition to blunt notch N^* can be obtained from Equation (2.23) and (2.25) and the full S/N curve to predict the notch constant amplitufe behavior through the TCD-P can be drawn. The predictions in an S/N plot are shown in Figure 2.11 for RQC-100 (Left) and Man Ten (Right).

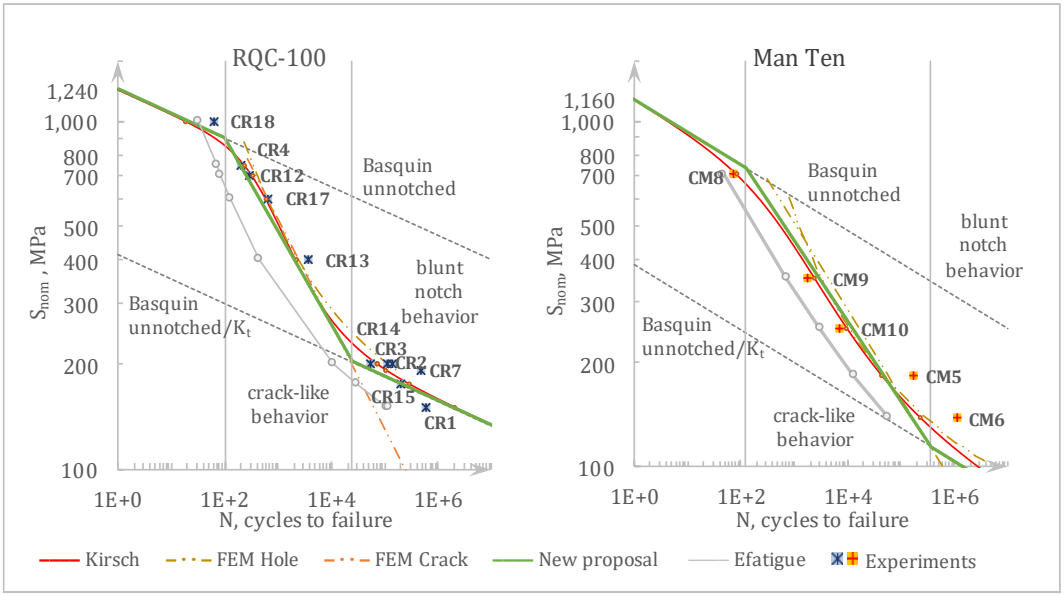

Figure 2.11: SAE Keyhole test program: comparison of experimental data for constant amplitude fatigue of the RQC-100 (Left) and Man Ten (Right) specimen with the proposed TCD-P based model for notched or cracked specimen. (Left) Strain-life predictions are added to show. The alphanumeric code next to the experiment represents the type of loas history, the material and the applied load

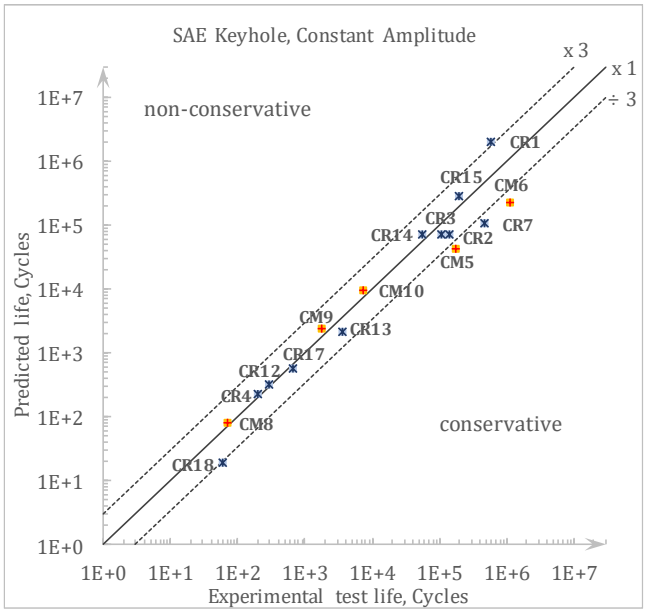

Figure 2.12: SAE Keyhole test program: Comparison of predictions and test results for constant amplitude loading. The accuracy is always within a factor 3 and almost always in the conservative half of the plane

Results are satisfactory and tendentially conservative, as also shown in Figure 2.12. The use of the actual stress profile from finite elements analysis would not improve significantly the fitting capabilities of the method. A simple suggestion to simplify the model could be to assume a power law behavior also in the crack like region from N_0/η up to N^* on the reduced Basquin's law. For this problem η=10 for both materials, but the factor can vary in other cases. Besides, a strain-life analysis has been performed through the website Efatigue which uses the full Coffin-Manson model with Neuber's rule. Predictions are much poorer than the ones with the current model.

Conclusion

It has been shown that the S/N curves obtained through the TCD-P for a crack and a notch are very close each other within a certain range of medium cycle fatigue life. Such region, denominated crack like behavior of the notch then undergoes a transition to another regime addressed as blunt notch, i.e. where the fatigue resistance is very close to the Basquin's law reduced by the stress concentration factor. This allows to define some conservative and accurate design criteria which have been proven to be very satisfactory when compared to the experimental data from the SAE Keyhole test program once the only free parameter of the model has been calibrated. The model here proposed is going to be combined with the one in the following Chapter to define a variable amplitude fatigue criterion for the life prediction of notched members.

References

[1] R. A. Smith and K. J. Miller, 'Prediction of fatigue regimes in notched components', *Int. J. Mech. Sci.*, vol. 20, no. 4, pp. 201–206, 1978.

[2] B. Atzori and P. Lazzarin, 'Notch Sensitivity and Defect Sensitivity under Fatigue Loading: Two Sides of the Same Medal', *Int. J. Fract.*, vol. 107, no. 1, pp. 1–8, Jan. 2001.

[3] B. Atzori and P. Lazzarin, 'A three-dimensional graphical aid to analyze fatigue crack nucleation and propagation phases under fatigue limit conditions', *Int. J. Fract.*, vol. 118, no. 3, pp. 271–284, Dec. 2002.

[4] B. Atzori, P. Lazzarin, and G. Meneghetti, 'Fracture mechanics and notch sensitivity', *Fatigue Fract. Eng. Mater. Struct.*, vol. 26, no. 3, pp. 257–267, 2003.

[5] B. Atzori, P. Lazzarin, and G. Meneghetti, 'A unified treatment of the mode I fatigue limit of components containing notches or defects', *Int. J. Fract.*, vol. 133, no. 1, pp. 61–87, Jan. 2005.

[6] P. C. Paris and F. Erdogan, *A Critical Analysis of Crack Propagation Laws*. ASME, 1963.

[7] T. Nicholas, *High Cycle Fatigue: A Mechanics of Materials Perspective*. Elsevier Science, 2006.

[8] H. Kitagawa and S. Takahashi, 'Applicability of fracture mechanics to very small cracks or the cracks in the early stage', in *Proc. of 2nd ICM, Cleveland, 1976*, 1976, pp. 627–631.

[9] M. H. El Haddad, N. E. Dowling, T. H. Topper, and K. N. Smith, 'J integral applications for short fatigue cracks at notches', *Int. J. Fract.*, vol. 16, no. 1, pp. 15–30, 1980.

[10] D. Taylor, 'The theory of critical distances', *Eng. Fract. Mech.*, vol. 75, no. 7, pp. 1696–1705, 2008.

[11] W. Yao, K. Xia, and Y. Gu, 'On the fatigue notch factor, Kf', *Int. J. Fatigue*, vol. 17, no. 4, pp. 245–251, May 1995.

[12] H. Neuber, *Theory of notch stresses: Principles for exact stress calculation*, vol. 74. JW Edwards, 1946.

[13] P. Kuhn and H. F. Hardrath, 'An engineering method for estimating notch-size effect in fatigue tests on steel', National Advisory Committee for Aeronautics, Langley Field, Va, NACA Technical Note NACA-TR-2805, 1952.

[14] R. Peterson, Ed., *Manual on Fatigue Testing*. West Conshohocken, PA: ASTM International, 1949.

[15] T. Topper, R. M. Wetzel, and J. Morrow, 'Neuber's rule applied to fatigue of notched specimens', *Illinois University at Urbana Dept of Theoretical and Applied Mechanics*, 1967.

[16] M. Ciavarella and G. Meneghetti, 'On fatigue limit in the presence of notches: classical vs. recent unified formulations', *Int. J. Fatigue*, vol. 26, no. 3, pp. 289–298, Mar. 2004.

[17] P. Lukáš and M. Klesnil, 'Fatigue limit of notched bodies', *Mater. Sci. Eng.*, vol. 34, no. 1, pp. 61–66, Jun. 1978.

[18] Z. P. Bazant, 'Scaling of quasibrittle fracture : asymptotic analysis', *Scaling Quasibrittle Fract. Asymptot. Anal.*, vol. 83, no. 1, pp. 19–40, 1997.

[19] L. Susmel and D. Taylor, 'A novel formulation of the theory of critical distances to estimate lifetime of notched components in the medium-cycle fatigue regime', *Fatigue Fract. Eng. Mater. Struct.*, vol. 30, no. 7, pp. 567–581, 2007.

[20] L. Susmel and D. Taylor, 'On the use of the Theory of Critical Distances to predict static failures in ductile metallic materials containing different geometrical features', *Eng. Fract. Mech.*, vol. 75, no. 15, pp. 4410–4421, Oct. 2008.

[21] L. Susmel and D. Taylor, 'The Theory of Critical Distances to estimate lifetime of notched components subjected to variable amplitude uniaxial fatigue loading', *Int. J. Fatigue*, vol. 33, no. 7, pp. 900–911, Jul. 2011.

[22] L. Susmel and D. Taylor, 'A critical distance/plane method to estimate finite life of notched components under variable amplitude uniaxial/multiaxial fatigue loading', *Int. J. Fatigue*, vol. 38, pp. 7–24, May 2012.

[23] C. Kirsch, 'Die theorie der elastizitat und die bedurfnisse der festigkeitslehre', *Z. Vereines Dtsch. Ingenieure*, vol. 42, pp. 797–807, 1898.

[24] H. M. Westergaard, 'Bearing pressures and cracks', *Trans AIME J Appl Mech*, vol. 6, pp. 49–53, 1939.

[25] M. Ciavarella and F. Monno, 'On the possible generalizations of the Kitagawa–Takahashi diagram and of the El Haddad equation to finite life', *Int. J. Fatigue*, vol. 28, no. 12, pp. 1826–1837, Dec. 2006.

[26] N. Pugno, M. Ciavarella, P. Cornetti, and A. Carpinteri, 'A generalized Paris' law for fatigue crack growth', *J. Mech. Phys. Solids*, vol. 54, no. 7, pp. 1333–1349, Jul. 2006.

[27] M. Ciavarella, 'Crack propagation laws corresponding to a generalized El Haddad equation', *Int. J. Aerosp. Lightweight Struct. IJALS*, vol. 1, no. 1, 2011.

[28] M. Ciavarella, 'A simple approximate expression for finite life fatigue behaviour in the presence of "crack-like" or "blunt" notches', *Fatigue Fract. Eng. Mater. Struct.*, vol. 35, no. 3, pp. 247–256, 2012.

[29] H. O. Fuchs and R. I. Stephens, *Metal fatigue in engineering*. Wiley, 1980.

[30] R. I. Stephens, A. Fatemi, R. R. Stephens, and H. O. Fuchs, *Metal Fatigue in Engineering*. John Wiley & Sons, 2000.

[31] B. Atzori and P. Lazzarin, 'Analisi delle problematiche connesse con la valutazione numerica della resistenza a fatica', in *AIAS National Conference, Lucca Italy, also Quaderno AIAS*, 2000, pp. 33–50.

[32] B. Atzori, G. Meneghetti, and M. Ricotta, 'Fatigue and Notch Mechanics', in *Applied Mechanics, Behavior of Materials, and Engineering Systems*, 2017, pp. 9–23.

[33] B. S. Company, *Bethlehem RQC-80, RQC-90, RQC-100, Roller Quenched and Tempered Carbon Steel Plate: Fabrication and Welding Data*. Bethlehem Steel, 1972.

[34] AISC, Ed., *Hot Rolled Steel Shapes and Plates*, Second. United States Steel - USS, 1963.

[35] H. M. Westergaard, 'Stresses At A Crack, Size Of The Crack, And The Bending Of Reinforced Concrete', *J. Proc.*, vol. 30, no. 11, pp. 93–102, Nov. 1933.

[36] L. Tucker and S. Bussa, 'The SAE Cumulative Fatigue Damage Test Program', *SAE Trans.*, vol. 84, pp. 198–248, 1975.

[37] R. W. Landgraf, F. D. Richards, and N. R. LaPointe, 'Fatigue Life Predictions for a Notched Member Under Complex Load Histories', *SAE Trans.*, vol. 84, pp. 249–259, 1975.

[38] J. M. Potter, 'Spectrum Fatigue Life Predictions for Typical Automotive Load Histories and Materials Using the Sequence Accountable Fatigue Analysis', *SAE Trans.*, vol. 84, pp. 260–269, 1975.

[39] H. Neuber, 'Theory of stress concentration for shear-strained prismatical bodies with arbitrary nonlinear stress-strain law', *J. Appl. Mech.*, vol. 28, no. 4, pp. 544–550, 1961.

[40] D. V. Nelson and H. O. Fuchs, 'Predictions of Cumulative Fatigue Damage Using Condensed Load Histories', *SAE Trans.*, vol. 84, pp. 276–299, 1975.

3 Gaßner curves as shifted Wöhler curves

Introduction

In this Chapter a criterion for the life prediction under variable amplitude spectrum loads for both smooth and notched specimens is presented. The criterion is obtained from the Basquin's law for constant amplitude loading and arrives to define the S/N curve for spectrum load simply as a shifted Basquin's law. Further, it is shown that the shift factor obtained for the smooth specimen is also valid for the cracked and notched one, where in these cases the S/N curve models obtained through the TCD-P in the previous Chapter have been used. Some comparisons with Literature data are added to substantiate the findings and finally, the possibility of defining a shift factor for damage accumulation rules different from the Palmgren-Miner rule is discussed.

3.1 Variable amplitude loading

Fatigue under cyclic loading with a constant amplitude and a constant mean load is addressed as constant-amplitude (CA) fatigue loading, classical example of it being the sinusoidal loading applied in many fatigue tests. Nevertheless, many components undergo complex load histories in their operating life, called variable-amplitude (VA) loading. The study of this phenomenon is still of great interest both in academia and in industry, and this is confirmed by the multiple authors that keep studying this topic although there have been thousands of experimental campaigns, analytical and numerical models trying to predict the VA fatigue behavior of materials in the last century. The simplest VA fatigue prediction rule has been proposed for the first time in 1924 by Palmgren [1] for the fatigue calculation of ball-bearings. Supposing that the load history is made of N_B load blocks, each one containing n_j cycles at the stress amplitude S_{mj}, S_{aj} and the corresponding fatigue life $N(S_{aj})=N_j$, the rule can be expressed as

$$D = \sum_{j=1}^{N_B} \frac{n_j}{N_j} = 1 \tag{3.1}$$

In other words, Palmgren postulated the linear accumulation of the fatigue damage, stating that the failure occurs when the damage D=1. Anyway, Palmgren did not

provide a derivation for the rule, and the same holds for Langer [2] that in 1937 postulated the same rule applied separately to the crack initiation and the crack propagation phases. The first derivation of the linear damage accumulation rule has been proposed by Miner [3]. His hypothesis was that the work that can be adsorbed until failure is a constant value and that the amount of work adsorbed during n_j is directly proportional to n_j. Thus, if W is the total work and w_j the work adsorbed during the block n_j, the criterion is $\Sigma_j w_j = W$. The use of Miner hypothesis ($n_j/N_j = w_j/W$) leads immediately to Equation (3.1). Miner conducted a series of tests on smooth and riveted 2024-T3 aluminum alloy sheet specimens by applying load histories having $2 \leq N_B \leq 4$ and found $0.61 \leq \Sigma_j n_j/N_j \leq 1.45$, very close to 1 on average. Since then the linear damage accumulation rule has been addressed very often as Miner's rule, but probably Palmgren-Miner's (PM) rule is the more corrected form and it is how the rule will be called in this work. Starting from the 1950s, tens of works have been published to verify the PM rule and to find its limits of validity, and also Ciavarella et al. [4] have shown that the limit values of PM rule range from 0.001 to 10. Furthermore, several theories trying to overcome this limit have been proposed; some of them where quite simple, e.g. Leve [5] in 1960 postulated the first simple nonlinear damage accumulation rule $\Sigma_j (n_j/N_j)^{CL}$ with $c_L > 1$, whilst others were much more complicated, like Park and Padgett's [6] general class of cumulative damage models which defined the damage as function of a statistical "strength reduction function". Despite all the interest in defining a generalized damage accumulation model, PM remains by far the most used rule in fatigue design. Thus, to increase its conservativism, some handbooks (e.g. the FKM-Guideline [7]) suggest reducing the critical damage from 1 to 0.3 for steels, steel castings, aluminum alloys, while keeping 1 for ductile iron, gray cast iron, malleable cast iron, albeit Sonsino [8]–[10] and Schijve [11], [12] suggest that testing is always the best choice. However, even testing can be extremely expensive and very difficult both in the setup of the VA experiments and in the interpretation of the results. Indeed, carrying a VA fatigue test campaign is an art on its own involving the concepts of safety factors both in life and in stress [13]: essentially, under a given service loading history, a single test can assess a given same reliability (typically assuming a Weibull distribution) only by increasing the load or the number of cycles/blocks to failure with respect to the mission. The former version is preferred because of the obvious time (and cost) savings that it implies, although special attention is needed when testing at high loads; in fact, during the test of a complex component with a complex loading, local plasticization phenomena (not foreseen via previous finite elements analyses)

might arise. On the other hand, a VA test with higher expected cycles to failure might (and usually it does) last too long if the bandwidth of the rig actuators is limited with respect to the load amplitude they should provide, plus, if time-dependent phenomena affect the fatigue process, the results obtained with a high loading frequency would be partially or completely unreliable. Often, small amplitude cycles are omitted for simplicity and to accelerate testing (and similarly in the original PM rule the cycles below fatigue limit are omitted from the computation of the damage), although in some design handbooks, especially in welded joints, these are known to produce fatigue damage. Indeed, low amplitude cycles can be dealt with according to the PM rule with prolongation of the Wöhler curve below the knee point with the same slope, or according to Haibach [14] with a reduced slope. The former method is the most conservative amongst the listed ones and has been adopted in the current methodology without loss of generality, i.e. for VA fatigue calculations the S/N power law curve for CA is supposed to extend for $N \rightarrow \infty$. This is particularly true for materials which do not show a clear fatigue limit, like aluminum or especially magnesium alloys, for which Haibach correction would not be required anyway. At the other extreme, it is demonstrated that the application of some isolated high amplitude cycles has a beneficial effect on the total life since it induces compressive residual stresses at notch roots. These effects are not considered in the current methodology for the sake of conservativism; furthermore, the model is suitable for fast and simple design level assessment, hence it is in the authors' intent to keep it as slender as possible. Moreover, in many cases, it is still debatable whether load spectra are known with satisfying accuracy, or if cycle-counting methods (such as rainflow or range-pair) are reliable (i.e. if load sequence effects are not important); therefore Miner's law is still very much used, and this is why predictions cannot completely substitute testing. They are just going to suggest better ways to plot Gaßner curves than what presently done, or and what one may expect when applying PM rule according to the theory of the critical distances (TCD) in complex situations, perhaps coming from finite element results of the stress fields, though in the case studies under exam finite elements have been avoided through analytical considerations.

3.2 Gaßner curves for smooth specimen

Under the hypothesis that Basquin's law holds

$$N_u S_u^k = N_e S_e^k = N S^k = C_B \tag{3.2}$$

Where the equation has been written also at the extreme points of the classical domain of validity of Basquin's law, i.e. at some low number of cycles N_u corresponding to the static strength S_u and at a high number of cycles N_e corresponding to the fatigue limit S_e. In the VA case the existence of the fatigue limit is disregarded and the Wöhler curve is extended to infinity. According to PM rule, the damage D in function of the alternate stress S_a for a given load history containing N_B blocks and a total number of cycles N_H would be

$$D = \sum_{j=1}^{N_B} \frac{n_j}{N_j} = \sum_{j=1}^{N_B} \frac{n_j}{N_H} \cdot \frac{N_H}{N_j} = N_H \sum_{j=1}^{N_B} \frac{\nu_j}{N_j} = \frac{N_H}{C_B} \sum_{j=1}^{N_B} \nu_j S_{aj}^k \tag{3.3}$$

Where $\nu_j = n_j/N_H$ is the proportion of cycles spent at level j on the total number N_H. The life under the sum of all j blocks is $\overline{N}$

$$\frac{1}{\overline{N}} = \frac{D}{N_H} = \frac{1}{C_B} \sum_{j=1}^{N_B} \nu_j S_{aj}^k \tag{3.4}$$

Therefore, normalizing the history by its peak tension $S_{a.max}$ such that $\overline{S} = \beta S_{a,max}$ (and $\overline{S}_{aj} = \beta S_{aj}$) and by varying the factor β a full Gaßner curve is obtained

$$\frac{1}{\overline{N}(\overline{S})} = \frac{\overline{S}^k}{C_B} \sum_{j=1}^{N_B} \nu_j \left(\frac{S_{aj}}{S_{a,max}}\right)^k = \frac{\overline{S}^k}{C_B} \cdot G \tag{3.5}$$

Where G has been addressed as shift factor and has the following expression

$$G = \sum_{j=1}^{N_B} \nu_j \left(\frac{S_{aj}}{S_{a,max}}\right)^k \tag{3.6}$$

G depends on the spectrum and the fatigue exponent only. In this way the Gaßner curve for a smooth specimen can be interpreted as a shifted Wöhler curve in the Log(S)/Log(N) coordinates. Equation (3.5) can be rewritten as

$$\left(\frac{\overline{S}}{G^{-\frac{1}{k}}}\right)^k \overline{N} = C_B \tag{3.7}$$

Besides, the Gaßner curve can be plotted as overlapped to the Wöhler curve by using the scale $\mathrm{Log}(S/G^{-1/k})$ instead of the common Log(S). Such scale will be used for all

the Gaßner curves plotted in this Chapter because it will be shown that this result has much wider and interesting generalizations.

3.3 Gaßner curve in the crack like region

In the previous Chapter (as in Ciavarella et al. [15]) it has been shown that in many cases when notches are sufficiently "sharp" their behavior is not too dissimilar from cracks in a certain span of fatigue cycles ranging from the quantities N_0 and N^* defined in Chapter 2. Then this hypothesis has been generalized to a wider family of problems through Susmel and Taylor's [16]–[20] theory of the critical distances in its point variant (TCD-P) exhaustively explained in § . The aim was the formulation of an analytical S/N curve model which could account for the effect of notches in medias to estimate their fatigue life under CA loading with satisfying accuracy. In the current section instead, under the proper hypotheses, such model will be extended to the estimation of VA fatigue life by demonstrating that the shift factor G is not affected by the presence of notches, thence it can be applied also to the more sophisticated S/N curves previously defined. For instance, considering the asymptotic part ($x \to 0$) of the Westergaard [21] solution for a crack of length 2a immersed in an infinite plate and subjected to opening mode loading with asymptotic nominal stress S_{nom} (cfr. Figure 2.3), i.e.

$$S(x) = \frac{K_I}{\sqrt{2\pi\, x}} = \frac{S_{nom}}{\sqrt{2\, x/a}} \tag{3.8}$$

The TCD-P suggests evaluating the stress at a distance $a_0(N)$ from the crack, resulting in $S(x(N))$ to evaluate the fatigue life. This means that there is a spectrum of S_{ej} values giving a spectrum of $S(x(N))$ values, where one takes (either Ciavarella [22] or Susmel and Taylor variants [16]–[20]) a critical distance of the form

$$x(N) = \frac{a_0(N)}{2} = A_{C-ST}\, N^{B_{C-ST}} \tag{3.9}$$

Where the subscript C-ST stands for Ciavarella-Susmel and Taylor (anyway ST is going to be used here, congruently with Chapter 2). Equation (3.9) constants shall be calibrated either according to some dedicated tests or with some material constants. Substituting (3.9) into (3.8)

$$S_j\big(x(N)\big) = \frac{S_{nom,j}}{\sqrt{\frac{A_{ST}}{a}\, N^{B_{ST}}}} \tag{3.10}$$

In order to use Equation (3.10) in VA loading, it must be hypothesized that the intrinsic defect size a_0 is not dependent on the spectrum, but only on the final life of the specimen for a given load history. Hence, using PM rule

$$\frac{1}{\overline{N}} = \frac{D}{N_H} = \frac{1}{C_B}\sum_{j=1}^{N_B} \nu_j \, S_{nom,j}^{k} \left(\frac{A_{ST}}{a}\,\overline{N}^{B_{ST}}\right)^{-\frac{k}{2}} = \frac{1}{C_B}\left(\frac{A_{ST}}{a}\right)^{-\frac{k}{2}} \overline{N}^{-\frac{B_{ST}k}{2}} \sum_{j=1}^{N_B} \nu_j \, S_{nom,j}^{k} \tag{3.11}$$

Notice that this (3.11) is explicit in $\overline{N}$

$$\overline{N}^{\frac{B_{ST}k}{2}-1} = \frac{1}{C_B}\left(\frac{A_{ST}}{a}\right)^{-\frac{k}{2}} \sum_{j=1}^{N_B} \nu_j \, S_{nom,j}^{k} \tag{3.12}$$

Therefore, normalizing the history by the peak tension $S_{nom,max}$ so that $\overline{S}=\beta S_{nom,max}$ the Gaßner curve in the crack like region is

$$\left(\overline{N}(\overline{S}_{nom})\right)^{\frac{B_{ST}k}{2}-1} = \frac{\overline{S}_{nom}^{k}}{C_B}\left(\frac{A_{ST}}{a}\right)^{-\frac{k}{2}} \sum_{j=1}^{N_B} \nu_j \left(\frac{S_{nom,j}}{S_{nom,max}}\right)^{k} = \frac{\overline{S}_{nom}^{k}}{C_B}\left(\frac{A_{ST}}{a}\right)^{-\frac{k}{2}} G \tag{3.13}$$

Where the shift factor G is the same as for the smooth material. However, notice that the new curve can be written as

$$\overline{S}_{nom}^{\,k_{CL}}\ \overline{N} = \left(\left(\frac{A_{ST}}{a}\right)^{-\frac{k}{2}} \cdot \frac{G}{C_B}\right)^{-k_{CL}/k} \tag{3.14}$$

Where the new slope $k_{CL}=k/(1-B_{ST}k/2)$. Consequently, this curve would have the same slope as the smooth one only if $B_{ST}=0$, i.e. if a_0 stayed constant. As done for Equation (3.7), Equation (3.14) can be rearranged as

$$\left(\frac{\overline{S}_{nom}}{G^{-\frac{1}{k}}}\right)^{k_{CL}}\ \overline{N} = \left(\left(\frac{A_{ST}}{a}\right)^{-\frac{k}{2}} \cdot \frac{1}{C_B}\right)^{-k_{CL}/k} \tag{3.15}$$

From Equation (3.15), a bigger crack like notch implies a shorter life, consistently with what expected. Besides, this equation means that, in terms of nominal stress amplitude the S/N curve in the crack like region is shifted exactly of the same amount of the unnotched S/N curve when obtaining VA data.

3.4 Gaßner curve in the blunt notch region

Considering the piecewise power law defined in § 2.5 for Wöhler curves, there is a region for $N>N^*$ where the fatigue behavior can be approximated with enough accuracy by the Wöhler curve of the smooth specimen reduced by the stress concentration factor, i.e.

$$(S\,K_t)^k\,N = C_B \tag{3.16}$$

Or

$$S^k\,N = C_B\,K_t^{-k} \tag{3.17}$$

This region is addressed as blunt notch region, as also stated by Ciavarella [23]. Obviously, through the same passages made here above, the Gaßner curve in the blunt notch region becomes

$$\left(\frac{\bar{S}}{G^{-\frac{1}{k}}}\,K_t\right)^k \bar{N} = C_B \tag{3.18}$$

Being G the same shift factor defined for the smooth material. This means that in the entire domain of N, the Gaßner curve for a notched body defined through the TCD-P (and approximated with a piecewise power law) is equivalent to a Wöhler curve shifted by $G^{-1/k}$.

3.5 Practical example

In this practical example it will be shown that the result obtained for the piecewise power law has even a wider validity and it will be extended to a life-dependent stress concentration factor. To this end, the S/N curves deriving from the usage of the TCD-P in the full Westergaard [21] and Kirsch [24] solutions (cfr. respectively Figure 2.3 and 2.5) are applied to an example steel having K_{Ic}=950 Mpa $mm^{1/2}$, ΔK_{th}=85 Mpa $mm^{1/2}$, S_u=900 MPa at N_u=1,000 cycles and ΔS_e=400 MPa at N_e=1,000,000 cycles. These values imply k=8.55 and $C_B=1.82\cdot10^{28}$. If the TCD-P constants are calibrated according to Susmel and Taylor's [16]–[20] variant, it results a_0=14.5 μm, a_0^u=0.35 mm, A_{ST}=8.62 mm and B_{ST}=-0.46. From the definition of the exact TCD-P Wöhler curves in these cases it is not so simple to isolate smoothly the shift factor as done before. For this reason, a fundamental postulate has been made: the Gaßner curves deriving from the exact solution of the stress field ahead of the notch/crack can be obtained by shifting of the corresponding Wöhler curves through the factor G, i.e.

$$\bar{N}\left(\bar{S}\,\kappa(\bar{N})\right)^{k} = C_B \quad \text{Wöhler}$$
$$\bar{N}\left(\frac{\bar{S}}{G^{-\frac{1}{k}}}\,\kappa(\bar{N})\right)^{k} = C_B \quad \text{Gaßner} \tag{3.19}$$

Where $\kappa(\bar{N})$ has been defined in Chapter 2 as the life dependent stress concentration factor. Equation (3.19) cannot be made explicit in $\bar{N}$, but can be rearranged as an explicit function of $\bar{S}$. This postulate is justified by the findings on the piecewise curve and has been verified by applying the benchmark variable amplitude load history presented as a solid black line in Figure 3.1. The shift factor calculated from the non-dimensional load history and k=8.55 is G≈0.15, or equivalently $G^{-1/k}$≈1.25. The VA results (from the application of numerous amplification factors β to the loading history) plotted as $\bar{S}(\bar{N})/G^{-1/k}$, as suggested by Equation (3.7) are almost perfectly overlapped to the CA S/N curves. Therefore the iterative procedure suggested by Susmel and Taylor [19] seems not needed. It is noteworthy that the difference between a crack and a hole is almost negligible at low number of cycles, as it is relatively established fact, whereas starts to be much more important at longer lives, where for the crack a truncation below the fatigue threshold levels should be needed.

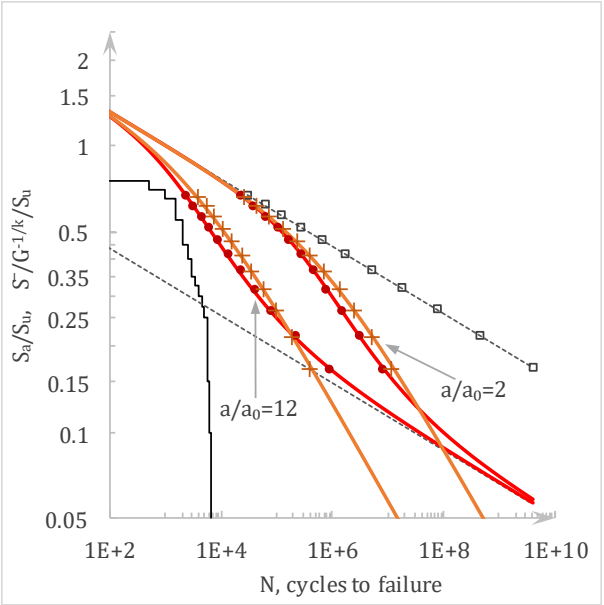

Figure 3.1: S/N curves for notched specimen using the TCD-P: notched specimen (red), cracked specimen (orange) and smooth specimen (gray dashed). Markers have been used to plot VA data (the scale $S_u/G^{-1/k}$ has been used, as suggested by Equation (3.7)) for the cumulative loading history shown with the black line. Gaßner results· are almost indistinguishable from the Wöhler lines

3.6 Quantitative validation

Susmel and Taylor [19] have already provided some evidence of the validity of their method, despite the main general warnings about the PM rule should be taken into account. Therefore, what really needs a validation is that the VA and CA curves can be superposed as it is beautifully indicated in Figure 3.1. It is difficult unfortunately to find known and reliable data from the literature about Gaßner curves, including details

of the spectra. One simple semi-direct way to do this is to use data from Sonsino and Dieterich [9]. To estimate the Wöhler k slope, their Table 3 has been considered (Cyclic material data for unnotched specimen). There is the entire Coffin Manson law which for cast magnesium alloys AZ 91 and AM50 and strain ratio R=–1 gives very similar slope factors, i.e. k≈5.60 to k≈5. This is extremely close to the slope k_{CL}=5 for the notched data (K_t=2:5 in Figures 7–9 under both R=–1 ratio, for all alloys. As a result, the following observations can be made: (i) the slope of Gaßner curve for notched data is indeed unchanged for CA or VA loading (cfr. Figures 6, 8, 9 of Sonsino and Dieterich [9]) in the entire set of tests and within the measured life intervals; actually a similar number of cycles to failure is obviously expected for very high stress amplitudes. This confirms, independently, the curve exponents in Equations (3.7), (3.14), (3.18); (ii) considering N=100,000 as reported in Table 4 of [9], the shift factor using smooth or notched in fatigue data should remain unchanged. In Table 3.1 the ratio N_{CA}/N_{VA} is reported for both notched and smooth data. As evident from the last column of Table 3.1, the difference in this ratio is in the range ~–10%÷10% (it is perfectly within the expected scatter of fatigue data), and this confirms again the finding; (iii) the knee point in correspondence of the fatigue limit is more difficult to estimate from the analytical point of view.

Table 3.1: Elaboration of data from Sonsino and Dieterich's [9] Table 4. Fatigue strength amplitudes S_a at N=100,000 cycles with confidence level CL=50%. The ratio of N_{CA}/N_{VA} is nearly the same for notched and smooth data, as predicted

	K_t=1			K_t=2.5			$\frac{\frac{N_{CA}}{N_{VA}}\Big\vert_{K_t=1} - \frac{N_{CA}}{N_{VA}}\Big\vert_{K_t=2.5}}{N_{CA}/N_{VA}\,\vert_{K_t=1}}\%$
	N_C Λ	N_V Λ	N_{CA}/N_V Λ	N_C Λ	N_V Λ	N_{CA}/N_V Λ	
$AZ91_{R=-1}$	84	163	0.52	61	132	0.46	-11.5
$AZ91_{R=0}$				38	91	0.42	
$AM50_{R=-1}$	70	157	0.45	49	101	0.49	8.9
$AM50_{R=0}$				36	82	0.44	
$AM20_{R=-1}$	61	126	0.48	43	85	0.51	5.9
$AM20_{R=0}$				32	72	0.44	

In some cases, the Gaßner curve is seen to have a slope which differs (albeit slightly) from Wöhler law; this may be a sign of invalidity of the PM rule: indeed, the simple use of non-unitary value of critical damage sum doesn't change the slope of Gaßner curves. Unfortunately, despite some data are available in the literature indicating the modest change of slope [10], they are not sufficiently detailed to comment on the frequency and relevance of this effect.

3.7 Mean stress effect on the shift factor

3.7.1 A brief outline on models

The study of mean stress effect on fatigue loading is probably almost as old as the study of fatigue itself. Indeed, in the very old days of fatigue, Wöhler [25]–[27] between 1858 and 1870 already mentioned a possible detrimental effect of positive mean cyclic stresses on life of railway axles. The first quantitative model relating the stress amplitude S_a and mean stress S_m through the ultimate tensile strength S_u dates 1874 from Gerber [28], who introduced the famous Gerber parabola

$$\left(\frac{S_m}{S_u}\right)^2 + \frac{S_a}{S_{ae}} = 1 \tag{3.20}$$

Where S_{ae} is the effective stress amplitude in fully reversed loading conditions. In this model, the equivalent stress amplitude can be expressed as a function of the mean and alternate stress, being the ultimate tensile strength a material constant. This means that for a given couple (S_m, S_a) there exists an equivalent condition (0, S_{ae}) (fully reversed loading) providing the same number of cycles to failure as (S_m, S_a). Forty years later, in 1914, Equation (3.20) has been "replaced" by the modified Goodman [29] line

$$\frac{S_m}{S_u} + \frac{S_a}{S_{ae}} = 1 \tag{3.21}$$

Which today is (maybe because of its simplicity) the most commonly used mean stress correction in industry and probably the most "popular" model with engineering students. In 1939 a more conservative version of the Goodman line has been proposed by Söderberg [30] who replaced the ultimate tensile strength with the yielding stress of the material, i.e.

$$\frac{S_m}{S_y} + \frac{S_a}{S_{ae}} = 1 \tag{3.22}$$

Anyway, the Söderberg correction is considered by many authors way overconservative, in fact Woodward et al. [31] stated *"The Söderberg line is safe for nearly all materials, but in very many instances the line seriously over-estimates the effect of mean stress"*. Moreover, it has been demonstrated that for many types of steels even the modified Goodman line (and consequently Söderberg line) provides too conservative corrections [32], [33], and for this reason sometimes it is replaced by the Morrow [34] line which substitutes the ultimate tensile strength with the fatigue strength at one cycle, namely

$$\frac{S_m}{S'_f} + \frac{S_a}{S_{ae}} = 1 \tag{3.23}$$

S'_f is not much higher than S_u for materials that do not exhibit a pronounced necking, thus Goodman and Morrow lines provide similar corrections. However, in the case of materials which show high plastic deformations, the fatigue strength at one cycle can be much higher than the ultimate tensile strength resulting in a highly less conservative Morrow line with respect to Goodman's. Dowling [32] in his Figure 3 and Figure 4 has shown this phenomenon, with Morrow correction giving highly non-conservative estimates in the case of 2024-T3 aluminum, while providing very good estimates in the case of AISI 4340 steel. It is very common to find Equations (3.20)–(3.23) expressed as a function of the effective stress amplitude S_{ae} which in fact usually is the unknown of the problem. In 1970 the Smith-Watson-Topper [35] (SWT) proposed an equation where the mean stress effect was not dependent on any material properties, but only on the loading history itself. The model can be written equivalently as:

$$\begin{aligned} S_{ae} &= \sqrt{S_{max}\, S_a} && \text{(a)} \\ S_{ae} &= S_{max}\sqrt{\frac{1-R}{2}} && \text{(b)} \\ S_{ae} &= S_a\sqrt{\frac{2}{1-R}} && \text{(c)} \end{aligned} \tag{3.24}$$

Where S_{max} is the maximum stress in the cycle and R)S_{min}/S_{max} is the load ratio. Equations (3.24) (a), (b) and (c) are equivalent since $S_a = ½ \cdot S_{max} \cdot (1-R)$, as can be easily recovered from Figure 3.2, where an example constant amplitude cyclic loading history has been plotted. A generalization of SWT model is the one from Walker [36] which can be interpreted as a modified SWT model with a fitting exponent γ. Therefore, Walker equation can be written similarly to Equation (3.24), i.e

$$\begin{aligned} S_{ae} &= S_{max}^{1-\gamma}\, S_a^{\gamma} && \text{(a)} \\ S_{ae} &= S_{max}\left(\frac{1-R}{2}\right)^{\gamma} && \text{(b)} \\ S_{ae} &= S_a\left(\frac{2}{1-R}\right)^{1-\gamma} && \text{(c)} \end{aligned} \tag{3.25}$$

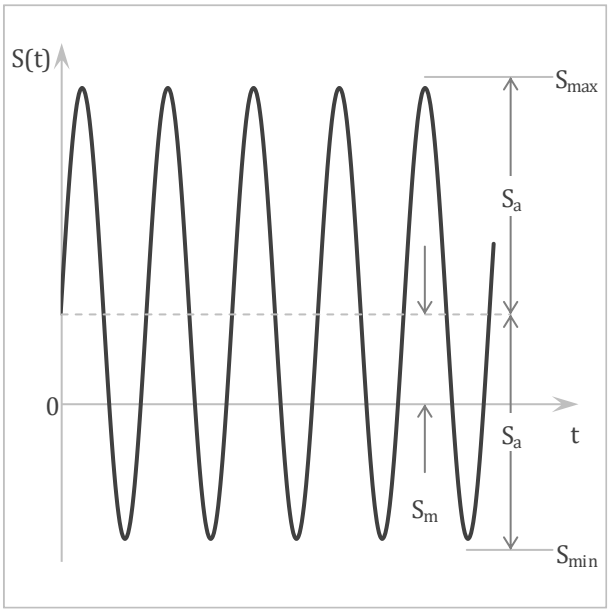

Figure 3.2: Definitions for fatigue stress cycle

Which for γ=½ obviously returns Equation (3.24). Dowling [32] in his Figure 5 and Figure 6 shows that for Al 2024-T3 and AISI 4340 steel the Walker and SWT equations overcome the limitations of Goodman and Morrow lines discussed above related with the ductility of the material. Dowling concludes his work stating that Walker and SWT models are the most accurate for general use, precising obviously that Walker model gives higher ac curacy when the exponent γ is known or can be estimated. In the current work SWT and Walker models are going to be used since, besides Dowling conclusions, they are independent of the material constants, which means that they can lead to more general conclusions on the shift factor definition for variable amplitude life prediction.

3.7.2 Generalized shift factor with mean stress effect

The definition of G given in §§ 3.2, 3.3, 3.4 does not account for mean stress effect, therefore it is only suitable for variable amplitude fatigue in fully reverse loading conditions. In order to introduce a mean stress effect correction in the definition of the G, Equation (3.3) has to be rewritten in terms of effective stress amplitude, viz.

$$D = \sum_{j=1}^{N_B} \frac{n_j}{N_j} = \sum_{j=1}^{N_B} \frac{n_j}{N_H} \cdot \frac{N_H}{N_j} = N_H \sum_{j=1}^{N_B} \frac{\nu_j}{N_j} = \frac{N_H}{C_B} \sum_{j=1}^{N_B} \nu_j \, S_{aej}^k \tag{3.26}$$

3.7.2.1 Smith Watson Topper mean stress effect correction

SWT mean stress correction (3.24) shall be substituted into Equation (3.26). With this correction Equation (3.4) becomes

$$\frac{1}{\bar{N}} = \frac{D}{N_H} = \frac{1}{C_B} \sum_{j=1}^{N_B} \nu_j \left(S_{maxj} \, S_{aj}\right)^{k/2} \tag{3.27}$$

And normalizing the history by its peak tension $S_{a,max}$ such that $\bar{S} = \beta S_{a,max}$ (and $\bar{S}_{aj} = \beta S_{aj}$, $\bar{S}_{maxj} = \beta S_{maxj}$) and by varying the factor β the full Gaßner curve is obtained again as

$$\frac{1}{\overline{N}(\overline{S})} = \frac{\overline{S}^k}{C_B} \sum_{j=1}^{N_B} \nu_j \left(\frac{S_{maxj}\, S_{aj}}{S_{a,max}^2} \right)^{k/2} = \frac{\overline{S}^k}{C_B} \cdot G \tag{3.28}$$

Where G has a slightly different definition from Equation (3.6), viz.

$$G = \sum_{j=1}^{N_B} \nu_j \left(\frac{S_{maxj}\, S_{aj}}{S_{a,max}^2} \right)^{k/2} \quad (a)$$

$$G = \sum_{j=1}^{N_B} \nu_j \left(\frac{S_{maxj}}{S_{a,max}} \sqrt{\frac{1-R_j}{2}} \right)^{k} \quad (b) \tag{3.29}$$

$$G = \sum_{j=1}^{N_B} \nu_j \left(\frac{S_{aj}}{S_{a,max}} \sqrt{\frac{2}{1-R_j}} \right)^{k} \quad (c)$$

Equation (3.29) returns equal to Equation (3.6) for R=–1 (i.e. if $S_{aj}=S_{maxj}$).

3.7.2.2 Walker mean stress effect correction

As done with the SWT model, if Walker equation (3.25) is substituted into (3.26) and the usual passages are performed, the following definition of G holds

$$G = \sum_{j=1}^{N_B} \nu_j \left(\frac{S_{maxj}^{1-\gamma}\, S_{aj}^{\gamma}}{S_{a,max}^2} \right)^{k} \quad (a)$$

$$G = \sum_{j=1}^{N_B} \nu_j \left(\frac{S_{maxj}}{S_{a,max}} \left(\frac{1-R_j}{2} \right)^{\gamma} \right)^{k} \quad (b) \tag{3.30}$$

$$G = \sum_{j=1}^{N_B} \nu_j \left(\frac{S_{aj}}{S_{a,max}} \left(\frac{2}{1-R_j} \right)^{1-\gamma} \right)^{k} \quad (c)$$

Again, the first definition of G is retrieved under fully reversed loading. As regards the mean stress effect correction in the crack like notch and the blunt notch region, it is trivial to demonstrate that the current definition of G applies to Equation (3.13) and (3.18), too.

3.8 Quantitative validation with experiments

The validation of the model proposed has been done again by using the data deriving from the SAE Keyhole test program, beautifully explained by Tucker and Bussa [37]. Indeed, the main scope of the test program was variable amplitude fatigue testing and prediction using three loading histories at several load levels. To this purpose many different prediction models for constant and variable amplitude have been collected in the SAE Transactions Vol. 84, 1975, § 1. For example, Landgraf et al. [38] and

Potter [39] adopted a strain-life approach through Neuber's rule [40] whilst Nelson and Fuchs [41] decided to work with stress-life models called nominal stress range I and II methods. As also stated in Chapter 2, the TCD has been used in 2008 also to predict with an acceptable level of accuracy the static failure of notched cold rolled low carbon steel and in presence of large plastic deformation before failure [17]. Nonetheless, in order to state that the TCD is a fully established approach, a large number of tests is still needed on larger notch radii $a>a_0^u$ and on a wider amount of material classes; for this reason, albeit accurate in the cases analyzed, the current linear elastic approach does not expect to supersede the elastoplastic fracture mechanics, neither in constant nor in variable amplitude fatigue. It is however noteworthy that no other simple methods amongst the ones collected in the SAE Transactions Vol. 84, 1975, § 1, including strain-life approach applied to notched geometries, seem to give higher accuracy.

3.8.1 Loading histories

The loading histories used in the Test Program are (B) Bracket: narrow band load history, (T) Transmission: strong tensile bias with several compressive reversals and (S) Suspension: strong compressive bias. Some additional tests were done with the same truncated (mini) spectra, namely mB, mT, mS. All the spectra are shown here in Figure 3.3.

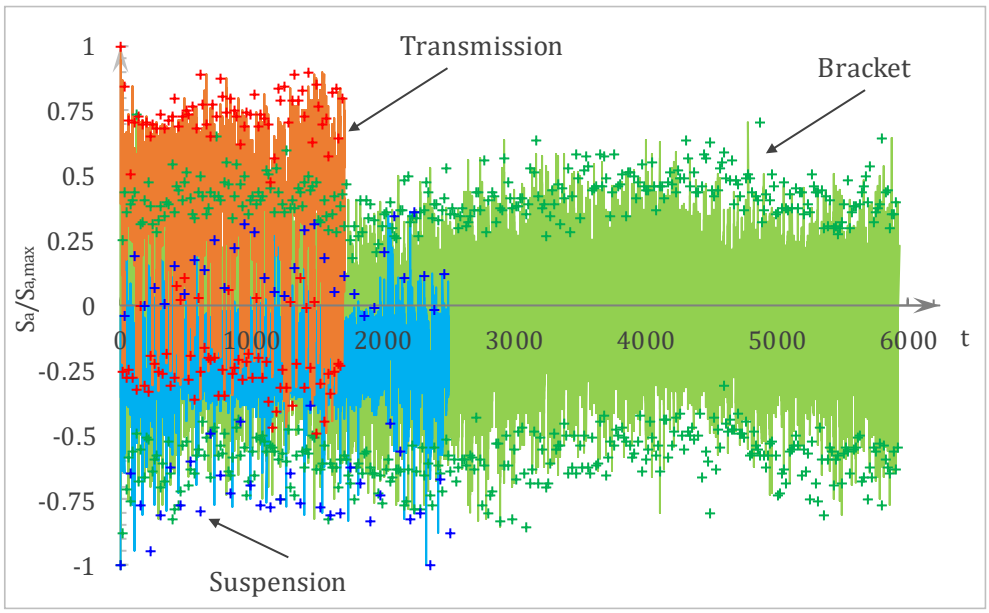

Figure 3.3: SAE Keyhole Test Program: load histories used in the tests. With solid lines are represented the full histories, the mini histories are shown with "+" markers. The data have been downloaded from the website https://www.efatigue.com/benchmarks/ under "SAE Keyhole Test Program"

The spectra have been cycle counted through the rainflow counting algorithm (cfr. Matsuishi and Endo [42]) shown in Appendix. Once the cycle counting is done, it is possible to calculate the summation for G. In this case, since no data on Walker's exponent γ were available in Literature, SWT method has been used. In this way it has been possible to plot an unusual representation of the rainflow, i.e. all the SWT corrected addenda G_j have been plotted as a function of the j-th stress amplitude S_{aj} (cfr. Figure 3.4). From Figure 3.4 some interesting considerations can be made: (i) for higher non-dimensional stress amplitude there is usually a higher contribution to the G_j: indeed, G would have been a monotonic increasing function only if the loading spectra had been at R=–1; (ii) G at R=–1 (solid thick lines) is higher than G(R≠–1) if R<–1 and smaller than G(R≠–1) if R>–1. This implies that if the spectrum has compressive average mean stress then a longer life is predicted (high shift $G^{-1/k}$), vice versa for tensile mean stress a shorter life is predicted (shift $G^{-1/k}$ is lowered), coherently with the mean stress effect correction; (iii) a higher Basquin's law exponent k tends to lower the $G^{-1/k}$. This effect is visible by comparison of the two different materials, with Man-Ten which provides higher values of $G^{-1/k}$.

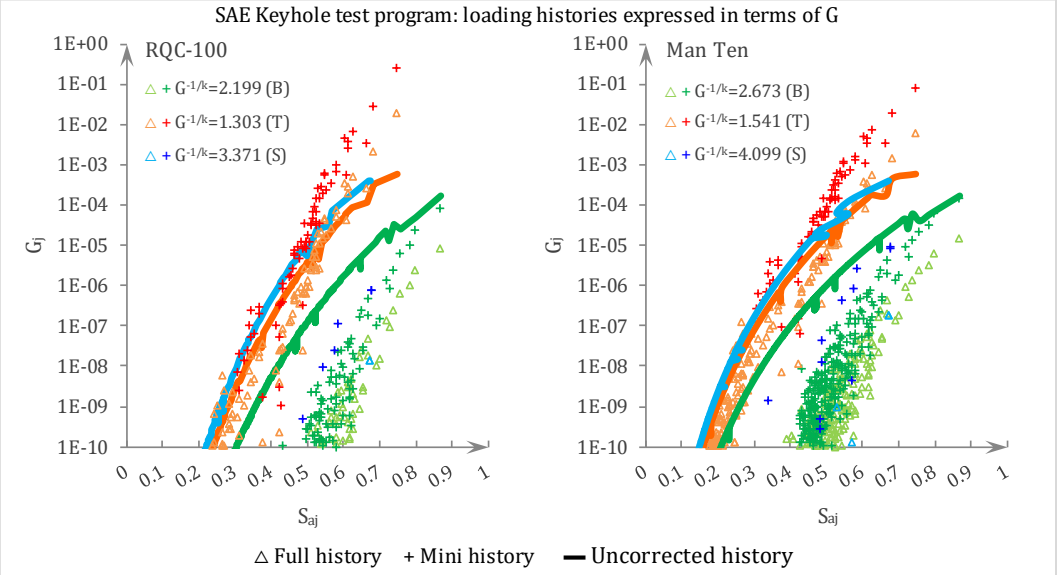

Figure 3.4: SAE Keyhole test program: loading histories here expressed in terms of G_j, i.e. the j-th contribution to the shift factor for every material is here provided as a function of the non-dimensional stress amplitude. Letters B, T, S are the initials of the spectra: (B) Bracket, (T) Transmission (S) Suspension

The VA life predictions have been calculated by shifting the green S/N curves shown in Chapter 2 by $G^{-1/k}$ for each one of the six spectra and the experimental results are plotted in Figure 3.5 for both RQC-100 (left) and for Man Ten (right). Predictions are satisfactory and are always in a scatter factor of ±3 times the predicted life. As regards

RQC-100, almost all the predictions seem to be collocated on the conservative side of the bisector, while for Man Ten predictions are simply within the scatter bands.

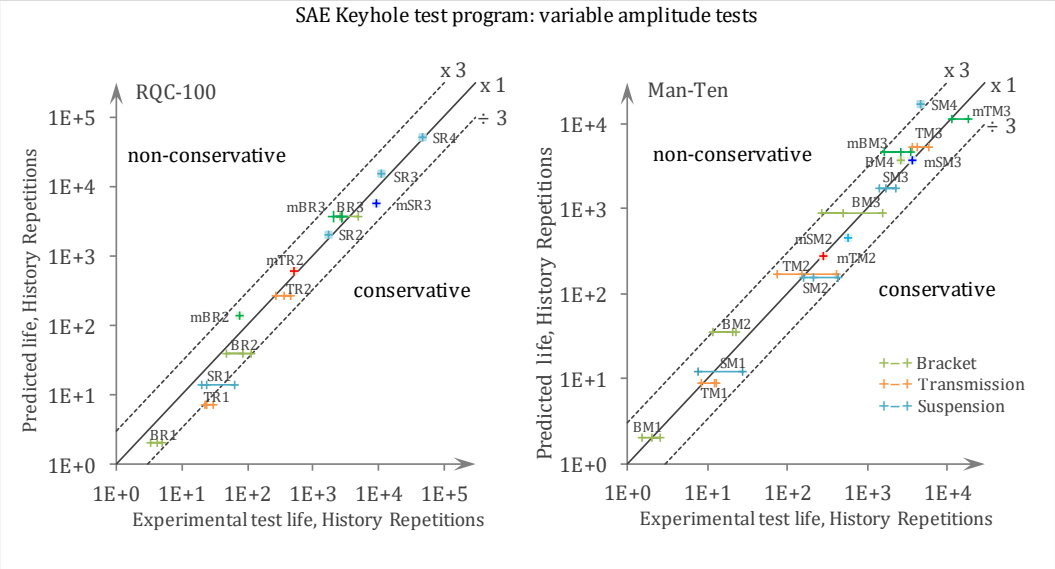

Figure 3.5: SAE Keyhole test program: experimentally measured vs. predicted life through the shift factor approach. On the left predictions for RQC-100 and on the right for Man Ten. The solid line (bisector) is the prefect correspondence and the dashed lines are the scatter bands with multiplicative factors ±3. The alphanumeric codes are explained in Table 3.2

Table 3.2: Specimen code number (from Tucker and Bussa [37])

1st letter	B	-	Bracket
(History Identification)	T	-	Transmission
	S	-	Suspension
2nd letter	R	-	RQC-100
(Material Identification)	M	-	Man Ten
3rd number	1	-	Highest Load
	2	-	
	3	-	
	4	-	
	5	-	Lowest Load

3.9 Discussion

3.9.1 Shift factor with nonlinear damage accumulation rule

As abovementioned, the first simple nonlinear damage rule was proposed by Leve [5] in 1960. Leve's model simply postulates a load-level dependency of the damage according to:

$$\sum_{j=1}^{N_B}\left(\frac{n_j}{N_j}\right)^{c_L}=1 \tag{3.31}$$

With $c_L \geq 1$ constant. Equation (3.31) obviously returns to PM rule when $c_L=1$. The damage curves associated with this rule are plotted as solid green lines in Figure 3.6 to varying of c_L. An attempt to calculate the shift factor through Leve's damage accumulation rule gives no simple definition of G, viz.

$$D=\left(\frac{N_H}{C_B}\right)^{c_L}\bar{S}^{kc_L}\sum_{j=1}^{N_B}\left[\nu_j\left(\frac{S_{aj}}{S_{a,max}}\right)^{k}\right]^{c_L} \tag{3.32}$$

Nevertheless, considering only the summation and applying the well-known power mean inequality [43] yields

$$\left\{\frac{1}{N_B}\sum_{j=1}^{N_B}\left[\nu_j\left(\frac{S_{aj}}{S_{a,max}}\right)^{k}\right]^{c_L}\right\}^{1/c_L}\geq\frac{1}{N_B}\sum_{j=1}^{N_B}\nu_j\left(\frac{S_{aj}}{S_{a,max}}\right)^{k} \tag{3.33}$$

Which may be rewritten as

$$\left\{\sum_{j=1}^{N_B}\left[\nu_j\left(\frac{S_{aj}}{S_{a,max}}\right)^{k}\right]^{c_L}\right\}^{1/c_L}\geq N_B^{\frac{1-c_L}{c_L}}G \tag{3.34}$$

Or

$$\sum_{j=1}^{N_B}\left[\nu_j\left(\frac{S_{aj}}{S_{a,max}}\right)^{k}\right]^{c_L}\geq\left(N_B^{\frac{1-c_L}{c_L^2}}G\right)^{c_L} \tag{3.35}$$

Inequation (3.35) is a lower limit for the estimated total damage, in fact from its substitution into (3.32) it results that

$$D\geq\left(\frac{N_H}{C_B}\right)^{c_L}\bar{S}^{kc_L}\left(N_B^{\frac{1-c_L}{c_L^2}}G\right)^{c_L} \tag{3.36}$$

Which can be rearranged as

$$\frac{1}{\bar{N}} = \frac{D}{N_H} \geq \frac{\bar{S}^{kc_L}}{C_B} \left(\frac{N_H}{N_B^{c_L}}\right)^{c_L-1} G^{c_L} \tag{3.37}$$

Or, in a more familiar way as

$$\frac{1}{\bar{N}} \geq \frac{\left(\frac{N_H}{N_B^{c_L}}\right)^{c_L-1}}{C_B} \left(\frac{\bar{S}}{G^{-\frac{1}{k}}}\right)^{kc_L} \tag{3.38}$$

Therefore, the lower limit S/N curve is

$$\left(\frac{\bar{S}}{G^{-\frac{1}{k}}}\right)^{kc_L} \bar{N} \geq C_{Bc_L} \tag{3.39}$$

With $C_{BcL}=C_B(N_H/N_B^{cL})^{1-cL}$.

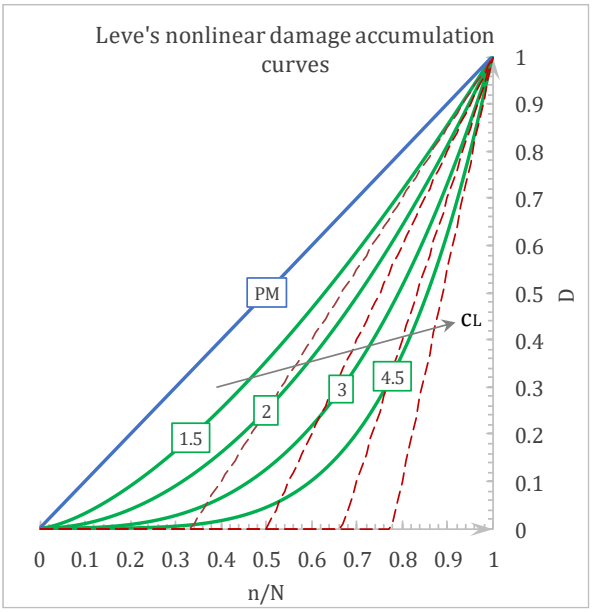

Figure 3.6: Damage curves for PM rule (solid blue), Leve's nonlinear rule (solid green) and the corresponding approximating double linear damage accumulation curves (dashed red)

Obviously (3.38) returns to the "classical" definition of Gaßner curve (3.5) when $c_L=1$. Inequation (3.38) underestimates the cycles to failure deriving from the application of a nonlinear damage accumulation rule of the Leve's type, henceforth it shall not be used for practical computation, but only in very preliminary assessment. It is noteworthy, anyway, that the use of a nonlinear damage accumulation rule entails an increase in the slope of the Gaßner curve from k to kc_L, meaning that this nonlinearity might be the cause of the slight difference between the slopes of the Wöhler and the Gaßner curves experimentally measured for example by Sonsino and Bacher-Höchst [44]or by Sonsino et al. [45].

3.9.2 Introduction of a fatigue limit in the shift factor model using a double linear damage rule

An exact solution, function of the shift factor, can be retrieved again if the Leve's rule is approximated through its first derivatives in (n/N, D)=(0,0) and (n/N, D)=(1,1). In fact, the slope of Leve's rule is 0 in the origin and c_L in 1 (cfr. the red dashed lines in Figure 3.6), therefore the following double linear damage model can be defined.

$$D = \sum_{j=1}^{N_B} c_L \frac{n_j}{N_j} + 1 - c_L = N_B(1 - c_L) + c_L \sum_{j=1}^{N_B} \frac{n_j}{N_j}, \quad \text{with } \frac{n_j}{N_j} \geq \frac{c_L - 1}{c_L} \tag{3.40}$$

As evident from Equation (3.40) and Figure 3.6, this model introduces a rather peculiar definition of fatigue limit in the damage rule. Indeed, substituting Basquin's law into the limit value of N_j returns the expression of the fatigue limit at the j-th load level

$$S_{ej} = \left(\frac{c_L - 1}{c_L} \cdot \frac{C_B}{n_j} \right)^{\frac{1}{k}} \tag{3.41}$$

From equation (3.41) c_L can be calibrated to obtain the correct fatigue limit, and its value is unique only if all the blocks contain the same number of cycles.

$$c_L = \left(1 - \frac{S_{ej}^k \, n_j}{C_B} \right)^{-1} \tag{3.42}$$

Using the proportion of cycles ν_j spent at level j allows to rewrite (3.40) as

$$D = N_B(1 - c_L) + \frac{N_H}{C_B} c_L \sum_{j=1}^{N_B} \nu_j \, S_{aj}^k \tag{3.43}$$

After the normalization and the mean stress effect correction through Walker's model, the final shifted S/N curve equation can be written

$$\frac{1}{\bar{N}(\bar{S})} = \frac{D}{N_H} = \frac{N_B}{N_H}(1 - c_L) + \frac{\bar{S}^k}{C_B} c_L G \tag{3.44}$$

Where G has the general form defined in Equation (3.30). Equation (3.44) can be rearranged in a more convenient form to highlight the fatigue limit

$$\left(\frac{\bar{S}}{G^{-\frac{1}{k}}} \right)^k - S_e^k = \frac{1}{\bar{N}} \frac{C_B}{c_L} \tag{3.45}$$

The fatigue limit S_e has been defined by supposing for convenience that each load block has constant number of cycles $n_j = N_H/N_B$.

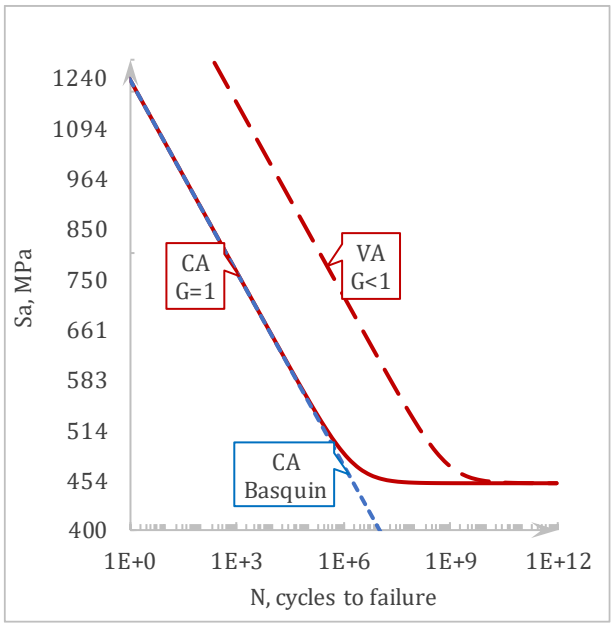

Figure 3.7: S/N curves for RQC-100 steel (data from Table 2.1). Comparison between Basquin's law, the CA S/N curve with G=1 and the VA S/N curve with G<1

Equation (3.45) returns to Basquin's law if c_L=1 and G=1, but if G=1 and c_L is used to define S_e, it is possible to modify also the CA S/N curve retrieving a non-pure power law. Indeed, in Figure 3.7 the S/N curves from (3.45) are plotted for RQC-100 steel (material properties in Table 2.1) considering both the case G=1, which corresponds to a CA S/N curve with fatigue limit and G<1 being a VA S/N curve deriving from a generic variable amplitude load history.

Conclusion

It has been demonstrated that the S/N curves under CA or VA loading can be obtained by a simple shift factor depending on the spectrum histogram and the Basquin's law slope, within the assumptions of PM rule. This holds true for both smooth and notched specimens and seems to be confirmed by some experimental data taken from the Literature. The finding is based on the TCD in its point variant proposed and validated by Susmel and Taylor. However, considering this result, there is no need to apply the iterative calculations that Susmel and Taylor propose, as the VA curves can be obtained directly from the CA curves, for which many proposals have already been put forward, also in closed form. Even the computation of the stress field from Finite Element Method does not seem necessary in many cases, as it does not add much accuracy to a problem where the number of assumptions is already quite strong, and more important, than the details of the stress field. As a first approximation, spectrum loading effects in notched or even cracked structures can be estimated easily from reduced amount of testing. Mean stress effect correction has been introduced in the definition of the shift factor through the SWT and the Walker equations and it has been demonstrated that under fully reversed loading the initial definition of shift factor is retrieved. Finally, it is proposed a discussion on the implications of using different damage accumulation rules in the calculation of the shift

factor and the concept of fatigue limit is introduced in the shift through a double linear damage rule.

References

[1] A. G. Palmgren, 'Die Lebensdauer von Kugellagern (Life Length of Roller Bearings. In German)', *Z. Vereines Dtsch. Ingenieure VDI Z. ISSN*, pp. 0341–7258, 1924.

[2] B. F. Langer, 'Fatigue failure from stress cycles of varying amplitude', *J. Appl. Mech.*, vol. 59, pp. A160–A162, 1937.

[3] M. A. Miner, 'Cumulative Damage in Fatigue', *J. Appl. Mech.*, vol. 3, pp. 159–164, 1945.

[4] M. Ciavarella, P. D'antuono, and A. Papangelo, 'On the connection between Palmgren-Miner rule and crack propagation laws', *Fatigue Fract. Eng. Mater. Struct.*, vol. 41, no. 7, pp. 1469–1475, 2018.

[5] H. L. Leve, 'Cumulative damage theories', *Met. Fatigue Theory Des.*, vol. A. F. Madayag Ed., pp. 170–203, 1960.

[6] C. Park and W. J. Padgett, 'A general class of cumulative damage models for materials failure', *J. Stat. Plan. Inference*, vol. 136, no. 11, pp. 3783–3801, Nov. 2006.

[7] E. Haibach, *Analytical Strength Assessment of Components in Mechanical Engineering: FKM-Guideline*. VDMA, 2003.

[8] C. M. Sonsino, 'Principles of variable amplitude fatigue design and testing', in *Fatigue Testing and Analysis Under Variable Amplitude Loading Conditions*, ASTM International, 2005.

[9] C. M. Sonsino and K. Dieterich, 'Fatigue design with cast magnesium alloys under constant and variable amplitude loading', *Int. J. Fatigue*, vol. 28, no. 3, pp. 183–193, Mar. 2006.

[10] C. M. Sonsino, 'Fatigue testing under variable amplitude loading', *Int. J. Fatigue*, vol. 29, no. 6, pp. 1080–1089, Jun. 2007.

[11] J. Schijve, *Fatigue of Structures and Materials*. Springer Science & Business Media, 2001.

[12] J. Schijve, Ed., 'Fatigue under Variable-Amplitude Loading', in *Fatigue of Structures and Materials*, Dordrecht: Springer Netherlands, 2009, pp. 295–328.

[13] J. Tomblin and W. Seneviratne, 'Determining the fatigue life of composite aircraft structures using life and load-enhancement factors. Final report', 2011.

[14] E. Haibach, 'Betriebsfestigkeit: Verfahren und Daten zur Bauteilberechnung. Düsseldorf: VDI-Verlag', ISBN 3–18–400828–2, 1989.

[15] M. Ciavarella, P. D'Antuono, and G. P. Demelio, 'Generalized definition of "crack-like" notches to finite life and SN curve transition from "crack-like" to "blunt notch" behavior', *Eng. Fract. Mech.*, vol. 179, pp. 154–164, Jun. 2017.

[16] L. Susmel and D. Taylor, 'A novel formulation of the theory of critical distances to estimate lifetime of notched components in the medium-cycle fatigue regime', *Fatigue Fract. Eng. Mater. Struct.*, vol. 30, no. 7, pp. 567–581, 2007.

[17] L. Susmel and D. Taylor, 'On the use of the Theory of Critical Distances to predict static failures in ductile metallic materials containing different geometrical features', *Eng. Fract. Mech.*, vol. 75, no. 15, pp. 4410–4421, Oct. 2008.

[18] L. Susmel and D. Taylor, 'The Theory of Critical Distances to estimate lifetime of notched components subjected to variable amplitude uniaxial fatigue loading', *Int. J. Fatigue*, vol. 33, no. 7, pp. 900–911, Jul. 2011.

[19] L. Susmel and D. Taylor, 'A critical distance/plane method to estimate finite life of notched components under variable amplitude uniaxial/multiaxial fatigue loading', *Int. J. Fatigue*, vol. 38, pp. 7–24, May 2012.

[20] D. Taylor, 'The theory of critical distances', *Eng. Fract. Mech.*, vol. 75, no. 7, pp. 1696–1705, 2008.

[21] H. M. Westergaard, 'Stresses At A Crack, Size Of The Crack, And The Bending Of Reinforced Concrete', *J. Proc.*, vol. 30, no. 11, pp. 93–102, Nov. 1933.

[22] M. Ciavarella, 'Crack propagation laws corresponding to a generalized El Haddad equation', *Int. J. Aerosp. Lightweight Struct. IJALS*, vol. 1, no. 1, 2011.

[23] M. Ciavarella, 'A simple approximate expression for finite life fatigue behaviour in the presence of "crack-like" or "blunt" notches', *Fatigue Fract. Eng. Mater. Struct.*, vol. 35, no. 3, pp. 247–256, 2012.

[24] C. Kirsch, 'Die theorie der elastizitat und die bedurfnisse der festigkeitslehre', *Z. Vereines Dtsch. Ingenieure*, vol. 42, pp. 797–807, 1898.

[25] A. Wöhler, 'Bericht über die Versuche, welche auf der Königl. Niederschlesisch-Märkischen Eisenbahn mit Apparaten zum Messen der Biegung und

Verdrehung von Eisenbahnwagen-Achsen während der Fahrt angestellt wurden', *Z. Für Bauwes.*, vol. 8, no. 1858, pp. 641–652, 1858.

[26] A. Wöhler, 'Versuche zur Ermittlung der auf die Eisenbahnwagenachsen einwirkenden Kräfte und die Widerstandsfähigkeit der Wagen-Achsen', *Z. Für Bauwes.*, vol. 10, no. 1860, pp. 583–614, 1860.

[27] A. Wöhler, *Ueber die Festigkeits-versuche mit Eisen und Stahl*. 1870.

[28] H. Gerber, *Bestimmung der zulässigen Spannungen in Eisen-Constructionen*. Wolf, 1874.

[29] J. Goodman, *Mechanics applied to engineering*. London [etc.] Longmans, Green & Co., 1914.

[30] C. R. Söderberg, 'Factor of safety and working stress', *Trans Am Soc Mech Eng*, vol. 52, pp. 13–28, 1939.

[31] A. R. Woodward, K. W. Gunn, and G. Forrest, 'The effect of mean stress on the fatigue of aluminum alloys', in *International Conference on Fatigue of Metals*, 1956, pp. 1156–1158.

[32] N. E. Dowling, 'Mean Stress Effects in Stress-Life and Strain-Life Fatigue', SAE International, Warrendale, PA, SAE Technical Paper 2004-01–2227, Apr. 2004.

[33] N. E. Dowling, C. A. Calhoun, and A. Arcari, 'Mean stress effects in stress-life fatigue and the Walker equation', *Mean Stress Eff. Stress-Life Fatigue Walk. Equ.*, vol. 32, no. 3, pp. 163–179, 2009.

[34] J. Morrow, 'Fatigue properties of metals', *Fatigue Des. Handb.*, pp. 21–30, 1968.

[35] K. N. Smith, P. Watson, and T. H. Topper, 'A Stress-Strain Function for the Fatigue of Metals', *J. Mater.*, vol. 5, pp. 767–778, Dec. 1970.

[36] K. Walker, 'The Effect of Stress Ratio During Crack Propagation and Fatigue for 2024-T3 and 7075-T6 Aluminum', *Eff. Environ. Complex Load Hist. Fatigue Life*, Jan. 1970.

[37] L. Tucker and S. Bussa, 'The SAE Cumulative Fatigue Damage Test Program', *SAE Trans.*, vol. 84, pp. 198–248, 1975.

[38] R. W. Landgraf, F. D. Richards, and N. R. LaPointe, 'Fatigue Life Predictions for a Notched Member Under Complex Load Histories', *SAE Trans.*, vol. 84, pp. 249–259, 1975.

[39] J. M. Potter, 'Spectrum Fatigue Life Predictions for Typical Automotive Load Histories and Materials Using the Sequence Accountable Fatigue Analysis', *SAE Trans.*, vol. 84, pp. 260–269, 1975.

[40] H. Neuber, 'Theory of stress concentration for shear-strained prismatical bodies with arbitrary nonlinear stress-strain law', *J. Appl. Mech.*, vol. 28, no. 4, pp. 544–550, 1961.

[41] D. V. Nelson and H. O. Fuchs, 'Predictions of Cumulative Fatigue Damage Using Condensed Load Histories', *SAE Trans.*, vol. 84, pp. 276–299, 1975.

[42] M. Matsuishi and T. Endo, 'Fatigue of metals subjected to varying stress', *Jpn. Soc. Mech. Eng. Fukuoka Jpn.*, vol. 68, no. 2, pp. 37–40, 1968.

[43] P. S. Bullen, *Handbook of means and their inequalities*, vol. 560. Springer Science & Business Media, 2013.

[44] C. M. Sonsino and M. Bacher-Höchst, 'Methodology for the safe and economical fatigue design of components in ABS/ETC braking systems under variable amplitude loadings', SAE Technical Paper, 1999.

[45] C. M. Sonsino, T. Łagoda, and G. Demofonti, 'Damage accumulation under variable amplitude loading of welded medium-and high-strength steels', *Int. J. Fatigue*, vol. 26, no. 5, pp. 487–495, 2004.

4 Limits of the Palmgren Miner rule

Introduction

In this Chapter the limits of validity of the Palmgren-Miner (PM) rule are discussed with special attention to its relationship with crack propagation laws of the generalized Paris type. An analysis of the connection between the linear accumulation damage rule and crack propagation laws is necessary also in order to have a better understanding regarding the subtle, yet clear, boundary dividing the phases of crack initiation (primarily studied in fatigue) and propagation (primarily studied in fracture mechanics). The Chapter is extracted directly from Ciavarella et al. [1] paper titled *"On the connection between Palmgren-Miner rule and crack propagation laws"*. The classical PM rule, despite clearly approximation, is commonly applied for life prediction under variable amplitude (VA) fatigue loading, and to date, there is no simple alternative. Multiple authors have previously commented in Literature that the PM hypothesis is based on an exponential fatigue crack growth law, i.e. when the crack propagation rate is proportional to the crack size a, the specific case including Paris' law for crack propagation exponent equal to 2. This is verified when PM is applied by updating the damage estimate during the crack growth. In this Chapter it is shown that applying PM to the "initial" and nominal (stress vs. number of cycles) curve of a cracked structure results exactly in the integration of the simple Paris' power law equation and more in general to any crack propagation law in the form $da/dN=H\cdot\Delta S^{\eta}a^{\zeta}$. This leads to an interesting new interpretation of the PM rule. Indeed, the fact that PM rule is often considered to be quite inaccurate probably pertains more to the general case when propagation cannot be simplified to this form (like when there are distinct initiation and propagation phases), rather than in long crack propagation. In fact, results from well-known round-robin experiments under VA loading confirm that, even using modified Paris' laws for crack propagation, the results of the non-interaction models, neglecting retardation and other crack closure or plasticity effects due to overloads, are quite satisfactory, and these correspond very closely to the application of PM rule, at least when geometrical factors can be neglected. The use of generalized exponential crack growth, even in the context of spectrum loading, seems to imply the PM rule applies. Therefore, this seems closely related to the so-called *lead crack fatigue lifing*

framework. The connection means however that the same sort of accuracy is expected from PM rule and from assuming exponential crack growth for the entire lifetime.

4.1 Description

The classical approach to VA fatigue loading is to apply the (PM) rule, proposed by Miner [2] at Douglas Aircraft in 1945, 21 years after Palmgren [3], which suggested that for a given block with a total number of cycles per block N_H, damage would be

$$D = \sum_{j=1}^{N_H} \frac{n_j}{N_j} \tag{4.1}$$

where n_j is the number of cycles spent at level j on the stress amplitude and N_j is the total number of cycles the specimen could resist at the stress level S_j according to the CA S/N (Wöhler) curve. Failure according to the PM hypothesis should occur when the damage reaches the critical value D_c=1. The linear damage accumulation rule is obviously quite approximate, neither load sequence nor memory effects are considered, and could be both on the unsafe and on the safe side, but it is by far the most well-known and used damage accumulation law (cfr. the review by Fatemi and Yang [4]). In order to achieve safety by design, handbooks suggest to simply assume a lower D_c. For instance, the FKM Guidelines [5] (Research Committee Mechanical Engineering) recommend D_c=0.3 for steels, steel castings, and aluminum alloys, while D_c=1 for ductile iron, grey cast iron, and malleable cast iron (therefore in these cases 1 seems to work quite well in general). Attempts to generalize the PM rule have had limited spread: for instance the first nonlinear damage accumulation rule by Leve [6] in 1960 encountered limited success; Miller and Zachariah [7] in 1977 proposed an exponential evolution of damage, and Manson and Halford [8] in 1981 proposed the "damage curve concept" and a double linear damage accumulation rule to weight initiation and propagation differently. Probably, these methods are not particularly diffused because they usually need calibration and can become very cumbersome when large number of blocks or random loading is considered. Concerning cracked structures, the PM rule has been applied much less, since the full integration of crack propagation equations is generally preferred with the hope of being more accurate [9]–[13], and the ultimate goal of obtaining eventually the full S/N curve solely via integration as a total-life analysis based on crack propagation, hence including the stage of (very) short cracks. This would hope to shed a light on the old problem of distinguishing between the initiation and propagation stages, which generally has only

a vague solution (the threshold *"has often been defined as a macrocrack, visible in a low-power microscope"* [14]). Notwithstanding, unsatisfactory prediction quality at times *"stems from an inadequate conception of the constraint factors incorporated in the NASGRO models."* [11] Clearly, the PM rule is not the way forward for very advanced designs of light structures, although it remains the basis for the applications where it started from, viz. rolling bearings, and many other applications. It is also commonly used in design of welded joints (cfr. Haibach [5] where variants are proposed to account for cycles below the fatigue limit, where it exists). In any case, it is appropriate to outline some possible conclusions, because some confusion may have originated from some authors who have noticed, like Miller and Zachariah [7], that *"the Palmgren-Miner hypothesis can be stated to be based on an exponential fatigue crack growth law."* Indeed, Miller and Zachariah [7] noticed that the integration of a law of the form

$$\frac{da}{dN} = \Gamma \, \Delta S^{\eta} a \tag{4.2}$$

Leads to the PM rule; in their case Miller and Zachariah referred to the type of equations originally proposed by Frost and Dugdale [15]. It should be noted immediately that the "exponential crack growth" was already proposed in 1952 by Shanley [16] in his Equation 4 to justify the S/N curves also under spectrum loading. His reference to h≈8 without much reference to actual real crack is rather similar to the equations by few authors (Nisitani [17], Goto and Nisitani [18], Nisitani et al. [19], [20], Murakami et al [21], and Murakami and Miller [22]; cfr. also Pugno et al. [23]). It is noteworthy that the integration of this type of crack growth laws leads to an S/N curve $\Delta S^{\eta} \cdot N = \text{const}$, in which the typical value of η is of the order of the Basquin's law exponent known from Textbooks. The logarithmic dependence on the initial crack size resulting from the integration has been obviously not observed in the classical studies and Textbooks (exception made for the empirical factors taking into account, for example, surface finish which might be an indication of a small initial crack), until recently when it was indeed observed [21], [24], [25]. The exponential crack growth sometimes is even recalled in the more general attempt to identify unified procedures for crack growth under spectrum loading [26], [27]. Indeed, the USAF report refers to exponential fits either for crack sizes a<0.005 in (which probably would be called short cracks) [21], or as an approximation in small increments of propagation. Indeed, on their page A10 it is explicitly written that exponential fits are assumed only over small increments *"Incremental crack growth is determined through log-linear interpolation of the crack growth curve. Crack growth curves typically increase at about the same rate as an exponential function.*

That is, although an exponential function may not fit the crack growth curve exactly, over a short interval the rate of increase of the crack growth curve is nearly exponential. Crack growth calculation errors can occur using linear interpolation even when many points are included in the crack growth table." Thus, it should not be concluded that exponential crack growth can be assumed for the entire lifetime. The present note starts from showing a disagreement with the Miller-Zachariah [7] statement that the Palmgren-Miner hypothesis should be valid only with exponential crack growth. This erroneous conclusion is shown to clearly come from updating the damage in each block starting from the initial crack size. This is not the correct interpretation of the PM rule, which in general never updates the damage during the calculation, being such simplification the basis for its simplicity. A more correct interpretation of the Palmgren-Miner hypothesis in the context of long cracks leads to quite more general conclusions. Indeed, it is here shown that a correct application of PM rule follows directly from any propagation law of the form

$$\frac{da}{dN} = \Gamma \, \Delta S^{\eta} a^{\zeta} \tag{4.3}$$

Covering the equation for short cracks which actually is a special case of Equation (4.3), as well as the best-known Paris' law [28] defining the advancement of the crack in terms of stress intensity factor range

$$\frac{da}{dN} = C \, \Delta K^{m} \tag{4.4}$$

Where C and m are material parameters to be experimentally calibrated. This is just the basic form of the Paris' law and, strictly speaking, the PM rule does not follow from application in range where da/dN vs. ΔK data show deviations from the power law, like near threshold or near static failure. The Chapter then concludes with a discussion about what may be the reasons why the linear accumulation damage rule does not seem to work so well in general and when it could work instead.

4.2 Palmgren-Miner hypothesis from crack propagation laws

The starting point is the application of PM rule to a crack of characteristic size a, considering that Paris' law defines a crack advancement per cycle in terms of stress intensity factor, $\Delta K = f \, \Delta S (\pi a)^{1/2}$. Under the hypothesis that the geometric factor f is independent of the crack size, Paris' law (Equation (4.4)) can be integrated within the load block j, i.e., assuming m>2, from a_j to a_{j+1}:

$$\pi^{\frac{m}{2}}\left(\frac{m}{2}-1\right)C\left(f\,\Delta S_j\right)^m N_j = a_j^{1-\frac{m}{2}} - a_{j+1}^{1-\frac{m}{2}} \tag{4.5}$$

Summing all the N_B blocks in the load history up to failure, all the intermediate terms cancel out (of course, retardation and interaction effects have been neglected in the current analysis), hence

$$\sum_{j=1}^{N_B} \Delta S_j^m N_j = \frac{a_i^{1-\frac{m}{2}} - a_f^{1-\frac{m}{2}}}{\pi^{\frac{m}{2}}\left(\frac{m}{2}-1\right)C\,f^m} \tag{4.6}$$

Where a_i and a_f are the initial and final crack sizes respectively. Writing the factor $\nu_j=N_{fj}/\overline{N}=n_j/N_H$, (proportion of cycles spent at level j on the total number N_H), the life under the sum of all N_B blocks is:

$$\Delta\bar{S}_j^m\,\overline{N}_j = \frac{a_i^{1-\frac{m}{2}} - a_f^{1-\frac{m}{2}}}{\pi^{\frac{m}{2}}\left(\frac{m}{2}-1\right)C\,f^m}\cdot\frac{1}{G} \tag{4.7}$$

Having defined again, as done in Chapter 3, an amplification factor β for the base spectrum such that $\Delta\bar{S}=\beta\Delta S_{max}$ is a Gaßner stress range and ΔS_{max} is the largest stress range of the spectrum, so that each individual block stress range is that $\Delta S_j=\beta\Delta\bar{S}_j$. Finally, the multiplicative factor can be computed from the base spectrum as

$$G = \sum_{j=1}^{N_B} \nu_j \left(\frac{\Delta S_j}{\Delta\bar{S}}\right)^m = \nu_j \left(\frac{\Delta\bar{S}_j}{\Delta S_{max}}\right)^m \tag{4.8}$$

This result looks identical to the result that was recently obtained for the VA S/N (Gaßner) curve (i.e., the Wöhler SN curve for spectrum loading); see Ciavarella et al [29] where it was found that Gaßner curve is simply shifted CA S/N curves starting from power laws for CA loading, like Basquin's [30] law, and even much more in general. The integrated form of Paris law for CA (4.4) with G=1 is also a power law of the Basquin type, $N\cdot\Delta S^k=C_B$ where m=k and $C_B=(a_i^{1-m/2} - a_f^{1-m/2})/(\pi^{m/2}(m/2-1)C)$. This result is the exact same as obtained from applying the linear damage sum rule of PM for which the damage sum will be given by

$$D = \sum_{j=1}^{N_B}\frac{n_j}{N_j} = \sum_{j=1}^{N_B}\frac{n_j}{N_H}\cdot\frac{N_H}{N_j} = N_H\sum_{j=1}^{N_B}\frac{\nu_j}{N_j} = \frac{N_H}{C_B}\sum_{j=1}^{N_B}\nu_j\,\Delta S_j^k \tag{4.9}$$

The life under the sum of all j blocks is $\overline{N}$

$$\frac{1}{\overline{N}} = \frac{D}{N_H} = \frac{1}{C_B}\sum_{j=1}^{N_B}\nu_j\,\Delta S_j^k \tag{4.10}$$

And the result follows. If G=1, one simply has the CA S/N curve. Indeed, in Ciavarella et al. [29] it was also found that starting from Basquin's law and applying the PM rule, gives a Gaßner curve which is shifted from the CA S/N curve, but here dealing with specimen with a long crack, there is also the independent integration of Paris law that results in the same final equation. For a plain specimen or a notched one (if the theory of the critical distances can be applied), Ciavarella et al. [29] proved only that VA S/N curves were shifted CA S/N curves with the factor G. An important consideration is that the same procedure just outlined can be generalized for the law of Equation (4.3) as the exponent in ΔS plays no role in the summation, and the result carries over to the more general crack growth curves. Therefore, it is concluded that in this general class of crack propagation laws, including many short crack laws proposed in the past, as well as Frost-Dugdale, the Palmgren-Miner rule follows naturally and is equivalent to the integration of the crack growth.

4.2.1 Mean stress effect

Mean stress effects can be accounted for in spectrum loading by using the modified definition of shift factor recently given by D'Antuono and Ciavarella [31]. In this case, the starting point is Walker [32] equation for crack growth

$$\frac{da}{dN} = C_0 \left(\frac{\Delta K}{(1-R)^{1-\gamma}} \right)^m \tag{4.11}$$

Where C_0 is the intercept of Paris' law calculated at R=0 and γ is Walker exponent for mean stress correction. Under the hypothesis that the geometric factor f is independent of the crack size, Walker equation (4.11) can be integrated within the load block j, i.e., assuming m>2, from a_j to a_{j+1}

$$\pi^{\frac{m}{2}} \left(\frac{m}{2} - 1 \right) C_0 \left(f \frac{\Delta S_j}{\left(1 - R_j\right)^{1-\gamma}} \right)^m N_j = a_j^{1-\frac{m}{2}} - a_{j+1}^{1-\frac{m}{2}} \tag{4.12}$$

As done for Paris' law, summing all the N_B blocks in the load history up to failure leads to

$$\sum_{j=1}^{N_B} \left(\frac{\Delta S_j}{\left(1 - R_j\right)^{1-\gamma}} \right)^m N_j = \frac{a_i^{1-\frac{m}{2}} - a_f^{1-\frac{m}{2}}}{\pi^{\frac{m}{2}} \left(\frac{m}{2} - 1 \right) C_0 f^m} \tag{4.13}$$

Writing the life proportion spent at level j, $\nu_j = N_{fj}/\overline{N} = n_j/N_H$, and rearranging (4.19) leads to

$$\frac{1}{\overline{N}} = \frac{D}{N_H} = \frac{\pi^{\frac{m}{2}}\left(\frac{m}{2}-1\right)C_0\, f^m}{a_i^{1-\frac{m}{2}} - a_f^{1-\frac{m}{2}}} \sum_{j=1}^{N_B} \nu_j \left(\frac{\Delta S_j}{(1-R_j)^{1-\gamma}}\right)^m \tag{4.14}$$

Then normalizing the spectrum by its peak stress range ΔS_{max} such that $\Delta\bar{S} = \beta\Delta S_{max}$ (and $\Delta\bar{S}_j = \beta\Delta S_j$, $\bar{S}_{maxj} = \beta S_{maxj}$) and by varying the factor β, the full Gaßner curve is obtained again as

$$\Delta\bar{S}_i^m\, \overline{N}_j = \frac{a_i^{1-\frac{m}{2}} - a_f^{1-\frac{m}{2}}}{\pi^{\frac{m}{2}}\left(\frac{m}{2}-1\right)C_0\, f^m} \cdot \frac{1}{G} \tag{4.15}$$

Where, as in Chapter 3, G now accounts for mean stress effect, being

$$G = \sum_{j=1}^{N_B} \nu_j \left(\frac{S_{maxj}^{1-\gamma}\, S_{aj}^{\gamma}}{S_{a,max}^2}\right)^k \quad (a)$$

$$G = \sum_{j=1}^{N_B} \nu_j \left(\frac{S_{maxj}}{S_{a,max}}\left(\frac{1-R_j}{2}\right)^{\gamma}\right)^k \quad (b) \tag{4.16}$$

$$G = \sum_{j=1}^{N_B} \nu_j \left(\frac{S_{aj}}{S_{a,max}}\left(\frac{2}{1-R_j}\right)^{1-\gamma}\right)^k \quad (c)$$

4.3 Applying Palmgren-Miner hypothesis in a refined sense

The reason why Miller and Zachariah [7] suggested PM rule stems from the exponential crack growth, and not from Paris' law, may be that they computed the damage by considering at the denominator the number of cycles N_j which would lead to failure at the given stress range level,

$$\pi^{\frac{m}{2}}\left(\frac{m}{2}-1\right)C\left(f\,\Delta S_j\right)^m N_j = a_j^{1-\frac{m}{2}} - a_{fj}^{1-\frac{m}{2}} \sim a_j^{1-\frac{m}{2}} \tag{4.17}$$

Where it has been supposed that the final crack size a_{fj} is large enough to be neglected. Hence, dividing the actual number of cycles spent at each level n_j by N_j, the total damage is obtained as

$$D = \sum_{j=1}^{N_B} \frac{n_j}{Nj} = \sum_{j=1}^{N_B} \frac{a_j^{1-\frac{m}{2}} - a_{j+1}^{1-\frac{m}{2}}}{a_j^{1-\frac{m}{2}}} \tag{4.18}$$

Which does not sum to 1. Indeed, considering small increments $a_{j+1}=a_j+\Delta a$, and then expanding in Taylor series

$$D = \sum_{j=1}^{N_B} \frac{n_j}{N_j} = \sum_{j=1}^{N_B} \frac{1}{2} \frac{a_j^{-\frac{m}{2}}}{a_j^{1-\frac{m}{2}}} (m-2)\,\Delta a$$

$$= -\left(1-\frac{m}{2}\right) \sum_{j=1}^{N_B} \frac{\Delta a}{a} \tag{4.19}$$

$$\xrightarrow{\Delta a \to 0} -\left(1-\frac{m}{2}\right) \int_{a_i}^{a_f} \frac{da}{a} = -\left(1-\frac{m}{2}\right) \ln \frac{a_f}{a_i}$$

That in general is $\gg 1$. For instance, if $a_f=1{,}000 \cdot a_i$, then $\ln(a_f/a_i) \approx 6.9$. This is only valid for $m>2$, and approximately as (4.19) was expanded in Taylor series, and neglected the final values of the crack at failure at each stress range level. For example, for $m=4$, this means a spurious artificial increase of damage of 7. There could be also an effect of load sequence for discrete spectra, if these approximations were removed. Miller and Zachariah [7] mention this interpretation of the PM rule and, therefore, state that the PM hypothesis is based on an exponential fatigue crack growth law, i.e., Paris for $m=2$, as in this case, repeating the process just completed for $m>2$, one obtains simply (similar to their Equation 3)

$$D = \sum_{j=1}^{N_B} \frac{n_j}{N_j} = D = \sum_{j=1}^{N_B} \frac{\ln a_j/a_i}{\ln a_{fj}/a_i} = \tag{4.20}$$

Neglecting the change of a_{fj} with ΔS (considering a given final crack size that is dictated by static failure $K_{Ic} \cdot (1-R) = f \cdot \Delta S_j \cdot (\pi a_{fj})^{1/2}$, where $R = S_{min}/S_{max}$ is the load ratio and K_{Ic} is static toughness) and neglecting the influence of ΔS_j on a_{fj}

$$D = \frac{1}{\ln \frac{a_f}{a_i}} \cdot \sum_{j=1}^{N_B} \ln \frac{a_{j+1}}{a_j} = \frac{1}{\ln \frac{a_f}{a_i}} \cdot \left(\ln \frac{a_2}{a_1} + \ln \frac{a_3}{a_2} + \cdots + \ln \frac{a_f}{a_{N_B-1}} \right)$$

$$= \frac{1}{\ln \frac{a_f}{a_i}} \cdot \ln \frac{a_f}{a_1} = 1 \tag{4.21}$$

Since $a_i=a_1$. This satisfies the PM hypothesis. In view of the general correct interpretation, the PM rule should apply rather commonly, including the case of short cracks. However, since it cannot be stated that "fatigue life is dominated" by initiation, as it is often believed for CA loading at low levels of stress range, in the case of short cracks there is inevitably the sum of the two fatigue phases (initiation and propagation),

and probably this makes the PM rule invalid. Indeed, as reported in previous studies [33], [34] and in the Q-Q plots of Figure 4.1, damage sum D_{real} can be as low as D_{real}=0.001 in extreme cases, or as large as D_{real}=10 in other extreme cases, although the distribution is rather of the extreme values type, so that only 10% of cases, for example, D_{real}<0.1, or in another 10% of cases, it is D_{real}>1.

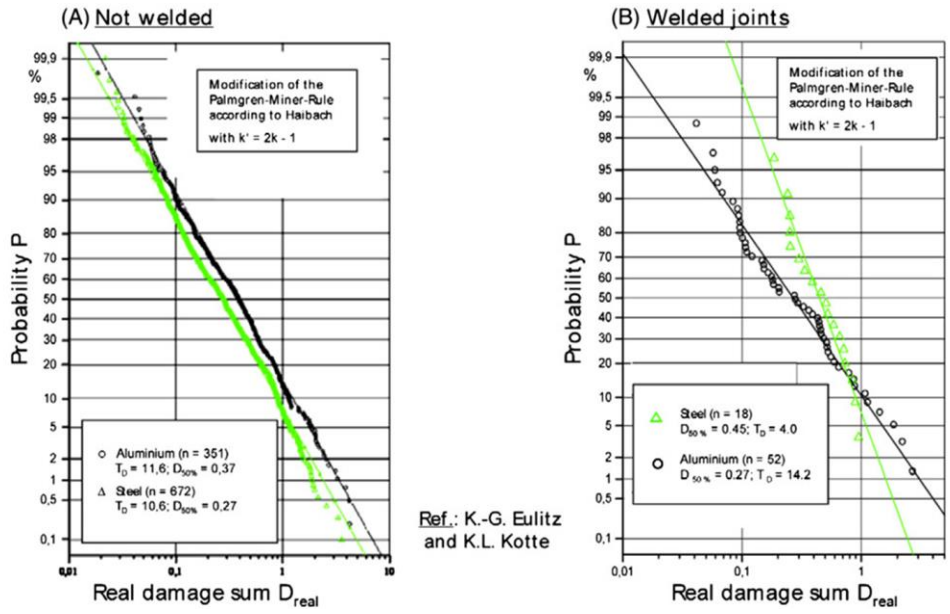

Figure 4.1: Adapted from Eulitz and Kotte [33] and Sonsino[34]: Damage sum D_{real} can be as low as D_{real}=0.001 in extreme cases or as large as D_{real}=10 in other extreme cases

It is found that the median value is rather 0.4, from which the standards obtain the safety factors suggested for design purposes mentioned in § 4.1. It is interesting to note that in double linear damage rules like Miller and Zachariah [7], and also Manson and Halford [8], it is said that cycles at high strains tend to decrease the initiation life at cycles at lower strains, so they introduce a negative effect, accelerating failure. In crack propagation, the opposite is normally found, as overloads give "crack retardation" effects. This means that even double linear damage rules would need to be adapted to crack propagation effects and tuned appropriately and it is not clear if this could be done in the general context. In the most common case, when there is crack initiation and propagation, it is unclear what their benefit could be, and indeed, this may explain their very limited success. When dealing with long cracks, there have been very few investigations of PM rule, perhaps because overload effects were found, and an attempt was immediately started to deal with them accurately. Not only Miller and Zachariah [7], but also in this context, early authors (Schijve and Broek [35]) interpreted PM rule in the "refined sense", exacerbating the increase of damage. Indeed, in Schijve and Broek [35] the ratio of final to initial crack length is 30/5=6, hence the spurious artificial increase of damage (4.20) is (for their material having

m=4), i.e. $(m-2)/2 \cdot \ln(a_f/a_i) \approx 1.8$. This means that their result that gust load fatigue tests the predicted damage at failure was fairly high, namely, of the order 2 to 4, should be significantly reconsidered to be not so high, of the order 1 to 2, which is very close to values of a round-robin exercise that is going to be described. Therefore, despite clearly there are overload effects as it is well known, they do not produce such tremendous effect on the linear damage accumulation. A fortiori one of the conclusions from Schijve and Broek [35] is valid: *"The Palmgren-Miner rule will give conservative crack rate predictions … it can be a useful tool to fix inspection periods for 'fail-safe' aircraft structure."* Today, NASGRO™ equation [10] (formerly known as Forman equation) is considered to be among the best possible crack growth prediction methods. It does attempt to consider load sequence effects with "interaction models" of various complexity. However, as it can be read in paragraph 2.1.7.6 (Notes on using the Load Interaction Models): "*In general, caution should be exercised when these models are used because they can be unconservative compared with the non-interaction model. This is so because the dominant effect modelled is retardation, even if accelerated growth is predicted in a few cases. Before applying these models for life predictions, it is recommended that the user gain sufficient experience and fine tune the various model parameters based on comparisons with test data for the kind of spectra relevant to the use."* Obviously, a calculation based on PM rule would work similarly to integration of Paris law with non-interaction models, at least in the sense that no overload effect and other memory effects are considered and within the assumption that geometrical factors in the crack size do not change during propagation, which is largely satisfied in cases when cracks are relatively small for much of their life. Hence, with respect to a full NASGRO™ calculation without load interaction, the PM rule will often be almost equivalent. Based on Table 4 of the NASGRO™ manual [10], which in turn reports a large set of data from a round-robin exercise [9] with a material having a rather good form of Paris law crack propagation law, with m very close to 3 (2219-T851 aluminum), some findings in the present paper seem confirmed. The paper deals with a center-cracked tension specimens (so that geometrical factors are probably constant over much of the fatigue propagation), under random spectrum loading of interest of a typical fighter aircraft air-to-air (A-A), air-to-ground (A-G), instrumentation and navigation (I-N), and composite missions. Indeed, even though the round-robin exercise was made with slightly different forms of crack propagation law than Paris law, the results are very encouraging, and they are relevant for spectrum loading of engineering interest, and with high quality data, although since 1981 of course the crack propagation codes may have improved. As in the previous studies[9], [10], load interaction models despite their

complexity lead to unconservative results unless the parameters are finely tuned; the non-interaction assumption seems to be more appealing (as indeed recommended in the NASGRO™ manual after all). Indeed, they lead to errors that are certainly not very large, with total life predicted very close to the real life measured, as reported in Table 4.1 (see second and third columns). And what is important to notice, with respect to the PM rule, is that they are much closer to correct than the real damage sum, D_{real}, from Table 4.1 was suggesting. Remarkably the damage sums in this round-robin exercise are not too different from those of Schijve and Broek [35], once the latter are corrected for the misinterpretation of PM damage rule. Hence, in general, the error in applying the PM rule in the most general cases could be attributed to various factors: (i) either the laws governing crack propagations are not correctly of the form above (separate variables power law forms) and in particular not of the exponential type (ii) or they are correct for short cracks, but differ largely when propagation stage is reached (and probably they are no longer exponential, but rather of the form expected from the integration of Paris law), in which case a single exponential law should not be used. These effects tend to make the damage sum too low; (iii) there are strong sequence effects (and, overloads) that make the damage sum too high.

Table 4.1: Ratio test over predicted life N_{test}/N_{pred} for ASTM (American Section of the International Association for Testing Materials)round-robin spectra

Loading Spectrum	Spec No	Stress, ksi	Test Cycles	Non Int NASGRO	Non Int Walker	Willenborg Walker R=3	Willenborg Generalized R=3	Willenborg Modified Φ_0=0.4	Strip Yeld	Constant Closure C_{fspec}=0.5
Air-Air	M-81	20	115700	0.78	0.71	0.49	0.54	0.54	0.62	0.7
	M-82	30	58585	1.27	0.92	0.62	0.87	0.92	1.27	1.15
	M-83	40	18612	1.28	0.79	0.54	0.88	0.94	1.71	1.16
Air-Grn	M-84	20	268908	0.86	0.77	0.51	0.57	0.55	0.52	0.6
	M-85	30	95642	1.25	0.98	0.63	0.81	0.82	0.98	0.87
	M-86	40	36397	1.24	1.04	0.67	0.99	1.04	1.64	1.06
Ins-Nav	M-88	30	380443	1.36	1.19	0.56	0.66	0.59	0.51	1.23
	M-89	40	164738	1.73	1.37	0.63	0.8	0.79	0.92	1.56

Note: Material 2219-T851, L-TAL. Data in Table 4 of NASGRO® manual [10] and in turn based on Chang and Hudson [9]. The non-interaction model prediction (which is a form very close to applying PM rule to crack propagation) is extremely close to real tests and often conservative by a little margin. Instead, interaction models predict often unconservative results and sometimes by larger margins.

Conclusion

There has been a suggestion in the literature that PM should follow from exponential crack growth only [7]. This is shown to stem perhaps from an incorrect interpretation of PM rule, updating the damage during the damage sum, which was repeated also in some early assessment of PM rule for long cracks [35]. In the correct version, the Palmgren-Miner hypothesis follows instead directly from a much more general crack growth law, where the crack growth is proportional to the product of powers of stress amplitude and crack length. This includes several laws proposed in the past for short or long crack growth, and obviously Paris law. The reason why PM does not apply very accurately in general may stem from its use in context involving a change from initiation to propagation laws (which tends to make the damage sum too low), or obviously also sequence effects and in particular overloads effects in long crack propagation, which tend to make the damage sum too high. When correcting for the "refined" interpretation of PM rule for long crack, the rule may work not too bad, as for some important round-robin data on spectrum loading for an aluminum alloy used in military aircrafts, moreover neglecting interaction effects was found to be perhaps better than including them. The application of the PM rule as suggested by Ciavarella et al [29] leads to VA S/N curves that are shifted power laws of the CA curve, similarly to what was found plain specimen having power law S/N curves (Basquin's law) but also for notched cases, whenever the theory of the critical distance applies. Therefore, this provides a general framework to consider Gaßner curves. The use of generalized exponential crack growth during the entire lifetime (which seems closely related to the "lead crack fatigue lifing framework" [27]), even in the context of spectrum loading, seems to imply that the PM rule applies. Therefore, the same sort of accuracy is expected.

References

[1] M. Ciavarella, P. D'antuono, and A. Papangelo, 'On the connection between Palmgren-Miner rule and crack propagation laws', *Fatigue Fract. Eng. Mater. Struct.*, vol. 41, no. 7, pp. 1469–1475, 2018.

[2] M. A. Miner, 'Cumulative Damage in Fatigue', *J. Appl. Mech.*, vol. 3, pp. 159–164, 1945.

[3] A. G. Palmgren, 'Die Lebensdauer von Kugellagern (Life Length of Roller Bearings. In German)', *Z. Vereines Dtsch. Ingenieure VDI Z. ISSN*, pp. 0341–7258, 1924.

[4] A. B. Fatemi and L. Yang, 'Cumulative fatigue damage and life prediction theories: a survey of the state of the art for homogeneous materials', 1998.

[5] E. Haibach, *Analytical Strength Assessment of Components in Mechanical Engineering: FKM-Guideline*. VDMA, 2003.

[6] H. L. Leve, 'Cumulative damage theories', *Met. Fatigue Theory Des.*, vol. A. F. Madayag Ed., pp. 170–203, 1960.

[7] K. J. Miller and K. P. Zachariah, 'Cumulative damage laws for fatigue crack initiation and stage I propagation', *J. Strain Anal. Eng. Des.*, vol. 12, no. 4, pp. 262–270, Oct. 1977.

[8] S. S. Manson and G. R. Halford, 'Practical implementation of the double linear damage rule and damage curve approach for treating cumulative fatigue damage', *Int. J. Fract.*, vol. 17, no. 2, pp. 169–192, Apr. 1981.

[9] J. Chang and C. Hudson, Eds., *Methods and Models for Predicting Fatigue Crack Growth Under Random Loading*. West Conshohocken, PA: ASTM International, 1981.

[10] S. R. Mettu *et al.*, 'NASGRO 3.0: A software for analyzing aging aircraft', 1999.

[11] M. Skorupa, T. Machniewicz, J. Schijve, and A. Skorupa, 'Application of the strip-yield model from the NASGRO software to predict fatigue crack growth in aluminium alloys under constant and variable amplitude loading', *Eng. Fract. Mech.*, vol. 74, no. 3, pp. 291–313, Feb. 2007.

[12] J. Maierhofer, R. Pippan, and H.-P. Gänser, 'Modified NASGRO equation for physically short cracks', *Int. J. Fatigue*, vol. 59, pp. 200–207, 2014.

[13] J. Maierhofer, R. Pippan, and H.-P. Gänser, 'Modified NASGRO equation for short cracks and application to the fitness-for-purpose assessment of surface-treated components', *Procedia Mater. Sci.*, vol. 3, pp. 930–935, 2014.

[14] J. Newman, E. Phillips, M. Swain, and R. Everett, 'Fatigue Mechanics: An Assessment of a Unified Approach to Life Prediction', in *Advances in Fatigue Lifetime Predictive Techniques*, M. Mitchell and R. Landgraf, Eds. West Conshohocken, PA: ASTM International, 1992, pp. 5–27.

[15] N. E. Frost and D. S. Dugdale, 'The propagation of fatigue cracks in sheet specimens', *J. Mech. Phys. Solids*, vol. 6, no. 2, pp. 92–110, Jan. 1958.

[16] F. R. Shanley, 'A theory of fatigue based on unbonding during reverse slip', RAND Corporation, Santa Monica, CA, RAND-P-350, Nov. 1952.

[17] H. Nisitani, 'Unifying treatment of fatigue crack growth laws in small, large and non-propagating cracks', *Mech. Fatigue*, vol. 151, 1981.

[18] M. Goto and H. Nisitani, 'Fatigue life prediction of heat-treated carbon steels and low alloy steels based on a small crack growth law', *Fatigue Fract. Eng. Mater. Struct.*, vol. 17, no. 2, pp. 171–185, 1994.

[19] H. Nisitani, M. Goto, V. Fourman, and R. Eliasi, 'A small-crack growth law and its application to the evaluation of fatigue life', in *EGF1*, 1986.

[20] H. Nisitani, M. Goto, and N. Kawagoishi, 'A small-crack growth law and its related phenomena', *Eng. Fract. Mech.*, vol. 41, no. 4, pp. 499–513, Mar. 1992.

[21] Y. Murakami, S. Harada, T. Endo, H. Tani-Ishi, and Y. Fukushima, 'Correlations among growth law of small cracks, low-cycle fatigue law and applicability of miner's rule', *Eng. Fract. Mech.*, vol. 18, no. 5, pp. 909–924, Jan. 1983.

[22] Y. Murakami and K. J. Miller, 'What is fatigue damage? A view point from the observation of low cycle fatigue process', *Int. J. Fatigue*, vol. 27, no. 8, pp. 991–1005, Aug. 2005.

[23] N. Pugno, M. Ciavarella, P. Cornetti, and A. Carpinteri, 'A generalized Paris' law for fatigue crack growth', *J. Mech. Phys. Solids*, vol. 54, no. 7, pp. 1333–1349, Jul. 2006.

[24] M. T. Todinov, 'Necessary and sufficient condition for additivity in the sense of the Palmgren–Miner rule', *Comput. Mater. Sci.*, vol. 21, no. 1, pp. 101–110, May 2001.

[25] M. Ciavarella and A. Papangelo, 'On the distribution and scatter of fatigue lives obtained by integration of crack growth curves: Does initial crack size distribution matter?', *Eng. Fract. Mech.*, vol. 191, pp. 111–124, Mar. 2018.

[26] A. P. Berens, P. W. Hovey, and D. A. Skinn, 'Risk Analysis for Aging Aircraft Fleets. Volume 1: Analysis', DAYTON UNIV OH RESEARCH INST, Oct. 1991.

[27] L. Molent, S. A. Barter, and R. J. H. Wanhill, 'The lead crack fatigue lifing framework', *Int. J. Fatigue*, vol. 33, no. 3, pp. 323–331, Mar. 2011.

[28] P. C. Paris and F. Erdogan, *A Critical Analysis of Crack Propagation Laws*. ASME, 1963.

[29] M. Ciavarella, P. D'antuono, and G. P. Demelio, 'A simple finding on variable amplitude (Gassner) fatigue SN curves obtained using Miner's rule for unnotched or notched specimen', *Eng. Fract. Mech.*, vol. 176, pp. 178–185, May 2017.

[30] O. H. Basquin, 'The exponential law of endurance tests', in *Proc Am Soc Test Mater*, 1910, vol. 10, pp. 625–630.

[31] P. D'Antuono and M. Ciavarella, 'Mean stress effect on Gaßner curves interpreted as shifted Wöhler curves', *ArXiv Prepr. ArXiv190913324*, 2019.

[32] K. Walker, 'The Effect of Stress Ratio During Crack Propagation and Fatigue for 2024-T3 and 7075-T6 Aluminum', *Eff. Environ. Complex Load Hist. Fatigue Life*, Jan. 1970.

[33] K. G. Eulitz and K. L. Kotte, 'Damage accumulation limitations and perspectives for fatigue life assessment', in *Proceedings of Materials week 2000*, 2000, pp. 25–28.

[34] C. M. Sonsino, 'Fatigue testing under variable amplitude loading', *Int. J. Fatigue*, vol. 29, no. 6, pp. 1080–1089, Jun. 2007.

[35] J. Schijve and D. Broek, 'Crack propagation: the results of a test programme based on a gust spectrum with variable amplitude loading', *Aircr. Eng. Aerosp. Technol.*, vol. 34, no. 11, pp. 314–316, 1962.

5 An analytical relation between Weibull's and Basquin's laws

Introduction

In this Chapter, the advantages of introducing a more versatile S/N curve model are investigated. Such necessity may arise from the need of having a more realistic S/N curve whose trend towards the fatigue limit can be controlled, instead of being a knee. The Chapter is directly extracted from an article by the author [1] titled *"An analytical relation between Weibull's and Basquin's laws for smooth and notched specimens and application to constant amplitude fatigue"*. Starting from the classical definition of stress-life Wöhler curve in the form of Basquin's law, an analytical procedure for the calibration of the four parameters Wöhler curve (Weibull's law) for a plain specimen is proposed. The higher precision of the four parameters S/N curve is highly evidenced by Weibull stating in his book [2], in disagreement with Moore and Kommers [3], that the knee that seem to show S/N diagrams *"is an accidental phenomenon caused by the joint effect of a large scatter in fatigue life and too small number of observations"*. Furthermore, as suggested by Shanley [18] in the 1956 "Colloquium on Fatigue" [19], Basquin's law fails to model low cycle fatigue since it does not predict correctly the strain at high stresses, while by using Weibull's law one supposes that a stress close to the ultimate tensile strength causes much lower strain, hence it can be applied a certain number of times without failure. This is also confirmed by Epremian and Mehl [20] that in 1952 showed that an S/N diagram when the alternate strength is close to the ultimate tensile strength, can be fit with very good agreement by a probability scale instead of a logarithmic scale and this suggests that at high stresses alternating plastic strain dependence on stress amplitude is primarily of statistic nature. Thence, for the reasons just evidenced the smooth Weibull's S/N curve model is certainly a more realistic form of modelling stress life fatigue data with respect to a Basquin's law truncated at the fatigue limit and at some low cycle fatigue strength. Similarly, in crack growth analysis the NASGRO™ equation in its original and modified forms [4]–[6] is a much more realistic representation of the Paris' law[7] truncated below the threshold stress intensity factor and above the limit stress intensity factor. Nevertheless, Basquin's law has been extensively used by most of the researchers and engineers until these days because of

its simplicity and consequently most of the fatigue databases for S/N curves available in literature are given in the form of Basquin's law truncated at the fatigue limit. To the author's knowledge, nobody before has ever tried to relate Basquin's and Weibull's laws and this shall be done in this work. The usefulness of this exercise can be found in the fact that many stress life models are based on Basquin's law, thus finding an analytical relationship with Weibull's law could make simpler to rewrite these models by means of a more sophisticated and realistic model, plus an entire database of Basquin's law coefficients might be converted into Weibull's law by simply applying an analytical formula. Moreover, since "the more parameters need to be calibrated, the more experimental data need to be known", having a direct link between a four and a two parameters model allows to reduce the amount of experimental data necessary to reliably characterize Weibull's law. Indeed, as also Weibull states in his book [2], tuning the parameters of Weibull's law is not as immediate as doing the same thing with a pure power law. On this purpose, Weibull suggests a graphical and a semi-analytical trial and error procedure to derive the parameters for his equation from experimental data. With the model described here, one could find the power law which interpolates the data in the high cycle fatigue regime and then the calculation of the four parameters is straightforward. Finally, the important matter of developing a unique S/N curve model based on Weibull's law which can account for the notch effect is addressed. The obtained parameters are then adjusted by means of an additional slope factor preserving the inflection point of the curve while changing its slope in order to model the experimental observations in which an increase of the scatter in life prediction is observed when reducing the stress amplitude. The same approach has then been adopted to calibrate the Weibull's law parameters for a notched specimen, and the fitting slope factor has been found to be a value that changes with the material but remains constant with the stress concentration factor. The findings have been validated with existing experimental data on 2024-T3 aluminum alloy and normalized SAE 4130 steel.

5.1 Wöhler curve in the form of Basquin's law

When dealing with Basquin's law, it must be considered that in its truncated form it depends on four parameters, i.e.

$$\begin{cases} S(N) = & S_u = \bar{b} \cdot N_u^{\bar{a}} & 1 \le N \le N_u \\ S(N) = & \bar{b} \cdot N^{\bar{a}} & N_u < N \le N_e \\ S(N) = & S_e = \bar{b} \cdot N_e^{\bar{a}} & N > N_e \end{cases} \tag{5.1}$$

Here the four parameters are the slope $\bar{a}$, the fatigue strength at 1 cycle (or at one reversal) $\bar{b}$, the ultimate tensile strength S_u (N_u) and the fatigue limit S_e(N_e). Equation (5.1) corresponds to a piecewise straight line in a log-log plot. Basquin's law is also currently the most used in the field of research since because of its simplicity it can be easily manipulated. Even the author used extensively Basquin's law in his works to derive new simplified models to predict variable amplitude fatigue life [8] or to derive another smoothed model which could account for the notch effect in the case of a plate with circular holes [9].

5.2 Wöhler curve in the form of Weibull's law

Finding an analytical link between Basquin's and Weibull's laws does not introduce new variables and complexity to the problem since in both cases four parameters are necessary to draw the Wöhler curve; on the contrary, the user will be able to condensate a piecewise function into a single equation and consequently, no further experimental analysis should be needed to re-characterize a material by means of Weibull's S/N curve model. In this way, Weibull's law can be intended as a direct smoothing of the truncated power law. Weibull's law was defined such that three constraints had to be satisfied when plotting it in semilogarithmic coordinates: (i) slope equal to zero for $N \to 0$, (ii) slope equal to zero for $N \to \infty$ and (iii) the curve must show an inflection point. The same constraints must be valid in a log-log plot. The law along with its derivatives w.r.t. N is

$$\begin{cases} S(N) = & b \cdot (N + B)^a + S_e & (a) \\ S'(N) = & \dfrac{dS(N)}{dN} = b \cdot a \cdot (N + B)^{a-1} & (b) \\ S''(N) = & \dfrac{d^2S(N)}{dN^2} = b \cdot a \cdot (a - 1) \cdot (N + B)^{a-2} & (c) \end{cases} \tag{5.2}$$

The parameters a, b, B, S_e must be calculated such that the new S/N curve respects the constraints defined by the Basquin's law. On this purpose, it is assumed that the

slope of the Basquin's law matches the first derivative of Weibull's law in the inflection point N_i of the log-log plot, i.e. $\log_{10} S(N)_{/\log_{10} N}\big|_{N=N_i} = \bar{a}$.

$$\begin{cases} \log_{10} S(N)_{/\log_{10} N}\big|_{N=N_i} = \bar{a} \\ \log_{10} S(N)_{/\log_{10} N \log_{10} N}\big|_{N=N_i} = 0 \end{cases} \tag{5.3}$$

Using the equations defined in Appendix gives

$$\begin{cases} \dfrac{b \cdot a \cdot (1 + B/N_i)^{a-1}}{b \cdot (1 + B/N_i)^a + S_e} = \bar{a} \quad (a) \\ (N_i + B) \cdot (1 - a) + N_i \cdot (a - 1) = 0 \quad (b) \end{cases} \tag{5.4}$$

The hypothesis on the slope of the inflection point is then combined with the static failure and the fatigue limit conditions, i.e.:

$$\begin{cases} b = (S_u - S_e) \cdot B^{-a} & (a) \\ S(N \to \infty) = S_e & (b) \end{cases} \tag{5.5}$$

Equation (5.4)(b) can be expressed as function of the auxiliary variable $\alpha = B/N_i$ corresponding to the exponent of Weibull's law in S/log(N) coordinates (it is a positive number since Weibull uses a minus sign at the exponent in his notation). With some simple passages the system of equations is then solved for α giving the following implicit equation

$$\left(\frac{\alpha + 1}{\alpha}\right)^{\alpha+1} = -\frac{\bar{a} S_e}{S_u - S_e} \quad \text{for } 0 < \alpha < 1 \tag{5.6}$$

Once numerically solved, Equation (5.6) gives the ratio $\alpha = B/N_i$. Then, the value of N_i is retrieved by considering that both the classical S/N curve and the smoothed one pass by $(N_i, S(N_i))$, i.e. equation (5.1) has to be equal to Equation (5.2)(a) for $N = N_i$

$$\bar{b}\, N_i^{\,\bar{a}} = b \cdot (N_i + B)^a + S_e \tag{5.7}$$

or

$$b = \frac{\bar{b}\, N_i^{\,\bar{a}} - S_e}{N_i^a \cdot (1 + \alpha)^a} \tag{5.8}$$

By using again Equation (5.4)(a) and the definition of α, an explicit expression of the inflection point N_i is found

$$N_i = \left(\left(\frac{1}{\alpha} + 1\right)^a \cdot \frac{(S_u - S_e)}{\bar{b}} + \frac{S_e}{\bar{b}}\right)^{1/\bar{a}} \tag{5.9}$$

The value of b can be found from Equation (5.5)(a) for N=0 or from Equation (5.8)s. From the above passages, the complete set of equations which "converts" Basquin's law into Weibull's law is

$$\begin{cases} \left(\dfrac{\alpha+1}{\alpha}\right)^{\alpha+1} = -\dfrac{\bar{a}\,S_e}{S_u - S_e} & \text{(a)} \\ a = \alpha\cdot(\bar{a}-1)+\bar{a} & \text{(b)} \\ B = \alpha\cdot\left(\left(\dfrac{1}{\alpha}+1\right)^{a}\cdot\dfrac{(S_u-S_e)}{\bar{b}}+\dfrac{S_e}{\bar{b}}\right)^{1/\bar{a}} & \text{(c)} \\ b = (S_u - S_e)\cdot B^{-a} & \text{(d)} \end{cases} \tag{5.10}$$

Note that for S_e=0 (no fatigue limit) the smoothed S/N curve shows no inflection point which implies $\alpha\rightarrow 0$, and the problem is again solvable in closed form. For a full analytical solution of the system shown in (5.10), an approximate form of Equation (5.10)(a) should be found. The basic consideration is that $\left(\frac{\alpha+1}{\alpha}\right)^{\alpha+1} = \left(\frac{\alpha+1}{\alpha}\right)\cdot\left(\frac{\alpha+1}{\alpha}\right)^{\alpha}$ and the approximate form to be found must be valid in the range $0<\alpha<1$. Hence, by studying the function $\left(\frac{\alpha+1}{\alpha}\right)^{\alpha}$, one finds that in the range of interest it can be approximated by an equilateral translated hyperbola $\frac{A_1x+A_3}{A_2x+A_3}$, where the coefficients A_1=5, A_2=2 and A_3=1 minimize the error between the correct and the approximated form, with a maximum error lower than 2.5%, as shown in Figure 5.1. Thus, the full analytical approximated solution to the classical Wöhler curve smoothing problem proposed in this work is

$$\begin{cases} \alpha = \dfrac{6-\gamma+\sqrt{(6-\gamma)^2+4(2\gamma-5)}}{2(2\gamma-5)} & \text{(a)} \\ a = \alpha\cdot(\bar{a}-1)+\bar{a} & \text{(b)} \\ B = \alpha\cdot\left(\left(\dfrac{1}{\alpha}+1\right)^{a}\cdot\dfrac{(S_u-S_e)}{\bar{b}}+\dfrac{S_e}{\bar{b}}\right)^{1/\bar{a}} & \text{(c)} \\ b = (S_u - S_e)\cdot B^{-a} & \text{(d)} \end{cases} \tag{5.11}$$

Where $\gamma=(-\bar{a}S_e/(S_u-S_e))^{1/(\bar{a}-1)}$.

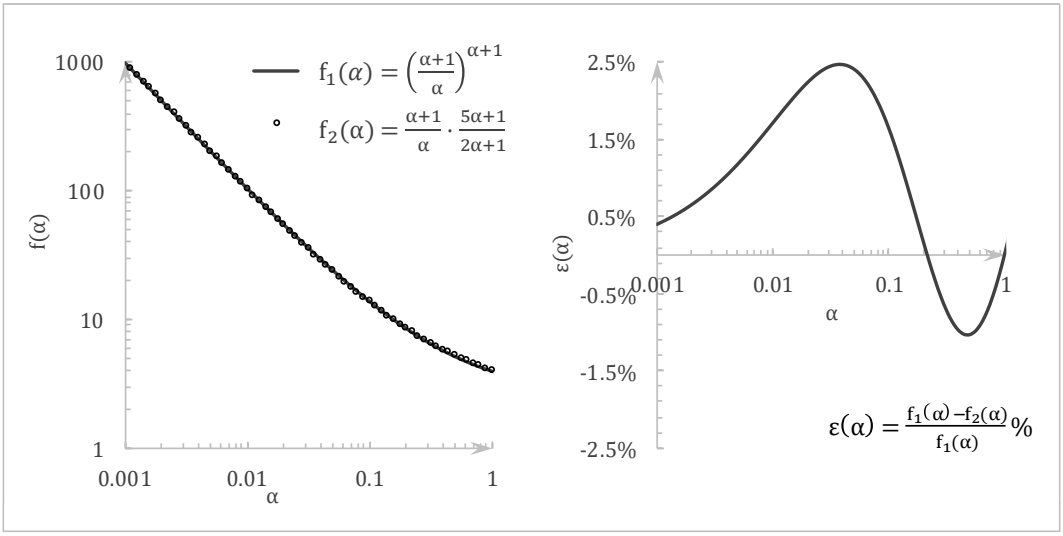

Figure 5.1: Approximate form of $\left(\frac{\alpha+1}{\alpha}\right)^{\alpha+1}$ (left side) and relative error between $\left(\frac{\alpha+1}{\alpha}\right)^{\alpha+1}$ and $\frac{5\alpha+1}{2\alpha+1}$ (right side) in the range $0<\alpha<1$

5.3 Discussion of the results

As written in the introduction, all the stress-life material data available in literature in terms of Basquin's law can be easily recalculated by means of the smoothing technique just explained providing Weibull's law data. As an example, consider a generic steel, in this case the material data for the two forms of S/N curve are:

Table 5.1: Example of material properties recalculation for a generic steel

Basquin's law		Weibull's law	
$\bar{b}$, MPa	1,796.4	b, MPa	6,715
$\bar{a}$	-0.1	a	-0.343
N_u, cycles	1,000	B, cycles	2,687
S_e, MPa	451.2	S_e, MPa	451.2

The truncated Basquin's law and Weibull's law are shown in Figure 5.2; in the low cycle fatigue regime Weibull's law is more conservative than the truncated Basquin's law, while almost a decade after the inflection point, the smoothed curve becomes less conservative w.r.t. the truncated power law since the transition to the fatigue limit appears too slow. A possible way to recalibrate these constants in order to get a more conservative curve and/or a better fit of experimental data shall be explained hereafter:

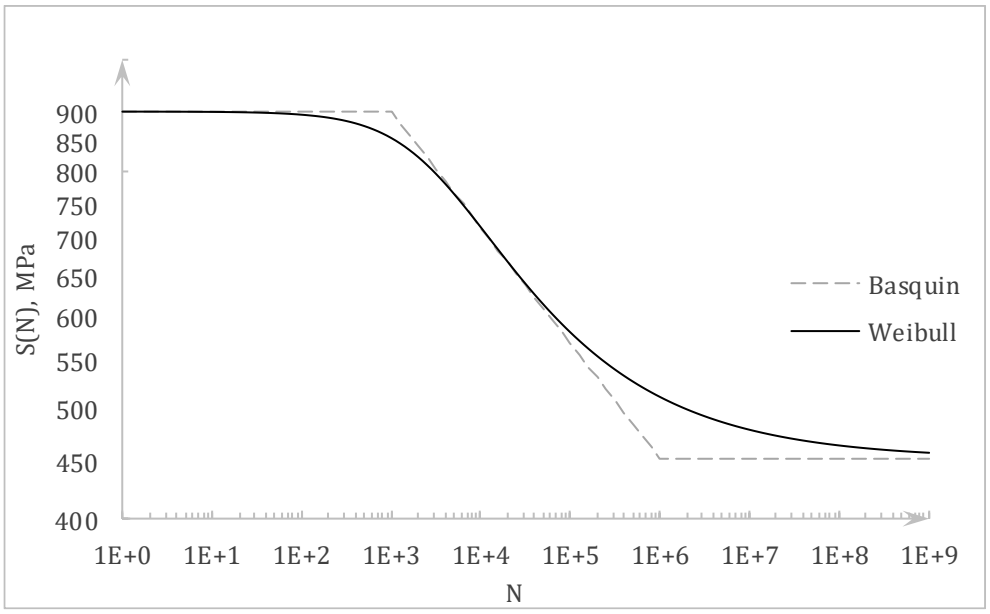

Figure 5.2: Comparison between Basquin's law and the corresponding derived Weibull's law

5.4 Techniques of recalibration of the constants

5.4.1 Graphical recalibration

If the experimental data require a steeper and more conservative curve in proximity of the fatigue limit, a smaller value of the exponent a should be chosen while keeping constant the inflection point N_i; on the contrary, if the transition to the fatigue limit is very smooth and should be modelled with a gentler slope, a higher value of the exponent should be used. In this way B, b, α vary consistently and the curve becomes more/less conservative in the very high cycle fatigue regime w.r.t. Basquin's truncated law, instead its first derivative for $N<N_i$ will not change too much. The definition of a slope factor f_a accomplishes the scope of changing the slope in the high cycle fatigue regime, i.e.:

$$\begin{cases} \check{a} = & f_a \cdot a & (a) \\ \check{\alpha} = & (a - \bar{a})/(\bar{a} - 1) & (b) \\ \check{B} = & N_i \cdot \check{\alpha} & (c) \\ \check{b} = & (S_u - S_e) \cdot \check{B}^{-\check{a}} & (d) \end{cases} \tag{5.12}$$

The family of curves deriving from changing the "slope" $\check{a}$ by multiplying a by $0<f_a<2$ is shown in Figure 5.3.

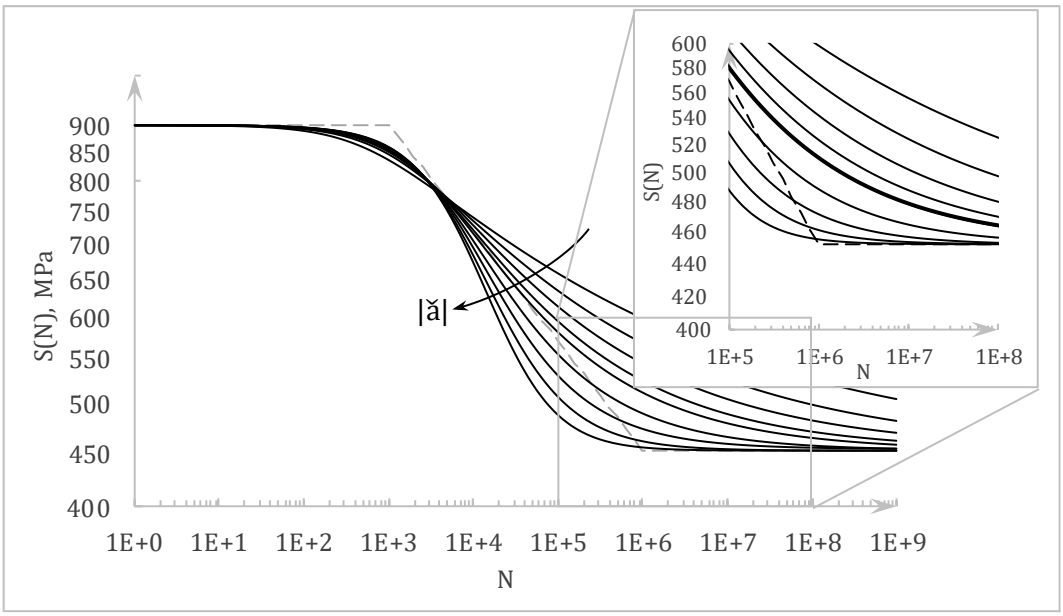

Figure 5.3: Family of S/N curves deriving from the analytical fitting of the basquin's law with decreasing $\check{\alpha}$

5.4.2 Statistical recalibration

The statistical calibration of the S/N curve parameters is usually done via least-squares method. The assumptions when approximating fatigue data with least squares by a pure power law are (i) that the N at prescribed S follows a lognormal distribution and (ii) that the variance of log(N) is constant over the tested range (hypothesis of homoscedasticity). The general equation of a least squares regression line is

$$Y = C_1 X + C_2 + \epsilon \tag{5.13}$$

Where ϵ is a random variable of error. The regression line is then

$$\hat{Y} = \hat{C}_1\, X + \hat{C}_2 \tag{5.14}$$

Where $\hat{C}_1, \hat{C}_2$ are the estimates obtained through the minimization of the sum of the squared deviations of the experimentally observed life from the predicted one considering n_f tests

$$\Delta^2 = \sum_{j=1}^{n_f} \left(Y_j - \hat{Y}_j\right)^2 = \sum_{j=1}^{n_f} \left(Y_j - (\hat{C}_1\, X_j + \hat{C}_2)\right)^2 \tag{5.15}$$

From the minimization of Δ^2 w.r.t. $\hat{C}_1, \hat{C}_2$, the estimated regression line is obtained:

$$\begin{cases} \hat{C}_1 = \dfrac{\sum_{j=1}^{n_f}(X_j - \overline{X})(Y_j - \overline{Y})}{\sum_{j=1}^{n_f}\left(X_j - \overline{X}\right)^2} & \text{(a)} \\ \hat{C}_2 = \overline{Y} - \hat{C}_1\overline{X} & \text{(b)} \end{cases} \tag{5.16}$$

Where $\overline{X} = 1/n_f \sum_{j=1}^{n_f} X_j$, $\overline{Y} = 1/n_f \sum_{j=1}^{n_f} Y_j$ are the average values of X and Y. The variance of Y_j on X_j is

$$\sigma^2 = \frac{1}{n_f - 1} \sum_{j=1}^{n_f} \left(Y_j - \left(\hat{C}_1 X_j + \hat{C}_2 \right) \right)^2 \tag{5.17}$$

Taking the decadic logarithm of the power law $S = \bar{b}\, N^{\bar{a}}$ gives $\mathrm{Log}(N) = \frac{1}{\bar{a}} \mathrm{Log}(S) + \frac{1}{\bar{a}} \mathrm{Log}(b)$, hence Y=Log(N) and X=Log(S), from which Basquin's law constants are

$$\begin{cases} \bar{a} = & 1/\hat{C}_1 & \text{(a)} \\ \bar{b} = & 10^{-\hat{C}_2/\bar{a}} & \text{(b)} \end{cases} \tag{5.18}$$

From Lee et al. [10], the coefficient of variation, defined as the ratio of the standard deviation to the mean, is estimated as $C_{\bar{a}} = \sqrt{10^{\bar{a}^2 \cdot \sigma^2} - 1}$. The design S/N curve deriving from this approach is obtained with a confidence level (CL) of 50%. The simplest strategy to obtain a design S/N curve with higher CL is to introduce the lower limit Y_L of Y at given X and level of confidence Kσ, where K is a multiplier, i.e.

$$Y_{L_j}(K) = \hat{Y}_j - K \cdot \sigma \tag{5.19}$$

Concerning the approximation of experimental data via Weibull's law and a required CL, the following three steps procedure could be applied: (i) calculate Basquin's law constants with the least squares method and the desired CL, (ii) calculate Weibull's law constants through Equations (5.11) and (5.12) with f_a=1 and (iii) calibrate the slope factor f_a through the least squares method considering Y=Log(N+B) and X=Log(S-S_e). In this way the smooth S/N curve can be represented as a power law from which $\check{a} = 1/\hat{C}_1$ and $\check{b} = 10^{-\hat{C}_2/\check{a}}$ and the value $\check{a}$ providing the 50% of CL can be found.

5.5 Notch effect

In the classical stress-life approach, the effect of notches can be accounted for through the definition of the material notch sensitivity factor q:

$$q = \frac{K_n - 1}{K_t - 1} \tag{5.20}$$

Where K_n is the technical stress concentration factor, i.e. the predicted ratio of the plain endurance limit to that for the notched member, and K_t is the theoretical elastic stress concentration factor. The notch sensitivity factor definition is based on Neuber's "building blocks" idea from 1946 [11], i.e. the material is not a continuum, but an

aggregate of building blocks and the stress gradient cannot develop across blocks. Thus, a characteristic length A_N, equal to the half-size of the block, was defined such that the notch sensitivity factor takes the form

$$q = \frac{1}{1 + \sqrt{A_N/\rho}} \tag{5.21}$$

Where ϱ is the notch root radius and A_N is Neuber's constant. In 1952 the effective stress concentration factor K_f was experimentally measured for many materials by Kuhn and Hardrath [12] and also by Kuhn in a work from "Colloquium on Fatigue" [13] and good agreement was found with K_n. Thus, the approximation $K_n \approx K_f$ will be taken as valid. From Kuhn and Hardrath's work [12], the values of Neuber's constants giving the ratios $0.9<K_n/K_f<1.1$ are 0.02 in for aluminum alloys and 0.027 in for steels with $S_u \approx 115$ ksi. In 1949 Peterson [14] based on the approximation of a linear variation of the stress near the crack tip modified Neuber's Equation (5.21) as

$$q = \frac{1}{1 + A_P/\rho} \tag{5.22}$$

Where A_P is Peterson's material constant. Thus, by considering the notch effect, Basquin's law is then modified as also done by Nelson and Fuchs in "nominal stress range II method" [15]

$$\begin{cases} S(N) = & S_u = b_n \cdot N_u^{a_n} & 1 \le N \le N_u \\ S(N) = & b_n \cdot N_u^{a_n} & N_u < N \le N_e \\ S(N) = & S_e/K_f = b_n \cdot N_u^{a_n} & N > N_e \end{cases} \tag{5.23}$$

Where $a_n = \bar{a} - \mathrm{Log}_{10}(K_f)/\mathrm{Log}_{10}(N_e/N_u)$ and $b_n = S_u/N_u^{a_n}$. Equation (5.23) can be used to obtain the same system of equations of (5.10) or (5.11) with a_n and b_n in place of $\bar{a}$ and $\bar{b}$. An example of application of Basquin's law smoothing for both plain and notched specimen is given in Figure 5.4.

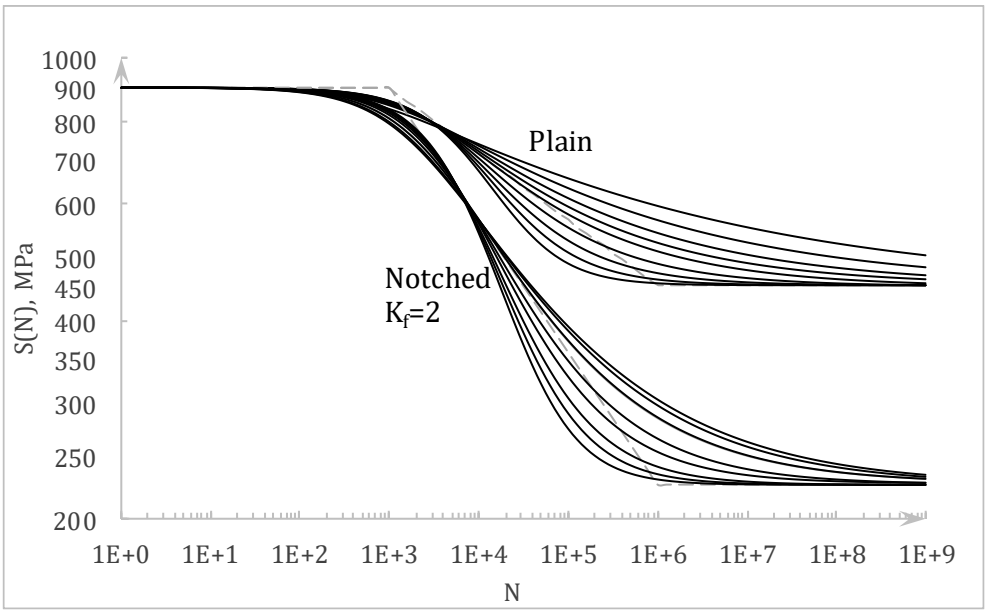

Figure 5.4: Comparison between an S/N curve for plain and notched member

5.6 Quantitative validation with experimental data

In 1956 the National Advisory Committee for Aeronautics (NACA) conducted a fatigue test program on plain and notched 2024-T3, 7075-T6 aluminum alloy and SAE 4130 steel sheet specimens [16]. The fatigue data from this program were merged with other previous test programs [17]–[21] to gather the huge amount of S/N data collected in the NACA Technical Note 3866 [16]. The materials tensile properties are listed in Table 5.2. The note was aimed to fully characterize the S/N curve shape for all the materials tested, from 10^0 to 10^8 fatigue cycles and for K_t=1.0, K_t=2.0 and K_t=4.0 with emphasis on the range between 2 and 10,000 cycles. The geometry of the specimens under test is shown in Figure 5.5. The specimens were axially loaded and, depending on the stress amplitude, the loading frequency was opportunely adjusted from 12 (manual control) to 1,800 (subresonant testing) cycles per minute. In the last figure of the note Illg [16] showed a plot of K_f vs the alternate stress observing that at very low number of cycles to failure $K_f \approx 1$ for all the materials testes, in good agreement with the S/N curve model later proposed by Nelson and Fuchs [15]. The maximum K_f is found when the alternate stress tends to the fatigue limit; this value is generally in good agreement with Neuber's empirical Equation (5.20). In this work the behavior of 2024-T3 aluminum alloy and normalized SAE 4130 steel have been considered in the case of fully reversed loading. Besides, results for 2024-T3 are applicable also to 7075-T6. In fact, *"due to the nearly identical fatigue properties of the T3, T351 and T4 conditions*

of 2024 and T6 and T651 conditions of 7075, no decision needs to be made between all these various conditions over the life region of interest" [22].

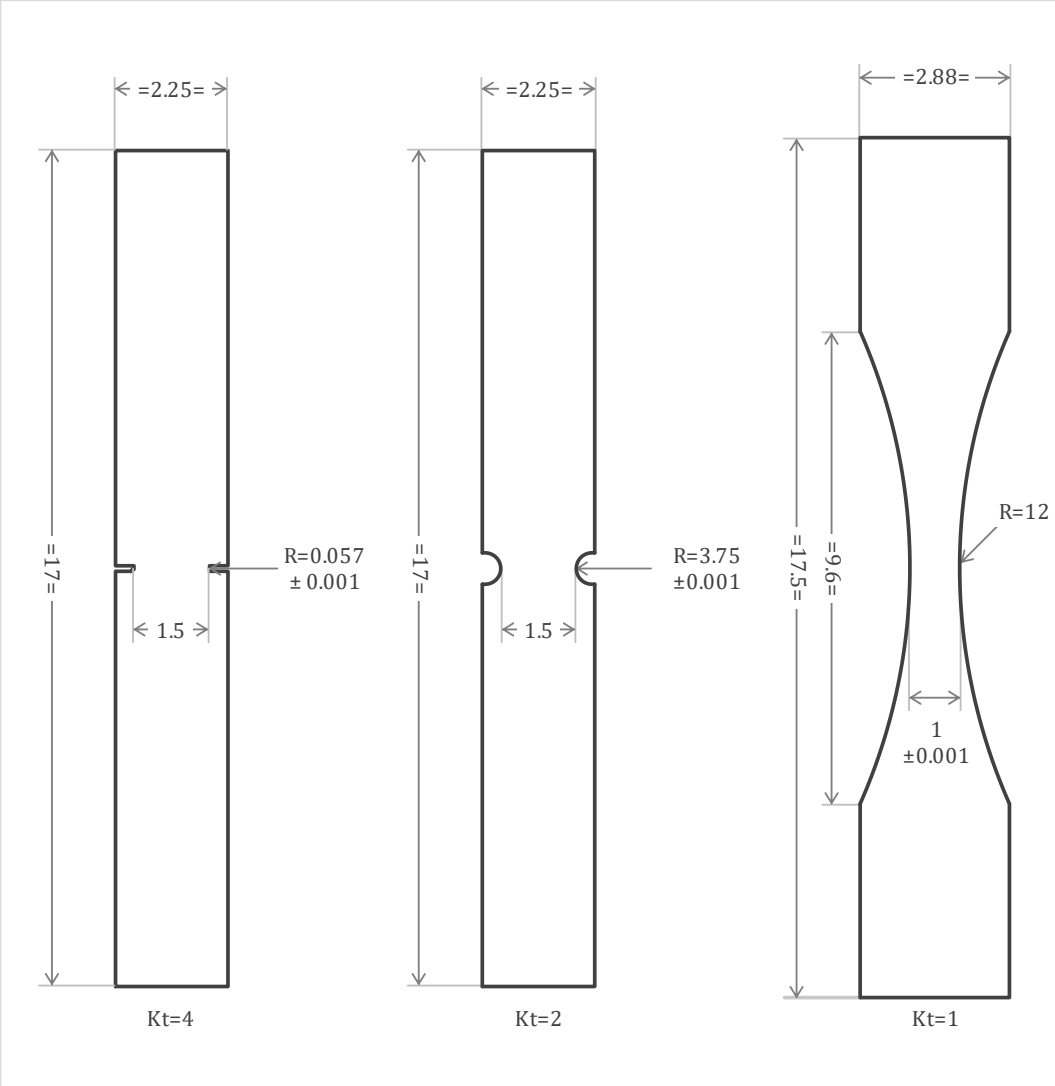

-

Figure 5.5– Configuration of sheet specimens, as in reference [16]. Lengths are in inches. Aluminum specimens are 0.09 inch thick; steel specimens are 0.075 inch thick

Table 5.2: Tensile properties of the materials analyzed (from Illg's Table 1 [16]) (*) σ^2 is the standard deviation

Material	Number of tests	Yield stress, (0.2 percent offset), ksi				Ultimate tensile strength, ksi				Total elongation, 2-inch gage length, percent				Young's modulus, ksi			
		Av.	Min.	Max.	σ (*)	Av.	Min.	Max.	σ (*)	Av.	Min.	Max.	σ (*)	Av.	Min.	Max.	σ (*)
2024-T3 aluminum alloy	148	52.1	46.9	59.3	1.7	72.1	70.3	73.4	0.9	20.3	15	25	1.89	10,500	10,150	10,750	134
7075-T6 aluminum alloy	152	75.5	70.7	79.8	1.4	83	79.8	84.5	1.1	12.3	7	15	1.27	10,200	10,000	10,550	104
Normalized SAE 4130 steel	149	93.9	87.4	102.2	2.1	115.9	111.4	124.6	1.8	15.2	12	18	1.06	29,400	28,200	31,500	660
Hardened SAE 4130 steel	9	174	168	178	---	180	178	183	---	8.3	8	9	----	29,900	29,200	30,800	---

Illg concludes his analysis with the following consideration: "The scatter in the results of the tests in the short-life range was remarkably small, whereas the tests at long lifetimes indicated considerably more scatter in the results" [16], in agreement with the capability of the model here described to vary consistently in proximity of the fatigue limit whilst keeping low scatter before the inflection point. All the S/N curves for the plain specimens have been calculated through the statistical procedure previously described with 50% of confidence level.

5.6.1 Plain specimens

As concerns the Al 2024-T3 plain specimens, from Table 5.2 $S_u = 72.1$ ksi, while Basquin's law parameters have been calculated with a linear regression in log(S)/log(N) coordinates between $2 \cdot 10^3$ and $5 \cdot 10^6$ cycles, consistent with the trend observed from experimental data, giving $\bar{b} = 308.34$ ksi and $\bar{a} = -0.191$; consequently $S_e(N_e) = 16.32$ ksi. Then, Weibull's law parameters have been calculated from Equation (5.11), giving $b = 1007.5$ ksi, $a = -0.347$ and $B = 4196$. In order to obtain the Weibull's law with 50% of confidence level, Equation (5.12) has been used to calculate and plot the linear regression in Log(S-S_e)/Log(N+B) coordinates. The factor $f_a = 1.15$ satisfies the required condition giving $\check{b} = 1743.9$ ksi, $\check{a} = -0.399$, and $B = 5591.7$. The S/N curve for normalized SAE 4130 steel has been calculated with the same procedure just introduced. All the fitting data are given in Table 5.3 and the final curves are shown in Log(S-S_e)/Log(N+B) coordinates in Figure 5.6. For both the materials it is evident a dramatic increase in the scatter of fatigue data with decreasing stress amplitude, as also underlined by Illg [16]. Hence, in this case the hypothesis of homoscedasticity is maybe too rough to draw the Wöhler curves with the desired CL.

Anyway, if the maximum variance is chosen to factorize the curve in stress (cfr. Equation (5.19)), the estimate will certainly be conservative.

Table 5.3: Fitting parameters for the S/N curve construction of the plain specimens

	Basquin		Weibull		Factorized Weibull	
2024-T3 aluminum alloy	$\bar{b}$, ksi	308.3	b, ksi	1007.5	$\check{b}$, ksi	1744
	$\bar{a}$	-0.191	a	-0.3469	$\check{a}$	-0.3989
	S_u, ksi	72.1	B, cycles	4196	$\check{B}$, cycles	5592
	S_e, ksi	16.3	S_e, ksi	16.3	S_e, ksi	16.3
					Implies f_a	1.15
Normalized SAE 4130 steel	$\bar{b}$, ksi	161.2	b, ksi	159.393	$\check{b}$, ksi	266.3
	$\bar{a}$	-0.0856	a	-0.1773	$\check{a}$	-0.257
	S_u, ksi	116	B, cycles	83	$\check{B}$, cycles	155
	S_e, ksi	43	S_e, ksi	43	S_e, ksi	43
					Implies f_a	1.45

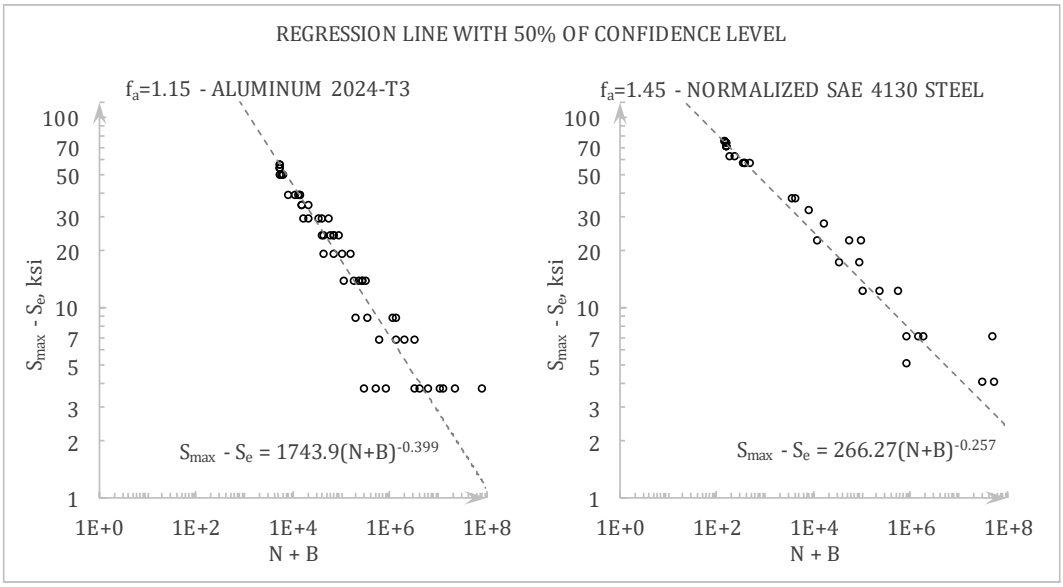

Figure 5.6: Statistical recalibration of Weibull's law parameters via least squares method for plain specimens. The scaling f_a used give 50% CL

5.6.2 Notched specimens

The S/N curves for the notched specimens have been calculated through the nominal stress range II method, i.e. Equation (5.23), applied to the best fit truncated Basquin's law for the plain specimen. The values of K_f have been calculated through Equation (5.20) and then compared with Figure 16 of the NACA Technical Note 3866 [16] where K_f is plotted vs the maximum stress. The values have been calculated through the Neuber's constants suggested by Kuhn and Hardrath's [12] which led to $K_f(K_t=2)\approx1.85$, $K_f(K_t=4)\approx2.90$ for aluminum and $K_f(K_t=2)\approx1.78$, $K_f(K_t=4)\approx2.78$ for steel. The effective stress concentration calculated for aluminum are confirmed by Figure 16 of the NACA Technical Note 3866 [16] and are also very similar to the values calculated by Topper et al. [22], while the values for steel at $K_t=4$ underestimated the actual notch effect, thence it had to be modified to $K_f(K_t=4)\approx3.65$ in accordance with Illg's Figure 16 [16]. Moreover, from Figure 16 [16] it is evident that the K_f tends to one when the maximum nominal stress approaches the ultimate tensile strength, confirming the hypothesis that the effect of the presence of notches only marginally affects the ultimate tensile strength. Anyway, as regards Al 2024-T3, notched specimens do not show the initial plateau characterizing the curve for $K_t=1$, consequently the nominal stress range II approach as is does not fit properly the experimental data. For this reason, N_u has been reduced from $2\cdot10^3$ to 20 for $K_t=2$ and to 2 for $K_t=4$, then the resulting Weibull's law has been recalibrated via Equation (5.12). For normalized 4130 steel the nominal stress range II approach provided a satisfying fit of experimental data. The final S/N curves obtained through

the model here introduced provide a smooth fit of the experimental data for both plain and notched experiments. The scaling factors remain unchanged with respect to the plain specimen, i.e. f_a=1.15 and f_a=1.45 for aluminum alloy and steel respectively. In Figure 5.7 the S/N curves obtained with the presented model are shown. Those curves are also compared with the non-corrected Weibull's law and with the truncated Basquin's law curves. The trend theorized by Weibull is globally confirmed, indeed Basquin's law through the present model appears to be an approximation of Weibull's law and the transition to the fatigue limit is smooth rather than a knee, especially when many data are available at $N \geq 10^7$ cycles.

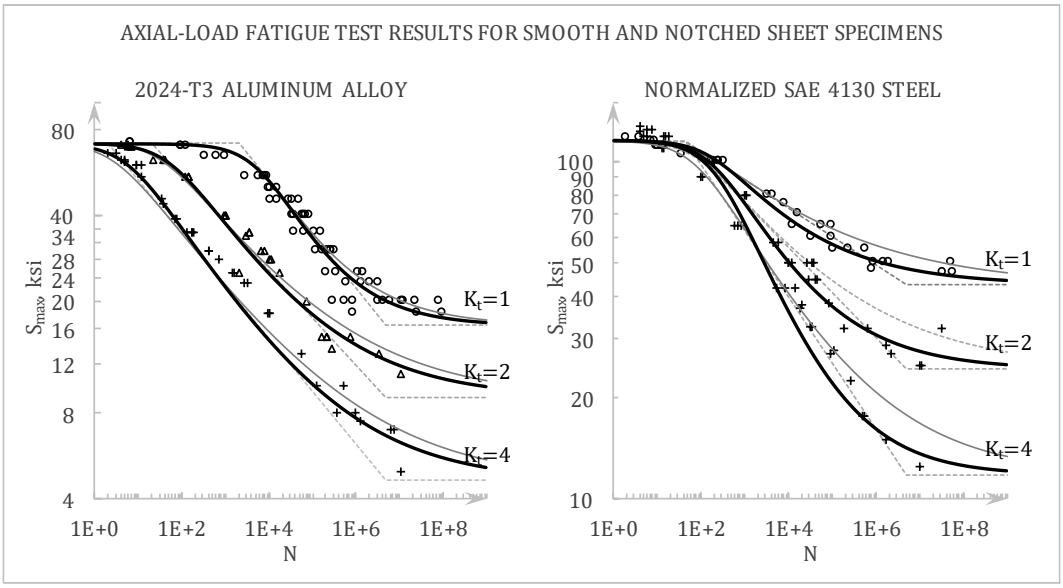

Figure 5.7: S/N curves for plain and notched sheet specimens. The dashed gray line represents the truncated Basquin's law, the solid gray line is Weibull's law with no modifications, and the black solid line is the updated Weibull's law

Conclusion

An analytical explicit model relating Basquin's law truncated at the fatigue limit and Weibull's law for a smooth four parameters S/N curve is proposed. Weibull's approach for the "determination of average load-life relations" [2] made use of graphical or approximate analytical trial and error procedures to determine the S/N curve equation in semilogarithmic axes. The Log(S)/Log(N) coordinates are helpful since the Basquin's power law can be used to represent the slope in the inflection point, thus making straightforward the analytical exact definition of Weibull's law parameters. The model can be used to define a family of S/N curves where the scatter increases with decreasing stress amplitude through the only introduction of a slope factor f_a and the hypothesis that N_i stays constant. This result is in agreement with Illg's

experiments [16] and shall be further studied from the statistical point of view. Finally, the effect of notches can be easily and successfully modelled only by knowing the effective stress intensity factor and the S/N curve for the plain specimen and it has been found that the parameter f_a is not affected by the presence of the notch.

References

[1] P. D'Antuono, 'An analytical relation between Weibull's and Basquin's laws for smooth and notched specimens and application to constant amplitude fatigue', *ArXiv Prepr. ArXiv190910741*, 2019.

[2] W. Weibull, *Fatigue Testing and Analysis of Results*. Elsevier, 1961.

[3] H. F. Moore, J. B. Kommers, and T. M. Jasper, 'Fatigue or Progressive Failure of Metals under Repeated Stress', in *Proceedings*, 1922, p. 266.

[4] S. R. Mettu *et al.*, 'NASGRO 3.0: A software for analyzing aging aircraft', 1999.

[5] J. Maierhofer, R. Pippan, and H.-P. Gänser, 'Modified NASGRO equation for physically short cracks', *Int. J. Fatigue*, vol. 59, pp. 200–207, 2014.

[6] J. Maierhofer, R. Pippan, and H.-P. Gänser, 'Modified NASGRO equation for short cracks and application to the fitness-for-purpose assessment of surface-treated components', *Procedia Mater. Sci.*, vol. 3, pp. 930–935, 2014.

[7] P. C. Paris and F. Erdogan, *A Critical Analysis of Crack Propagation Laws*. ASME, 1963.

[8] M. Ciavarella, P. D'antuono, and G. P. Demelio, 'A simple finding on variable amplitude (Gassner) fatigue SN curves obtained using Miner's rule for unnotched or notched specimen', *Eng. Fract. Mech.*, vol. 176, pp. 178–185, May 2017.

[9] M. Ciavarella, P. D'Antuono, and G. P. Demelio, 'Generalized definition of "crack-like" notches to finite life and SN curve transition from "crack-like" to "blunt notch" behavior', *Eng. Fract. Mech.*, vol. 179, pp. 154–164, Jun. 2017.

[10] Y.-L. Lee, J. Pan, R. Hathaway, and M. Barkey, *Fatigue testing and analysis: theory and practice*, 1st ed., vol. 13, 1 vols. Butterworth-Heinemann, 2004.

[11] H. Neuber, *Theory of notch stresses: Principles for exact stress calculation*, vol. 74. JW Edwards, 1946.

[12] P. Kuhn and H. F. Hardrath, 'An engineering method for estimating notch-size effect in fatigue tests on steel', National Advisory Committee for Aeronautics, Langley Field, Va, NACA Technical Note NACA-TR-2805, 1952.

[13] W. Weibull and F. K. G. Odqvist, *Colloquium on Fatigue / Colloque de Fatigue / Kolloquium über Ermüdungsfestigkeit: Stockholm May 25–27, 1955 Proceedings / Stockholm 25–27 Mai 1955 Comptes Rendus / Stockholm 25.–27. Mai 1955 Verhandlungen*. Springer Science & Business Media, 2012.

[14] R. Peterson, Ed., *Manual on Fatigue Testing*. West Conshohocken, PA: ASTM International, 1949.

[15] D. V. Nelson and H. O. Fuchs, 'Predictions of Cumulative Fatigue Damage Using Condensed Load Histories', *SAE Trans.*, vol. 84, pp. 276–299, 1975.

[16] W. Illg, 'Fatigue Tests on Notched and Unnotched Sheet Specimens of 2024-T3 and 7075-T6 Aluminum Alloys and of SAE 4130 Steel with Special Consideration of the Life Range from 2 to 10,000 Cycles', National Advisory Committee for Aeronautics, Langley Field, Va, NACA Technical Note NACA-TR-3866, Dec. 1956.

[17] S. I. Liu, J. J. Lynch, E. J. Ripling, and G. Sachs, 'Low Cycle Fatigue of Aluminum Alloy 24ST in Direct Stress', *Trans AIME*, vol. 175, p. 469, 1948.

[18] M. H. Weisman and M. H. Kaplan, 'The Fatigue Strength of Steel Through the Range from 1/2 to 30,000 Cycles of Stress', in *Proceedings-American Society For Testing And Materials*, 1950, vol. 50, pp. 649–667.

[19] H. F. Hardrath, C. B. Landers, and E. C. Utley Jr, 'Axial-load fatigue tests on notched and unnotched sheet specimens of 61S-T6 aluminum alloy, annealed 347 stainless steel, and heat-treated 403 stainless steel', National Advisory Committee for Aeronautics, Langley Field, Va, NACA Technical Note NACA-TR-3017, Oct. 1953.

[20] H. J. Grover, S. M. Bishop, and L. R. Jackson, 'Fatigue strengths of aircraft materials: axial-load fatigue tests on notched sheet specimens of 24S-T3 and 75S-T6 aluminum alloys and of SAE 4130 steel with stress-concentration factors of 2.0 and 4.0', National Advisory Committee for Aeronautics, Battelle Memorial Institute, NACA Technical Note NACA-TR-2324, Mar. 1951.

[21] H. J. Grover, W. S. Hyler, P. Kuhn, C. B. Landers, and F. M. Howell, 'Axial-load fatigue properties of 24S-T and 75S-T aluminum alloy as determined in several

laboratories', Battelle Memorial Institute, Langley Aeronautical Laboratories, Aluminum Company of America, NACA Technical Note NACA-TR-2928, May 1953.

[22] T. Topper, R. M. Wetzel, and J. Morrow, 'Neuber's rule applied to fatigue of notched specimens', *Illinois University at urbana Dept of Theoretical and Applied Mechanics*, 1967.

6 Appendix

Appendix A

Python implementation of Rainflow counting algorithm with Walker mean stress correction.

```
#!/usr/bin/env python
"""
------------------------------------------------------------------------------
Author: Pietro D'Antuono
------------------------------------------------------------------------------
"""
from numpy import fabs as fabs
import numpy as np

def rainflowSWT(array_ext,
                gamma=0.5, uc_mult=0.5):
    """
    Rainflow counting of a signal's turning points
    with Walker correction
        Args:
            array_ext (numpy.ndarray): array of turning points
        Keyword Args:
            gamma (float): Walker's constant [opt, default=0.5]
                           0.5 for SWT lmean effect correction
            uc_mult (float): partial-load scaling [opt, default=0.5]
        Returns:
            array_out (numpy.ndarray):
                (4 x n_cycle) array of rainflow values:
                    1) load range
                    2) range lmean
                    3) Walker-adjusted range
                    4) cycle count
    """

    tot_num = array_ext.size            # total size of input array
    array_out = np.zeros((4, tot_num-1)) # initialize output array

    pr = 0                              # index of input array
    po = 0                              # index of output array
    j = -1                              # index of temporary array "a"
    a  = np.empty(array_ext.shape)      # temporary array for algorithm

    # loop through each turning point stored in input array
    for i in range(tot_num):

        j += 1               # increment "a" counter
        a[j] = array_ext[pr] # put turning point into temporary array
        pr += 1              # increment input array pointer

        while ((j >= 2) & (fabs( a[j-1] - a[j-2] ) <= \
                fabs( a[j] - a[j-1]) ) ):
            lrange         = fabs( a[j-1] - a[j-2] )
            # partial range
            if j == 2:
                lmean      = ( a[0] + a[1] ) / 2.
                lmax       = lrange/2 + lmean
                if lmax > 0:
                    adj_lrange = 2 * lmax**(1 - gamma) * (lrange / 2)**gamma
                else:
```

```
                adj_lrange = 0
            a[0]=a[1]
            a[1]=a[2]
            j=1
            if (lrange > 0):
                array_out[0,po] = lrange
                array_out[1,po] = lmean
                array_out[2,po] = adj_lrange
                array_out[3,po] = uc_mult
                po += 1

        # full range
        else:
            lmean      = ( a[j-1] + a[j-2] ) / 2.
            lmax       = lrange/2 + lmean
            if lmax > 0:
                adj_lrange = 2 * lmax**(1 - gamma) * (lrange / 2)**gamma
            else:
                adj_lrange = 0
            a[j-2]=a[j]
            j=j-2
            if (lrange > 0):
                array_out[0,po] = lrange
                array_out[1,po] = lmean
                array_out[2,po] = adj_lrange
                array_out[3,po] = 1.00
                po += 1

# partial range
for i in range(j):
    lrange         = fabs( a[i] - a[i+1] );
    lmax           = lrange/2 + lmean
    if lmax > 0:
        adj_lrange = 2 * lmax**(1 - gamma) * (lrange / 2)**gamma
    else:
        adj_lrange = 0
    if (lrange > 0):
        array_out[0,po] = lrange
        array_out[1,po] = lmean
        array_out[2,po] = adj_lrange
        array_out[3,po] = uc_mult
        po += 1

# get rid of unused entries
array_out = array_out[:,:po]
return array_out
```

Appendix B

In order to define an analytical relationship between the variables S_U, $\bar{a}$, $\bar{b}$ and a, b, B of Chapter 5, the following definitions valid for the generic variable ψ have been used:

$$\log_{10}\psi = \frac{\ln\psi}{\ln\ 10} \tag{6.1}$$

Where ln stands for the natural logarithm.

Generic derivative of a quantity □ with respect to the decadic logarithm of N

$$\frac{d\psi(N)}{d\log_{10} N} = \log 10\,\frac{d\psi}{dN\,\frac{d\ln N}{dN}} = \ln 10 \cdot N \cdot \frac{d\psi}{dN} \tag{6.2}$$

First derivative of the decadic logarithm of a function □(N) with respect to the decadic logarithm of N:

$$\frac{d\log_{10}\psi(N)}{d\log_{10} N} = \log_{10}\psi_{/\log_{10} N} = N \cdot \frac{d\ln\psi}{dN} = N \cdot \frac{\psi'(N)}{\psi(N)} \tag{6.3}$$

Second derivative:

$$\begin{aligned}\frac{d^2\log_{10}\psi(N)}{d\,(\log_{10} N)^2} &= \log_{10}\psi_{/\log_{10} N\,\log_{10} N} = N \cdot \ln 10 \cdot \frac{d}{dN} \cdot \left[N \cdot \frac{\psi'(N)}{\psi(N)}\right] \\ &= N \cdot \ln 10 \cdot \frac{1}{\psi(N)} \\ &\cdot \left[\psi'(N) \cdot \left(1 - N \cdot \frac{\psi'(N)}{\psi(N)}\right) + N \cdot \psi''(N)\right] \\ &= N \cdot \ln 10 \cdot \frac{1}{\psi(N)} \\ &\cdot \left[\psi'(N) \cdot \left(1 - \log_{10}\psi_{/\log_{10} N}\right) + N \cdot \psi''(N)\right]\end{aligned} \tag{6.4}$$

Hence, substituting equation (5.2) into the generic derivatives written in equations (6.3) and (6.4) the following expressions are found:

$$\log_{10} S_{/\log_{10} N} = N \cdot \frac{b \cdot a \cdot (N+B)^{a-1}}{b \cdot (N+B)^a + S_e} \tag{6.5}$$

$$\begin{aligned}\log_{10} S_{/\log_{10} N\,\log_{10} N} &= \frac{N \cdot \log 10 \cdot b \cdot a \cdot (N+B)^{a-2}}{b \cdot (N+B)^a + S_e} \\ &\cdot \left[(N+B) \cdot \left(1 - \log_{10} S_{/\log_{10} N}\right) + N \cdot (a-1)\right]\end{aligned} \tag{6.6}$$